die talsperren österreichs

Large Dams in Austria/Volume 34

Embankment Dams

Research and development, construction and operation

W. Schober

Published by the **Austrian National Committee on Large Dams**
with the support of the Austrian Reservoir Commission (Staubeckenkommission).

die talsperren österreichs

Large Dams in Austria/Volume 34

Embankment Dams

Research and development, construction and operation

W. Schober

Innsbruck, September 2003

Translation by Professor Chris Marsh at Innsbruck University

About the author

Walter Schober, born in Klagenfurt/Austria (1924) received his civil engineering and doctoral degrees from the Technical University of Graz, where he was assistant at the Institute of Water Construction until 1953.

From 1953 until 1971 he worked as design engineer at the TIWAG – Tiroler Wasserkraft AG. During this time he was involved in the construction of Gepatsch dam and in the design of Finstertal dam.

After moving to Innsbruck University als professor he was head of the Institute of Soil Mechanics, Rock Mechanics and Foundation Engineering (BFG) until 1994. As Professor Emeritus he is now a member of the Institute of Geotechnic and Tunnel Engineering (IGT).

Edited and Published by:

ÖSTERREICHISCHES NATIONALKOMITEE FÜR TALSPERREN
(AUSTRIAN NATIONAL COMMITEE ON LARGE DAMS – ATCOLD)
Elisabethstrasse 59/4
A-8010 Graz

Published with the support of the
Austrian Federal Ministry of Agriculture and Forestry, Environment and Water Management,
and The Austrian Water and Solid Waste Management Association

Cover photo: Finstertal and Längental dams,
TIWAG – Tiroler Wasserkraft AG

Publishers foreword

The "Austrian National Committee on Large Dams" has published a series on "Dams in Austria" under the title "Talsperren in Österreich" for the past half century. As part of this series, and following a monograph on arch dams – published for the first time with a summary in English –, another monograph is now available, this time entirely in English.

This volume deals with embankment dams and their design, construction, maintenance, and surveillance. The author of this comprehensive work is Professor Walter Schober, who enjoys an international reputation among his expert colleagues. After working as an assistant professor at the Graz University of Technology, Professor Schober joined Tiroler Wasserkraftwerke AG (TIWAG, the Tyrolean hydroelectric company), where he rose to the position of Senior Design Engineer. This was followed by more than 20 years' teaching as a professor and head of the Department of Soil Mechanics, Rock Mechanics, and Foundation Engineering at the University of Innsbruck. During these decades his interest focused on embankment dams in both theory and practice, as witnessed by the design and construction of several fill dams, in particular two large rockfill dams in Austria. In his scientific studies, Professor Schober explored possible ways of further developing embankment technologies, publishing the results and passing them on to his students. Always keen to pursue innovative methods, he e.g. conceived and developed the "Prestressed Embankment Dam". Professor Schober is a member of several associations and commissions both on the national and international levels and, now a professor emeritus, he is still a sought-after expert.

Embodying in a concise form all the experience gathered by the author during decades of engineering work, this volume is valuable both as a documentary record and as a basis for further development studies. The ATCOLD board has decided to include this work in its series of publications, because of its great interest to us.

As Chairman of ATCOLD, I wish to express our thanks primarily to the author himself, but also to all the others who have helped to make this publication possible. May it stimulate the international attention it deserves.

G. Heigerth

Contents

Summary

It was not until the second half of the 20th century that high embankment dams came to Austria. A total of twenty dams with a height of between 25 m and 153 m were built, namely ten with asphaltic concrete facings, four with asphaltic concrete cores, two with concrete cores and four with earth cores. Material of high shear strength was available for the filter, transition and shell zones. Seven dams were located on compressible overburdens that were of considerable depth in places.

The purpose of this report is to summarize the Austrian contribution to the theory and practice of fill dam construction. One focus of the paper is to relate the research into embankment dams conducted at the University of Innsbruck from 1971 to 1993 to the empirical results of bearing behavior monitoring on the dams constructed. Attention is also paid to special aspects of the construction work involved, the sophisticated monitoring equipment installed and questions of dam safety.

Kurzfassung

Der Bau hoher Staudämme setzte in Österreich erst in der 2. Hälfte des 20. Jahrhunderts ein. Es wurden 20 Staudämme zwischen 25 m und 153 m Dichtungshöhe errichtet. 10 Dämme kamen mit Asphaltbeton-Oberflächendichtungen, 4 mit Asphaltbeton-Kerndichtungen, 2 mit Betonkerndichtungen und 4 mit Erdkerndichtungen zur Ausführung. Für Filter-Übergangs- und Stützkörperzonen stand scherfestes Material zur Verfügung. 7 Dämme wurden auf teilweise tiefreichender und zusammendrückbarer Felsüberlagerung gegründet.

Der vorliegende Bericht setzte sich zur Aufgabe, die österr. Beiträge zum Staudammbau in Forschung und Praxis zusammenzufassen. Es wird als Schwerpunkt der Bearbeitung ein Kontext zwischen der an der Universität Innsbruck von 1971 bis 1993 durchgeführten Staudammforschung und dem gemessenen Tragverhalten der ausgeführten Dämme hergestellt. Darüberhinaus werden auch Besonderheiten der Bauausführung, die hoch entwickelte messende Überwachung, sowie Fragen der Sicherheit von Stauanlagen behandelt.

1. Preface

Austria's last embankment dams with a height of over 30 m were finished in 1990. That marked the provisional end of an intensive period of dam construction that had lasted for over forty years. Fig. 1 shows the locations and Table 1 lists the main specifications of the twenty high dams involved [9] and [37]. Since 1990 several small fill dams have been built, primarily to provide pondage in ski areas for snowmaking systems.

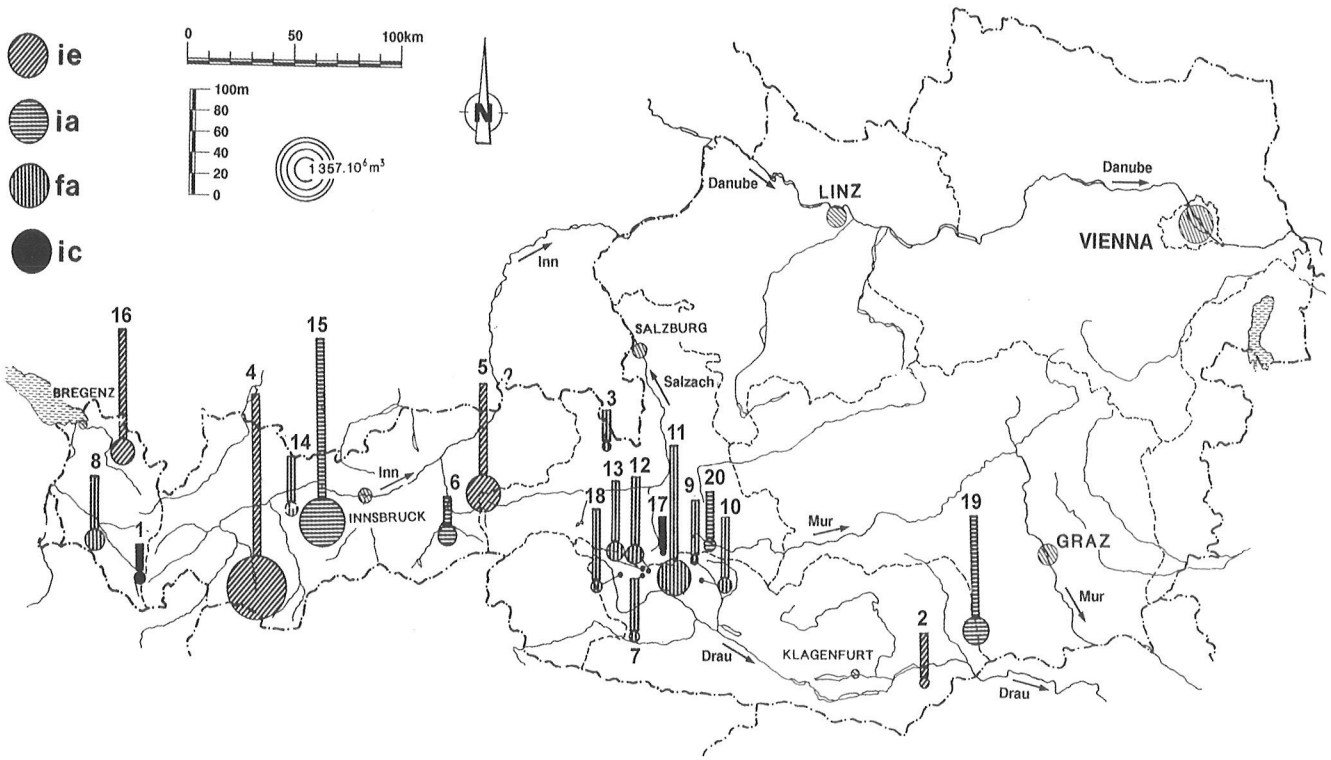

Fig. 1 *from [9]: Location of embankment dams over 25m high.*
ie: Earth core.
ia: Asphalt concrete core membranes.
fa: Asphalt concrete facings.
ic: Cement concrete core membranes.

As in all complex fields of engineering, embankment dam construction depends to a significant degree on the global exchange of experience. That makes organizations like ICOLD (International Commission on Large Dams) and the relevant publications such as [3] and [7] particularly important. The communication of experience is not the primary focus of this report, however; the main objective is to provide a compact summary of the contribution made by Austria to the theory and practice of embankment dam construction. A bibliography is provided for further reading on the various topics covered by the report.

Embankment dam engineering was made a focus of research by the author of this report in his capacity as head of the Institute of Soil Mechanics, Rock Mechanics and Foundation Engineering at Innsbruck University **(BFG Institute)** at the beginning of the 1970s, and research there continued for a period of over twenty years [1].

With three exceptions (dams nos. 3, 17 and 20), Austria's twenty high embankment dams were planned by Austrian hydro-electric companies with the help of external experts, and they were largely constructed by Austrian contractors.

This report is modeled on Volume 10: „Rockfill Dams, Design and Construction" of the series on „Hydropower Development" published by the Norwegian Institute of Technology [2] in 1992. The topics that have already received full coverage in the Norwegian publication are not repeated here,

No.	Name	Power company	Hmax[1] [m]	HDo[2] [m]	HDu[3] [m]	V[4] [10^6 m^3]	Type[5]	Year of completion
1	Bielerdamm	VIW	25	20	5	0.375	TE ic	1948
2	Freibach	KELAG	49	41	–	0.235	TE ie	1958
3	Diessbach	Sbg. AG	36	29	–	0.165	ER fa	1963
4	Gepatsch	TIWAG	153	153	–	7.100	ER ie	1965
5	Durlassboden	AHP	83	83	60	2.520	TE ie	1966
6	Eberlaste (Stillupp)	AHP	28	28	52	0.790	TE ia	1968
7	Wurten	KELAG	51	34	15	0.265	ER fa	1971
8	Latschau II	VIW	50	18	–	0.865	TE fa	1975
9	Galgenbichl	AHP	50	50	–	0.065	TE fa	1974
10	Gösskar	AHP	55	55	–	0.540	TE fa	1975
11	Oscheniksee	KELAG	116	61	–	2.250	ER fa	1978
12	Hochwurten	KELAG	55	50	16	0.600	TE fa	1979
13	Gross-See	KELAG	57	49	–	0.740	ER fa	1978
14	Längental	TIWAG	45	32	12	0.400	TE fa	1980
15	Finstertal	TIWAG	150	96	–	4.500	ER ia	1980
16	Bolgenach	VKW	102	92	–	1.200	TE ie	1978
17	Bockhartsee	Sbg. AG	69	31	–	0.228	ER ic	1982
18	Zirmsee	KELAG	44	37	–	0.525	ER fa	1983
19	Feistritzbach (Koralpe)	KELAG	88	85	–	1.500	ER ia	1990
20	Rotgüldensee	Sbg. AG	45	45	–	0.350	ER ia	1990

Table 1 *from [9]: Main data for embankment dams over 25m high.*
1) Maximum dam heigh.
2) Heigh of seal in dam body
3) Heigh of seal in dam foundation
4) Dam Volume.
5) ICOLD calssification.

but the relevant references are provided where necessary.

This report makes no claim to being a complete or definitive account. Given the subject concerned, that would not be appropriate in any case. Like all man-made structures that interact with the forces of nature, every embankment dam has its own unique character, and any attempt to describe its behavior will always involve a process of approximation of varying degrees of accuracy.

I should like to take this opportunity to thank all those who have contributed to this report, by providing documents, proof reading, producing the figures and so on. I am particularly indebted to the authors of the various research papers and data analyses from which the figures have been taken. To that extent this report must be seen as the result of a group effort. Finally, I wish to offer my sincere thanks to the Austrian National Committee on Large Dams (ATCOLD) for making it possible for the report to appear in its series of publications and the Honorary President of ICOLD W. Pircher for his encouragement and assistance.

W. Schober

2. General remarks

The planning work for the construction of a reservoir must always be performed in close co-operation with geologists, in particular with regard to the imperviousness of the reservoir, the state of the adjoining slopes, the characteristics of the foundations, especially of the dam itself, and the availability of the necessary fill materials. Once these aspects have been adequately documented, work can begin on the design of the dam itself. The first question to be decided is whether the site is better suited for a concrete dam or an embankment dam. The choice will fall on the type of dam that constitutes the best solution in terms of engineering and economics on the basis of investigations into the various alternatives.

The decision is simple in the case of dam foundations that are susceptible to settlements, where an embankment dam is the only possible solution. Under such conditions, only the type of embankment dam and foundation sealing works need to be decided. The principle requirement is a flexible dam body that will cope with the anticipated deformations without suffering damage.

The choice of the optimum type of dam is more complex and more difficult in those cases where either a concrete dam or a fill dam could be built. That is the case where the dam can be founded on competent bedrock. The progress made in adapting the design and construction of embankment dams to the conditions pertaining in narrow gorges made them a possible variant even on such sites.

Theoretically, an unchallengeable decision on the optimum type of dam would require a procedure in which the various possible solutions are planned to the same level of detail and made the subject of tender in open competition. In most cases, however, that is not practicable for reasons of time and expense.

Frequently the clients are influenced by their previous experience with dam construction projects. A company already operating dams of a certain type will tend to build the same type again unless there are serious objections, e.g. in terms of significantly higher construction costs. That can also apply to decisions on the variants available within one and the same type of dam. For embankment dams there is usually a number of alternative dam designs. Local availability of suitable materials will normally be a decisive aspect as that is the primary cost factor in the construction of fill dams. On the other hand, the serious dam engineer will not support the decision to build a certain type of embankment dam for reasons of estimated lower construction costs where the decision cannot be supported by structural arguments.

Every dam construction project must naturally be handled in accordance with the relevant standards and industry codes. That is only one aspect of dam safety, however. Equal importance must be attached to a high standard of workmanship, including the various aspects of materials testing and processing, and monitoring of the placement process. Foundation sealing works can also be of decisive importance with regard to dam safety.

Dam surveillance is always an essential element of dam safety and must be entrusted to duly appointed and qualified personnel. The dangers confronting a dam often derive from long-term processes. As a dam failure can have catastrophic consequences, great importance is attached to reliable dam monitoring throughout the world. In the case of Austria, all high dams are inspected by the federal authority every five years [35a, 35b, 35c, 35d]. The work is performed by a committee of experts who are especially well qualified for the task. In addition, annual inspections are performed by the regional authorities, who are also the supervisory authority for smaller dams. In this context it should be pointed out that it is becoming increasingly difficult to recruit personnel with the necessary expertise at a time of stagnating dam construction. It is therefore extremely important that the appropriate training facilities be created and the inspectors' qualifications duly tested in the future.

All dam construction projects involve a number of appurtenant systems in the form of spillways for flood water discharge and a bottom outlet for reservoir drawdown. It is essential that dam safety be maintained under every conceivable operational load case including extreme events. In the case of machinery and equipment, all necessary measures must be taken to ensure safe operation. For the safety of the construction pit, high standards of working must be observed with regard to the diversion structures built to control the flow of water.

3. Structure of the contents

The structure of this report is based on the seven topics formulated below, which served as a framework for the work done on sections 4 to 10. The report closes with a number of conclusions which are presented in section 11.

Topic 1: Types of embankment dams

By way of introduction to the subject of the report, the profiles of the different embankment dam types are presented, the wide variety of solutions explained and the corresponding Austrian examples highlighted. The various types are classified in groups and their structure described.

Topic 2: Bearing behavior of embankment dams

In this main section, each of the groups of dams as defined in Topic 1 is first considered in the light of the general research results followed by a presentation of observed behavior in the Austrian examples.

Topic 3: Additional problems

This section focuses on the following research projects: „Shear resistance of loose material on foundation rock", „Filter criteria for geotextiles", „Load calculations for rigid structures" and „The prestressed embankment dam".

Topic 4: Construction

Standardized processes are now largely employed to study material behavior, to extract, process and place the fill materials, and to monitor placement. For that reason only, special features of dam construction in Austria are discussed.

Topic 5: Monitoring dam behavior and incidents

A process of global harmonization can also be observed in the case of surveillance. Austria has made significant contributions over the years to today's high standards of monitoring equipment. This Topic also covers a number of incidents which were identified in good time with the monitoring systems in place.

Topic 6: Dam safety

This Topic is devoted to the Austrian situation. A research paper on the approximative quantification of three-dimensional effects is presented, and the stability of reservoir slopes discussed.

Topic 7: „Spillways and bottom outlets"

The situation in Austria is presented.

4. Types of embankment dams

As stated in section 2, the primary objective of dam design is to achieve the solution offering the best possible results in terms of engineering and economics based on the investigations conducted at the site of the dam and material extraction sites, and the results of materials testing. This will of necessity be a painstaking process in constant interaction with a growing store of knowledge.

Wide valleys with gently sloping flanks and foundation areas with good bearing capacity permit the use of all types of embankment dams. The choice is more limited in the case of deformable foundations, narrow valleys with steep flanks and areas of seismic activity.

Dam design must take account of the need for dam monitoring facilities and scope for remedial measures in the case of any negative developments. This includes the provision of inspection galleries and shafts in particular.

In this report the various types of embankment dams are defined in terms of their sealing elements. Their choice of these elements is of paramount importance. Impervious zones and membranes should be able to resist cracking in every conceivable load state. They are also decisive for the remaining design aspects of a dam as a structure that must offer a high level of stability and resistance to erosion. Two main types are distinguished in the following.

4.1 Type A: embankment dams with membrane seals

Artificial membrane seal elements were already in use worldwide in the early years of high embankment dam engineering at the beginning of the previous century. The main attraction was doubtless the independence they offered of the availability of natural impervious materials. Mechanized construction processes also meant a higher quality product was available and amenable to quality control measures. Apart from the - now obsolete - wooden plank seals [3], the materials listed in Table 2, which is taken from [4], are still in use. The distinctive feature proposed for these materials is flexural rigidity, which is a measure of the capacity of the membrane to adapt to various movements in the dam body and foundations.

The various possible locations of membranes and impervious layers in the dam cross-section are shown in Fig. 2/A. The seal is extended down into the foundations through the use of grout curtains, cutoff walls, thin diaphragm walls or pile walls. In the case of embankment dams founded on overburden, toe weights and relief wells located downstream from the toe of the dam also play an important role.

No.	Kind of diaphragm	E (KN/m²)	d(m)	E.I/m (kNm²/m)
1	Geomembrane	3×10^{3}**	4×10^{-3}	1.6×10^{-5}
2	Steel sheet	2.1×10^{8}	6×10^{-3}	3.8×10^{9}
3/1*	Asphaltic concrete	1×10^{5}**	1×10^{-1}	8.3×10^{9}
3/2*	Asphaltic concrete	1×10^{5}**	6×10^{-1}	1.8×10^{3}
4	Clay concrete	1×10^{5}**	6×10^{-1}	1.8×10^{3}
5	Cement concrete	3×10^{7}	6×10^{-1}	5.4×10^{5}

Table 2 *from [4]*
Types of diaphragms.
**) 3/1 surface diaphragms, 3/2 core diaphragms.*
***) Incorrect vallues.*

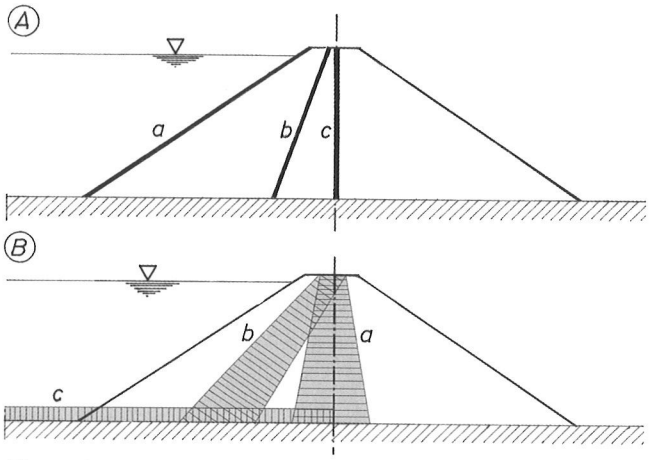

Fig. 2: *Locations of Seals*
A Membrane Seals
B Earth Seals
a, b, c, see text

The Austrian examples of embankment dams with membrane seals can be divided into two groups: those with surface diaphragms (A1) and those with core diaphragms (A2). The surface membranes in the A1 group all take the form of asphaltic concrete facings in the „a" position on the upstream surface. According to [56], the first high embankment dam with an asphaltic concrete facing was the 43 m high Genkeltal Dam in Germany, which was built in 1950 - 1952. Fig. 3 shows the main sections of Austria's ten high dams of this type. In the case of Dam no. 7, the surface diaphragm is continued as a grout curtain into the overburden, and in dams 12 and 14 as a concrete wall. In all cases grout curtains are used to seal the foundation rock. Five of the dams are built on bedrock, the others wholly or

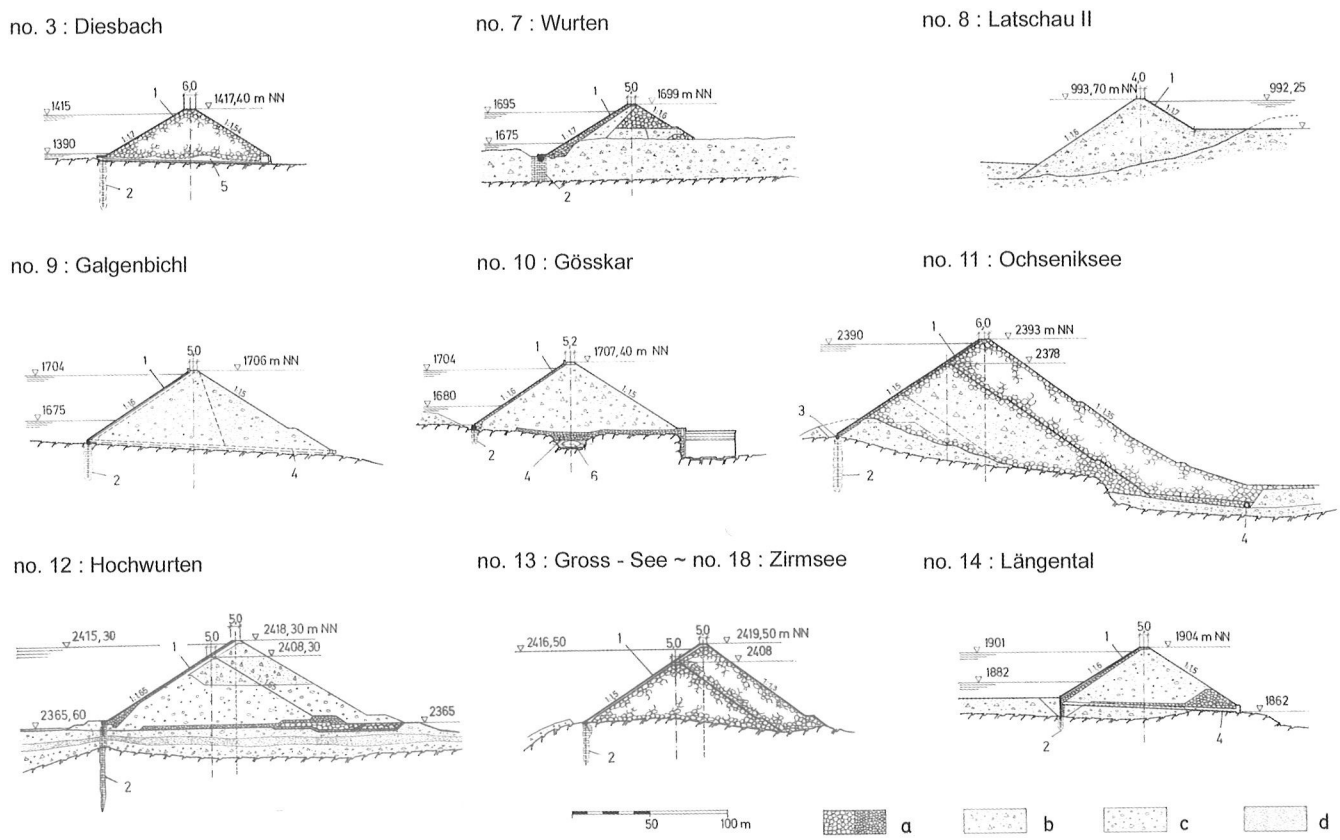

Fig. 3 *from [5]:*
Main sections of dams with asphaltic concrete facings – Type f_a
(1) Membrane Seal
(2) Grout curtain
(3) Inspection gallery
(4) Drainage gallery
(5) Bottom outlet
(6) Pressure tunnel
a: Rockfill coarse and fine grained
b: Moraine/Talus material
c: Sediment mixed grained
d: Sediment fine grained

in part on overburden. For the fill for the dam body, material of high shear strength was available, e.g. quarry-run material, tunnel spoil, moraine material, alluvial deposits, and talus.

The overburden is mainly made up of soils of high bearing capacity such as moraine material, talus or alluvial deposits, although fine grained strata like lacustrine clay sediments are also found.

There are several explanations for the clear preference given to Type A1. The main reasons, as mentioned above, are the resulting independence of natural impervious materials, the excellent flexibility of the continuous asphaltic concrete facing, long years of positive experience with earlier projects, and the capacity of the dam to resist hydrostatic pressure. In dams nos. 11, 12 and 13, the resulting potential for raising the height of the dam was a decisive argument. In the case of basins (Dam no. 8) and short-term storage reservoirs (dams nos. 9, 10 and 14), the autonomy of the dam in the face of rapid fluctuations in storage level also played a major role.

A characteristic of the design of Type A1 dams is the provision of a permeable filter zone beneath the upstream facing to ensure interception of any seepage (blanket drain) followed by a less permeable zone to permit the seepage to drain along its surface to the upstream toe of the dam. This zone could only be omitted in the case of dam bodies constructed with highly permeable quarry-run rockfill material offering high resistance to erosion (dams nos. 3, 11, 13 and 18). In the case of Dam no. 8, the binder course beneath the upstream facing also functions as a relief zone.

In general, Austrian dams with asphaltic concrete facing have proven very successful and have now been in operation for several decades. Damage to the upstream facing such as cracking at the edge of the crest as a result of creep, of pull exerted in high mountain locations by creeping ice with the ploughshare effect of the enclosed stones, and also of settlements at the connections to concrete structures and steep valley flanks was addressed through appropriate remedial measures in the case

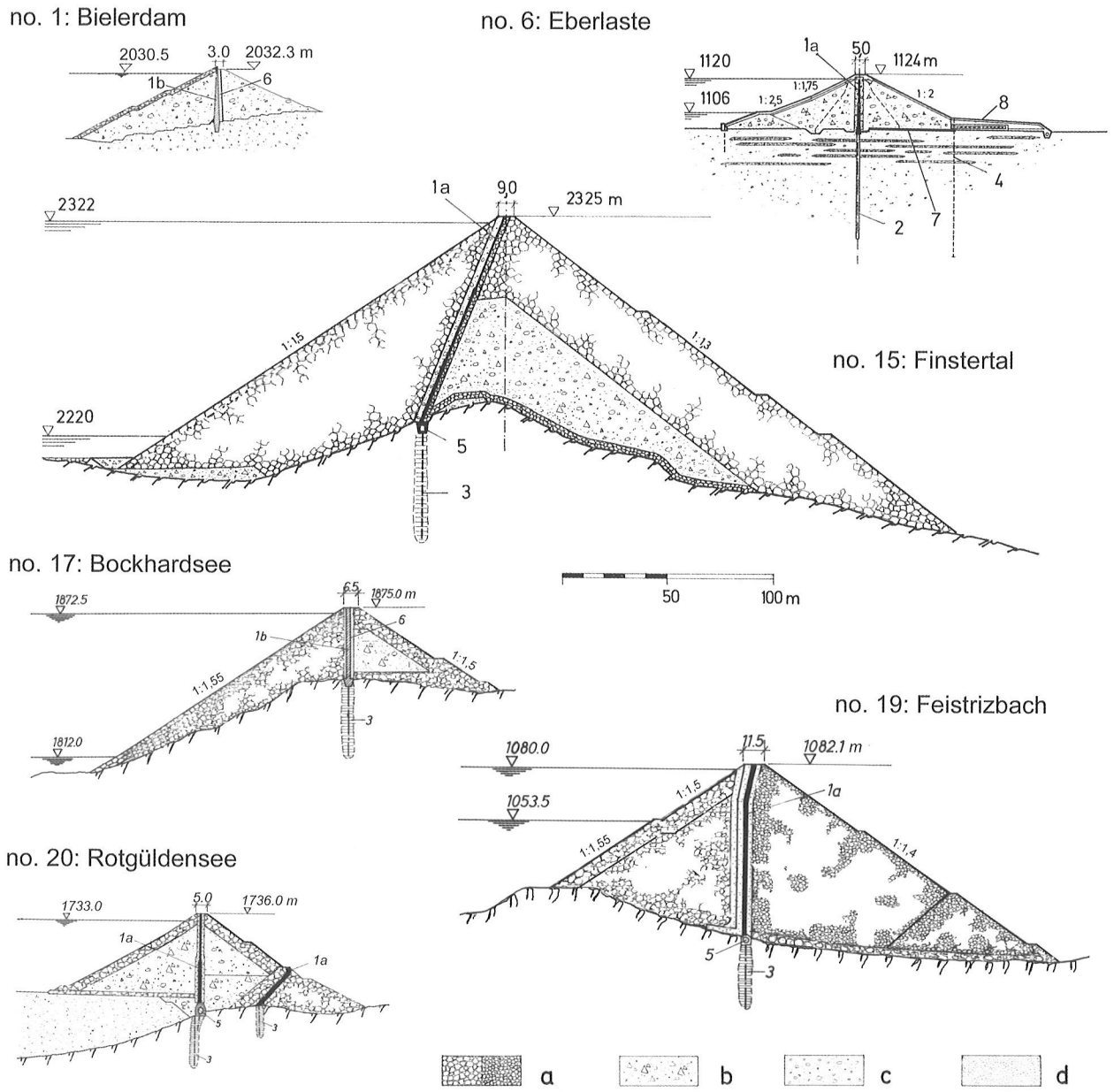

Fig. 4 *from [5,9,33b]: Main sections of dams with core membrane seals – Types ia and ic*
(1a) Asphaltic concrete core
(1b) Cement concrete core
(2) Cut-off wall
(3) Grout curtain
(4) Relief wells
(5) Inspection gallery
(6) Inspection shaft
(7) Asphaltic concrete blanket
(8) Toe weight

a: Rockfill coarse and fine grained
b: Moraine/Talus material
c: Sediment mixed grained
d: Sediment fine grained

of dams nos. 12 and 13, as reported in detail in [6]. Vapor pressure blistering, especially in double-course facings, and the resulting damage caused by cracking are also amenable to rehabilitation.

More recent asphaltic concrete facings comprise one single course. Improvements to the facing machines have made it possible to produce excellent compaction results on layers that are 10 cm thick and more. The highest facing placed in Austria to date is 61 m high (Dam no. 11). Such facings are at risk from erosion of the asphaltic concrete in the case of a leakage and are relatively susceptible to all kinds of mechanical damage. In a field test conducted on Dam no. 10, good penetration resistance was demonstrated in the case of rockfall. Increased thickness of the facing in the rock impact area was enough to counter the hazard. The world's highest dams with surface diaphragms were built with reinforced concrete facings. The 160 m high Foz do Areia Dam in Brazil has been operating successfully since 1980 [8]. Shuibuya Dam presently under construction in China will be 230 m high.

There are six dams in the A2 group of Austrian dams with membrane seals in the dam body. As shown in Fig. 4, the sealing elements occupy the

„c" position in five cases and the „b" position in one. Dams nos.1 and 17 have concrete core walls; in the other cases the sealing elements are made of asphaltic concrete. Whereas concrete core walls were among the first artificial sealing elements to be used in the construction of high dams [7], asphaltic concrete core walls were not developed until the second half of the previous century, thanks largely to work done by Strabag Bau AG of Cologne. As reported in [56] and [57], the German company retained the services of the Austrian Professor H. Breth as consulting engineer for the construction of the core diaphragm for the 30 m high Dhünntal Dam in 1961/62. In the first phase of construction in 1957, Dam no. 20 was sealed with a 15 m high asphaltic concrete membrane in the „b" position [49]. In this case, however, the asphaltic concrete was poured rather than placed and compacted in layers with machines developed for the purpose by the Strabag company [42]. The highest asphaltic concrete core in the „c" position was constructed for the 125 m high Storglomvatn Dam in Norway at the end of the 1990s. The world's highest asphaltic concrete core in the „b" position is to be found in Dam no. 15 (Finstertal), with a height of seal of 96 m. In the case of concrete core walls in the „c" position, the Tieton Dam in the USA achieved an impressive height of 97.5 m as early as 1923. As explained in section 5.1.1 below, development work done at the BFG Institute would permit concrete core diaphragms to be used for dam heights of well above 100 m. The slip layer needed to reduce negative skin friction at the concrete surface was tested successfully on Dam no. 17.

Dams nos. 1 and 6 were placed on thick overburden; in the case of the other four dams the sealing element is in direct contact with the bedrock, and the dam body is founded wholly or partly on bedrock. Unusual dam engineering solutions were adopted for Dam no. 1, with a concrete core founded on stiff and dense ground moraine, and Dam no. 6, which has an up to 52 m deep clay-concrete cutoff wall to provide a partial seal for an overburden that extends well beyond 100 m in depth [9]. The above mentioned Professor Breth was also the consultant for Dam no. 6 and as such provided the scientific basis for the design decisions taken and also pioneered the combination of a central asphaltic concrete core and a clay concrete cutoff wall to seal the foundations.

In the case of core diaphragms, filter or relief zones downstream from the sealing element and stiff shell zones are essential. It is also advantageous to provide a fine-grained zone upstream from the diaphragm as a second sealing element. The design should also provide for free drainage conditions in the upstream shell zone on rapid drawdown.

The main arguments for the use of core diaphragms rather than surface diaphragms relate to the reduced area of the sealing element and its location in the dam body where it is protected from weathering and mechanical damage. As will be shown in section 5.1.1, a high bearing capacity can be achieve with just the downstream dam body. In comparison with surface diaphragms, it is easier to tie in the core wall with the foundations in an area that is compressed by the weight of the fill and to achieve a sound connection to the foundation sealing works on steep slopes especially. The interior membrane seals in group A2 have also done good service to date.

4.2 Type B: embankment dams with earth cores

The core positions shown in Fig. 2/B represent the variants of this type of embankment dam. Earth sealing elements can extend to the upstream and downstream faces and can be continued with upstream sealing carpets. The Austrian dams of this type all have central cores - position a.

Earth cores are particularly suited to dams founded on overburden. As with Type A, the foundation sealing works can take the form of grout curtains, cutoff walls, thin diaphragm walls or pile walls. In the case of dams founded on overburden, toe weights and relief wells located downstream from the toe are typical additional measures.

Apart from the central position of the core, the four Austrian dams with earth cores to be seen in Fig. 5 all have their special features. The above-mentioned Professor Breth played a key role as consulting engineer for all earth core dams built in Austria. His theoretical and practical engineering contribution to Dam no. 2 (Freibach) included the introduction of advanced soil mechanics to Austrian embankment dam engineering. On the left slope, this dam connects to permeable colluvial and alluvial sediments. At the time of construction, Dam no. 4 (Gepatsch) was one of the world's highest earth core dams with a height of 153 m. It was the first dam in which the quarry-run rock for the shell zones was placed in layers and compacted using vibratory rollers. Dam no. 5 (Durlassboden) is founded on sediments up to 136 m deep

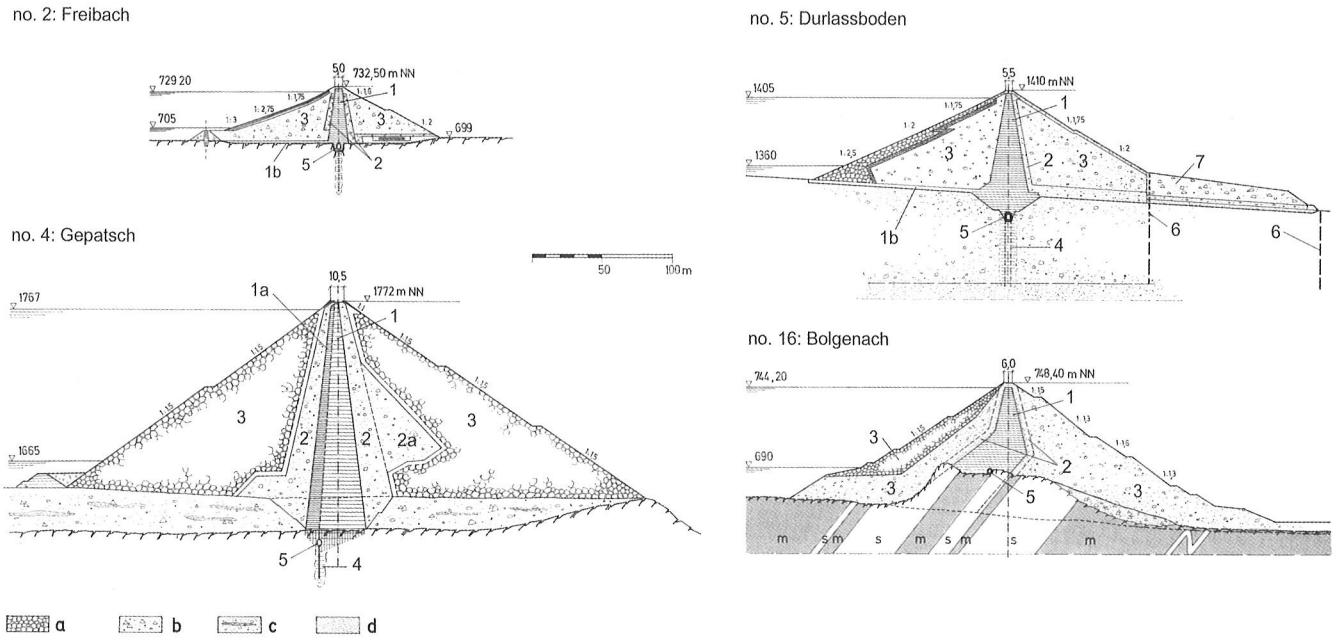

Fig. 5 *from [5]: Main sections of earthcore dams – Type ie*
(1) Earth core
(1a) Core with 1% bentonite
(1b) Seal carpet
(2) Transition zones
(2a) Extension of transition zone
(3) Shell zones
(4) Grout curtain
(5) Inspection gallery
(6) Relief wells
(7) Toe weight

a: Rockfill
b: Moraine/Talus material
c: Sediment mixed grained with sand lenses
d: Sediment fine grained
m: Marl
s: Sandstone

and ties in on the right embankment with a thick creeping slope. An unusual solution was also adopted for Dam no. 16 (Bolgenach), with its angled core dictated by dense strata of marl in the foundation contact area in a narrow valley with projecting ribs of sandstone.

Earth core dams always comprise a number of distinct zones. The core is flanked by upstream and downstream filter and transition zones followed by the external shell zones. They are designed for the decrease in piezometric level to be completed in the downstream filter zone. The embankment movements in the various zones should be as similar as possible so as to minimize load transfer between the zones. That constitutes one of the main problems in the construction of earth core dams, as the different requirements of the various zones can only be met through the use of different materials. Free drainage in the upstream shell zone on rapid drawdown is also required.

The main argument in support of earth cores is the use of natural impervious materials offering good stability with regard to long-term behavior. Stiff concrete core walls came to be considered unsuitable and were replaced by earth cores as a more adaptable solution. The scientific basis for the use of earth cores was supplied at the beginning of the 20th century by Professor Karl von Terzaghi, a citizen of the Austro-Hungarian Empire and founder of the new science of „soil mechanics on the basis of soil physics". His theory on the consolidation of fine-grained soils became the key to the reliable design of earth core dams. The highest dams constructed worldwide all have central earth cores. The 310 m high Nurek Dam in Central Asia, for example, has been in operation since 1980 [32].

5. Bearing behavior of embankment dams

Dam construction generates the greatest horizontal loads deriving from the works of man. The thrust of the impounded water behind a dam has a huge potential for destruction, which must be countered with a thorough knowledge of the processes involved in bearing behavior and a strong focus on safety. In addition to the hydrostatic load as the dominating external force, the deadweight of the fill materials and dynamic loads from seismic activity must also be transmitted safely to the foundations. In simplified terms, the earth mass of the dam body opposes the stored water of the reservoir [62].

In comparison with concrete dams, the hydrostatic load in a fill dam is contained by a much greater mass (e.g. five to eight times that of an arch dam). As a result, the dam foundation area is preloaded and support is provided for the abutments in particular. In addition, the loads are transferred to the foundations over a larger contact area, which is less stressful for the foundation. Load bearing in dams involves compressive stresses and shear stresses. Where differences in deformability occur in the dam, loads are transferred to stiffer zones.

In the case of embankment dams in wide valleys, load bearing takes place mainly by two-dimensional processes (2D) in the cross-section. In narrow valleys and gorges, however, major spatial bearing effects (3D) also occur.

As formulated in Topic 1 we shall first consider the bearing behavior of dams with membrane seals. **In general, the term „bearing behavior" is used in this report to describe all states of stress and strain in dam construction and operation until reversible (elastic) processes set in.** In addition to this static behavior, however, the term also includes all seepage and erosion processes and the processes involved in the decrease of the piezometric pressure.

5.1 Bearing behavior of embankment dams with membrane seals

5.1.1 Research results relating to 5.1

As mentioned in the preface, the BFG Institute had a main focus on the field of embankment dam research for over twenty years [1]. The various topics were addressed on a step by step basis in the form of theses and doctoral dissertations. Each paper treats a complete topic or chapter on a modular basis like the stones of a mosaic, which permitted the Innsbruck research project to be completed after a period of twenty years. The work was financed out of the institute's own funds, funds received from the Research Support Fund of Austrian Trade and Industry, and sponsorship provided by a number of hydro-electric companies.

As the basis of research, the program started with a series of investigations employing physical models [10]. This required the construction of a test box for plane strain model testing. Stress and strain analyses [22] were performed to verify the stresses measured in the models and to provide additional data on the calculated states of strain. In addition, finite-element based software developed for the purpose by Professor W. Swoboda at the University of Innsbruck was also used to verify data obtained from on-site monitoring at existing dams [22].

In an earlier paper [4], the author addresses the bearing behavior of dams with interior diaphragms. As stated in section 4.1, these sealing elements can be most easily distinguished in terms of their flexural rigidity $E \cdot 1/m = E \cdot d^3/12$ (E = modulus of elasticity, d = diaphragm thickness). The range of variation covers over ten decimals, from $1.6 \cdot 10^{-5}$ kN/m²/m for geomembranes to $5.4 \cdot 10^5$ kN/m²/m for a cement-concrete diaphragm. The location of the diaphragm in the dam is the dominant factor, as shown in a 2D diagrammatic view in Fig. 6. Although there is no difference between surface diaphragm A and central core wall B in load case (LC) I = deadweight in the case of the untensioned diaphragms assumed in Fig. 6, the differences are significant in LCII = top water level (AII and BII). In the case of BII, unlike the dam with the surface diaphragm, only the downstream half of the dam body

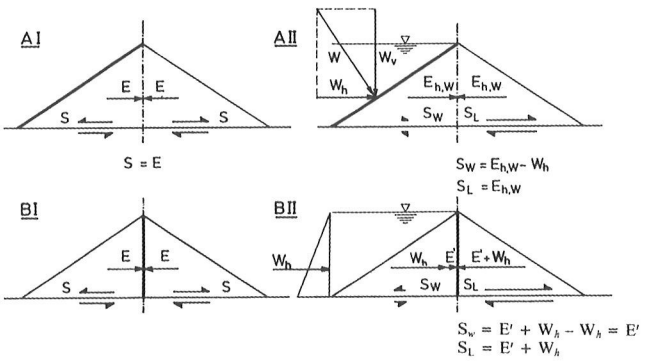

***Fig. 6** from [4]: Bearing effects*

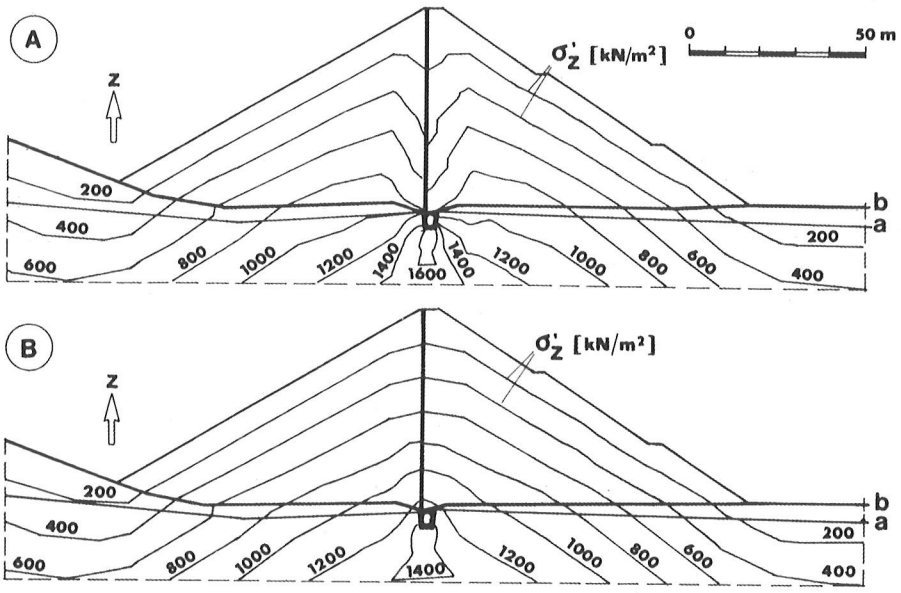

Fig. 7 *from [4] : σ_z – isobars LC deadweight for a 60 m high dam for comparison*
(A) Cement concrete core
(B) Asphaltic concrete core

plays a load-bearing role with regard to the hydrostatic load.

The model of a 60 m high dam with a central core wall in Fig. 7 illustrates the influence of skin friction on a concrete core. In the case of the untreated concrete core in Fig. 7/A, load is transferred from the fill to the core, whereas the asphaltic concrete core in Fig. 7/B cannot absorb any additional load.

Let us turn now to the 2D bearing behavior of a model dam. Figs. 8, 9 and 10 are taken from [4]. They illustrate the stress and strain conditions of a 1.3 m high dam with untensioned surface diaphragms and diaphragm walls. The calculations were performed with the help of FEM using the characteristic values listed in Table 3. In the figures, the measured stresses are compared with the results of the calculations. The data permit the following conclusions to be drawn.

Load case of deadweight for both diaphragm positions (Fig. 8)

Characteristic value	Unit	State of soil	
		Humid	Saturated (buoyancy)
Unit weight	kN/m³	γ = 25.86	(γ' = 19.36)
Poisson's ratio		μ = 0.254	μ = 0.286
Friction angle	degree	φ = 48°	φ' = 39°
Modulus of elasticity			
First loading I	kN/m²	E = 96.52 (σ' + 90)	E = 90.53 (σ' + 25)
Including creeping $I_{(k)}$	kN/m²	E = 62.0 (σ' + 110)	
Relief of load II	kN/m²		E = 452.65 (σ' + 25)
Saturation settlement	%	ε = 1 %	

Table 3 *from [4]: Characteristic values of soil for FEM calculation.*

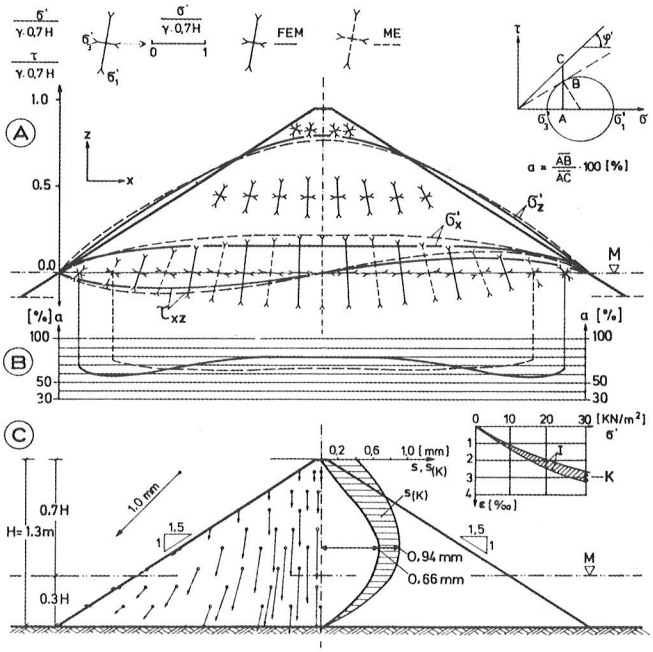

Fig 8 *from [4]: Model dam - LC deadweight*

- In view of the triangular shape of the dam body, load transfer occurs from the center of the dam to the embankments in the form of shear prestress in the shell zones.
- Material utilization varies between 58% and 80% of material strength.
- The dam body is subjected to rotating deformation from the inside to the outside, turning upstream on the right and downstream on the left, with uplift at the dam toes.

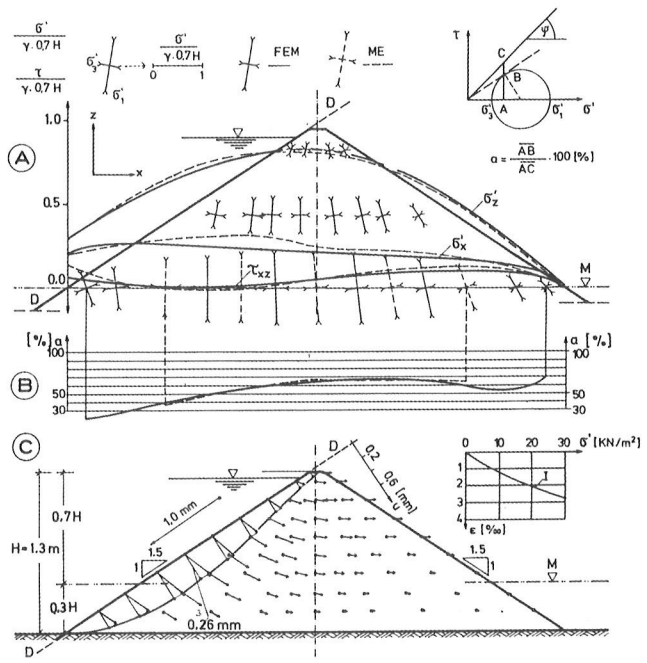

Fig. 9 *from [4]: Model dam - Surface diaphragm LC maximum reservoir level.*

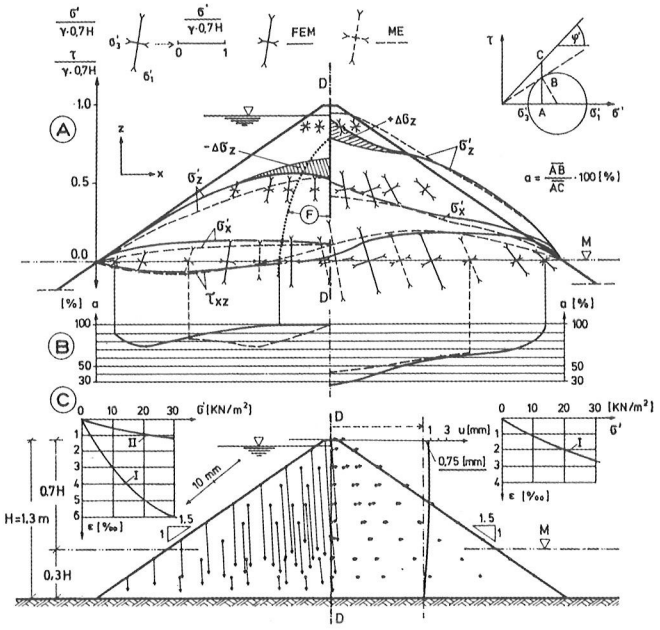

Fig. 10 *from [4]: Model dam - Core diaphragm LC maximum reservoir level.*

- The greatest settlements during fill placement occur at the middle levels, and the most pronounced post-construction settlements in the crest.

Load case of top water level - surface diaphragm (Fig. 9)

- The hydrostatic load is primarily absorbed in the upstream half of the dam.
- Material utilization in the upstream half of the dam is reduced at the measuring level to as little as 20% of material strength.
- The dam body is subjected to left-rotating deformation, with the vectors turning from roughly normal to the upstream diaphragm to approximately horizontal at the downstream embankment.
- The most pronounced movements in the upstream facing occur in the lowest third.

Load case of top water level - vertical diaphragm wall (Fig. 10)

- Saturation settlement in the upstream dam body is the cause of load transfer to the downstream body. Plastification of the upstream shell zone adjacent to the core occurs as a result of downstream deflection in the diaphragm.
- Material utilization in the downstream shell zone is reduced in the vicinity of the diaphragm to approx. 25% and increases towards the face to approx. 95%. In the crest, arching occurs with lower material utilization.
- The vectors of the downstream deformations are directed upwards in the vicinity of the core and right-rotating towards the dam faces (see also Fig. 33a).
- Pronounced saturation settlement in the upstream shell zone is due to the loose placement of the material in the model.

From this comparison of the two diaphragm positions it can be said that, in view of the low level of material utilization downstream from the diaphragms, they both offer significant reserve bearing capacities against the thrust of the impounded water. Agreement between the measured values and the calculations is satisfactory and the results appear logical.

Finally, when comparing the two diaphragm positions, it should be pointed out that the hydrostatic load is primarily absorbed via compressive stresses in the case of surface diaphragms and via shear stresses in the case of core walls (see Fig. 10a). As shown in Fig. 10b, the greater portion of shear deformation occurs in the lower half of the dam.

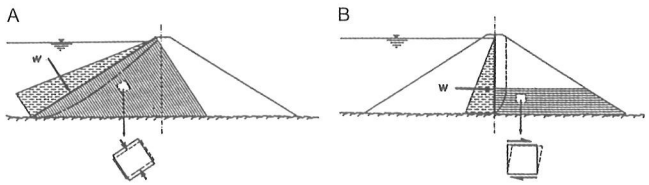

Fig. 10a *from [50]: Primary bearing behavior.*
(A) Surface diaphragm - mainly compression.
(B) Core diaphragm - mainly shear.

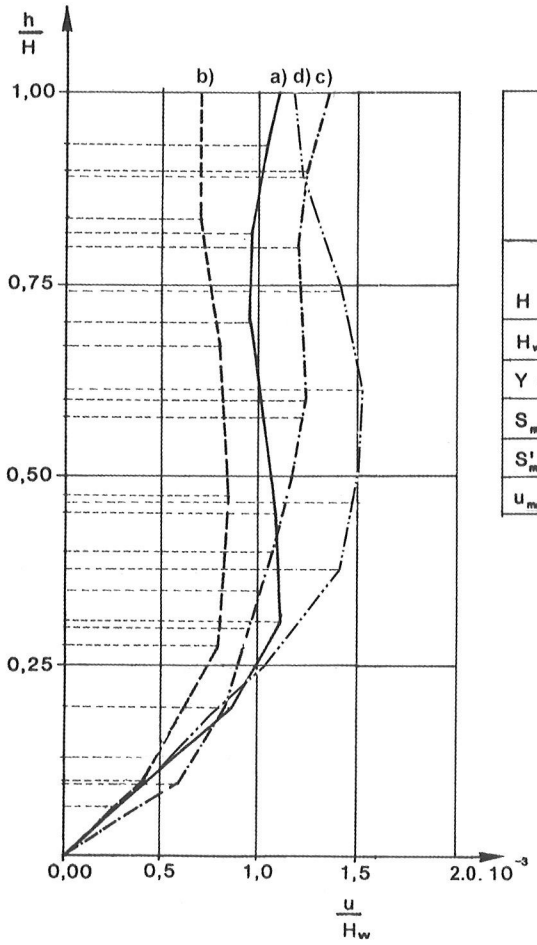

a ... Bockhardsee no. 17
b ... Neue Dhünn
c ... Finstertal no. 15
d ... Rotgüldensee no. 20

	a	b	c	d
H (m)	31	58	96	45
H_w (m)	28.5	54	93	42
Y of C	1982	1984	1981	1990
$S_{max.}$ (l/s)	0.02	0.23	4.2	0.1
$S'_{max.}$ (l/sm²)	$4.7 \cdot 10^{-6}$	$1.6 \cdot 10^{-5}$	$1.2 \cdot 10^{-4}$	$1.4 \cdot 10^{-4}$
$u_{max.}$ (cm)	3.8	4.6	14	6

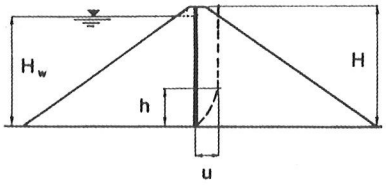

Fig. 10b *from [24]: Displacements of 4 dams with core diaphragm at LC max. reservoir level*
Y of C: Year of completion
S max: max. seepage
S'max: max seepage per m²

In order to also provide a qualitative insight into the three-dimensional supporting effects involved, small physical 2D and 3D models with a dam height of 45 cm were built and the downstream dam body loaded via an untensioned central diaphragm. As can be seen in Fig. 11, which is taken from [4], it was possible to increase the load to three, four and five times the hydrostatic load. The results show that the downstream movements in the diaphragm are significantly reduced as a result of spatial effects due to the ravine shape of the valley involved. These effects will be dealt with again in section 9 (Dam safety).

As a new development, a research project entitled „Concrete core diaphragm walls for high embankment dams" [14,21] was initiated to make the central concrete core wall, which had done such good service in many earlier dams, a viable solution for dams over 100 m high. The objective was to achieve crack-free results with unreinforced concrete paying due regard to the maximum permissible tensile and compressive stresses in the State I of concrete. In order to meet this requirement, a bitu-

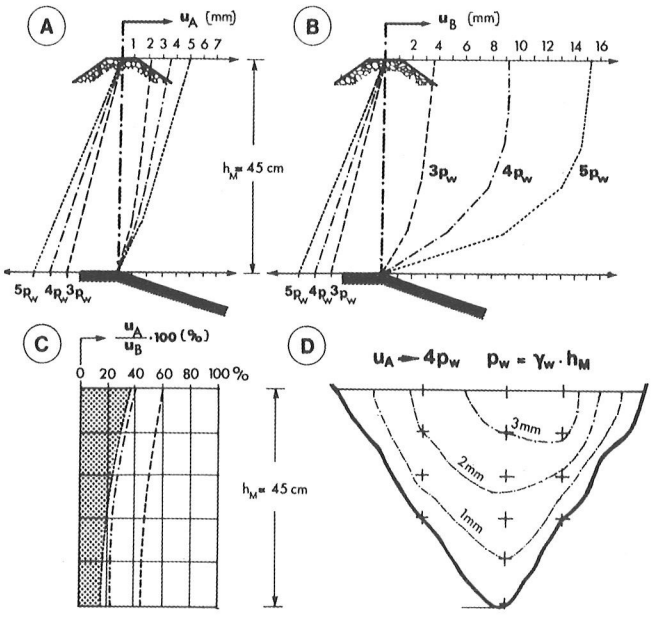

Fig. 11 *from [4]: Results of physical model tests*
A: Displacements of diaphragm u_A (3D model)
B: u_B – (2D model)
C: Reduction of u_B
D: Isolines of u_A

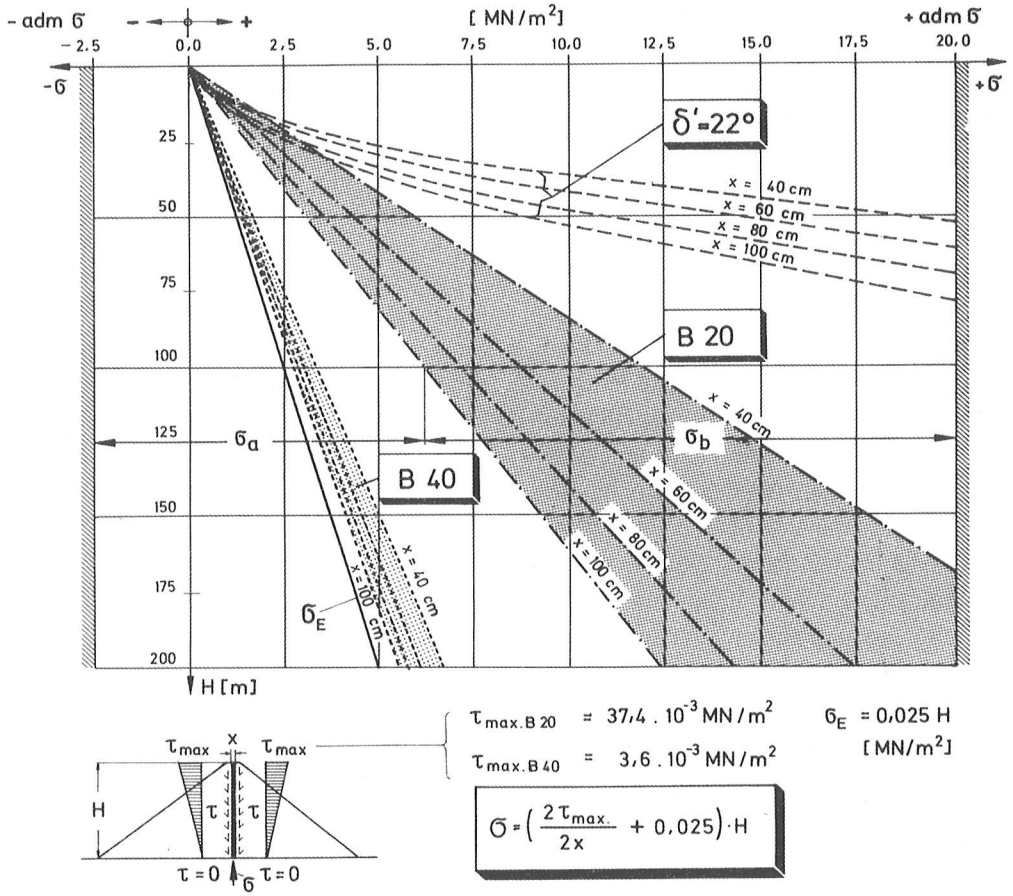

Fig 12 *from [14]: Normal stresses in the concrete core wall at dam height H, and variation of τ and x. B 20, B 40: Types of bitumen, σ_a, σ_b: Available stresses according to Fig. 13 and 14*

minous slip layer was developed to reduce skin friction.

As shown in Fig. 12, which is taken from [14], optimum choice of the type of bitumen for the slip layer permits central diaphragm walls to be built in over 200 m high dams. Without a slip layer, the compressive stresses in a 1.0 m thick concrete core reach limit values at a dam height of 80 m already. Depending on the individual situation, the slip layer can be applied in full or in part to either both core wall faces or just to the upstream face. The diagram in Fig. 12 only takes account of the

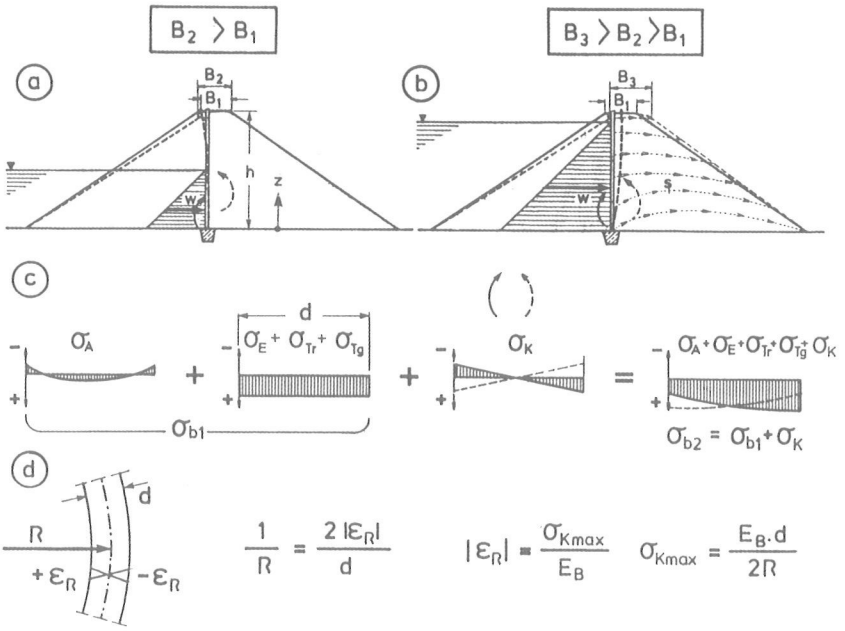

Fig 13 *from [15]: Displacements and stresses of the concrete core, for explanation see text.*

stresses deriving from deadweight and skin friction. Additional stresses are created, however, as a result of bending in the concrete core wall and the curing process. Fig. 13, which is taken from [15], takes account of all the stresses involved, namely σ_E (from deadweight), σ_A (from curing of the concrete), σ_{Tr} (from skin friction), σ_{Tg} (from the slip layer) and σ_K (from wall bending). Fig. 13 also illustrates the expected deformations in the dam in diagrammatic form. In addition to the initial settlements, Fig. 13/a also indicates settlements in the upstream shell zone as a result of partial filling. They cause the core wall to bend upstream and the crest to widen from B1 and B2. As top water level is reached, embankment movement occurs in the downstream shell zone in the downstream direction and the core wall moves with it, so that both upstream and downstream bending occur. A tilt movement is to be expected at the core wall footing without horizontal displacement. As mentioned above, the purpose of the exercise was to answer the question whether unreinforced concrete cores are capable of absorbing the resulting stresses without cracking and above all whether the concrete at the downstream core wall footing will spall as a result of excessive edge pressures.

Admissible bending in the concrete core wall at various thicknesses is presented in isolation in Fig. 14. Analysis of measured core wall bend demonstrated that maximum permissible bending is not exceeded in the case of stiff shell zones. In addition, concrete flaking at the downstream core wall footing is prevented by the above mentioned upward movements (convex path - see Figs. 10 and 33a) in the downstream shell zone in the passive load condition. [21] contains design charts for core heights of up to 200 m, which were developed on the basis of large-scale tests. Fig. 15 indicates the experimental set-up, while Fig. 16 shows the process of applying the bituminous slip layer to the core wall. The bituminous layer is bonded to a fabric protection layer and delivered in rolls. The bitumen is heated with a torch until bonding temperature is reached. Compression of a 10 cm thick layer of expanded polystyrene placed beneath the experimental fill permitted major shear displace-

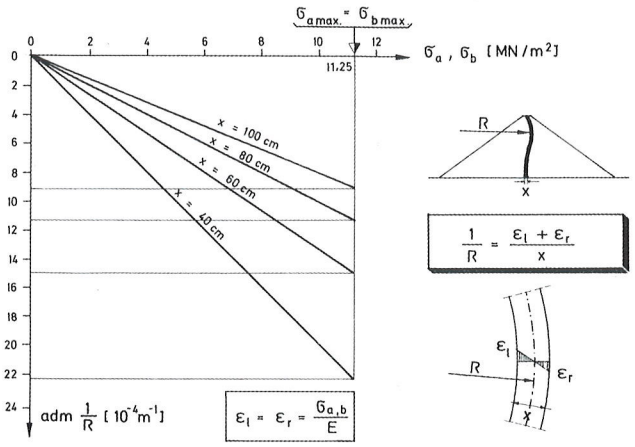

Fig. 14 *from [14]: Admissible values of wall bend (adm 1/R) at varying wall thickness x.*

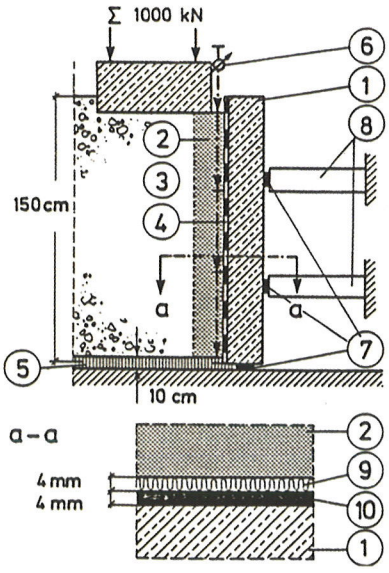

Fig. 15 *from [9, 43]: Large-scale tests for developing the bituminous slip layer.*
1: Tested concrete wall
2: Sand layer
3: Gravel fill
4: Slip layer
5: Polystyrene
6: Settlement gauges
7: Pressure cells
8: Steel support
9: Protection fleece
10: Bitumen layer

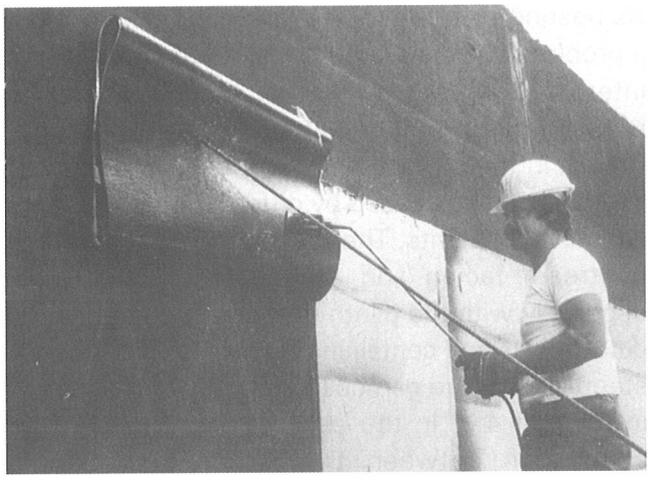

Fig. 16 *from [15]: Application of the bituminous slip layer.*

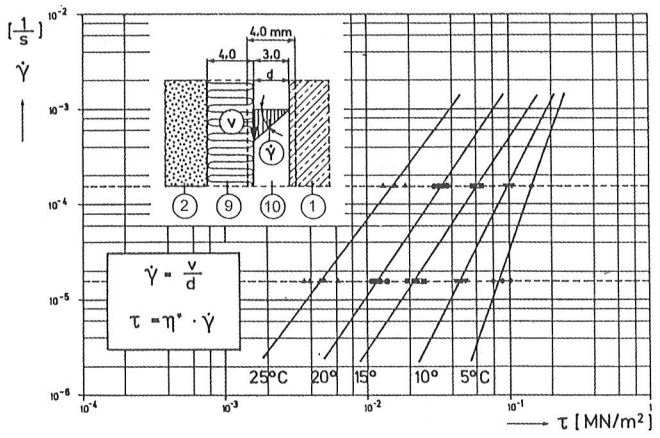

Fig. 17 *from [43]: Creep curves of slip layer (see Fig. 15)*

ments to be produced in the bituminous layer. One of the results of the project was a set of flow curves for the various bitumen hardness grades and test temperatures. These flow curves (Fig. 17) can be used to read off the sliding resistance of the bituminous layer for various displacement velocities.

The research into „Concrete core diaphragm walls for high embankment dams" closed with an investigation into the influence of different degrees of sliding resistance at the core wall faces in the case of an 80 m high dam [24]. A comparison of the core walls with and without slip layers based on stress and strain analysis permitted the following conclusions to be drawn:

- One effect of the two slip layers applied as proposed in [21] is to reduce contact stresses at the core wall footing at the end of the construction period from 25.2 MN/m² to 3.9MN/m², i.e. by 84.5%!

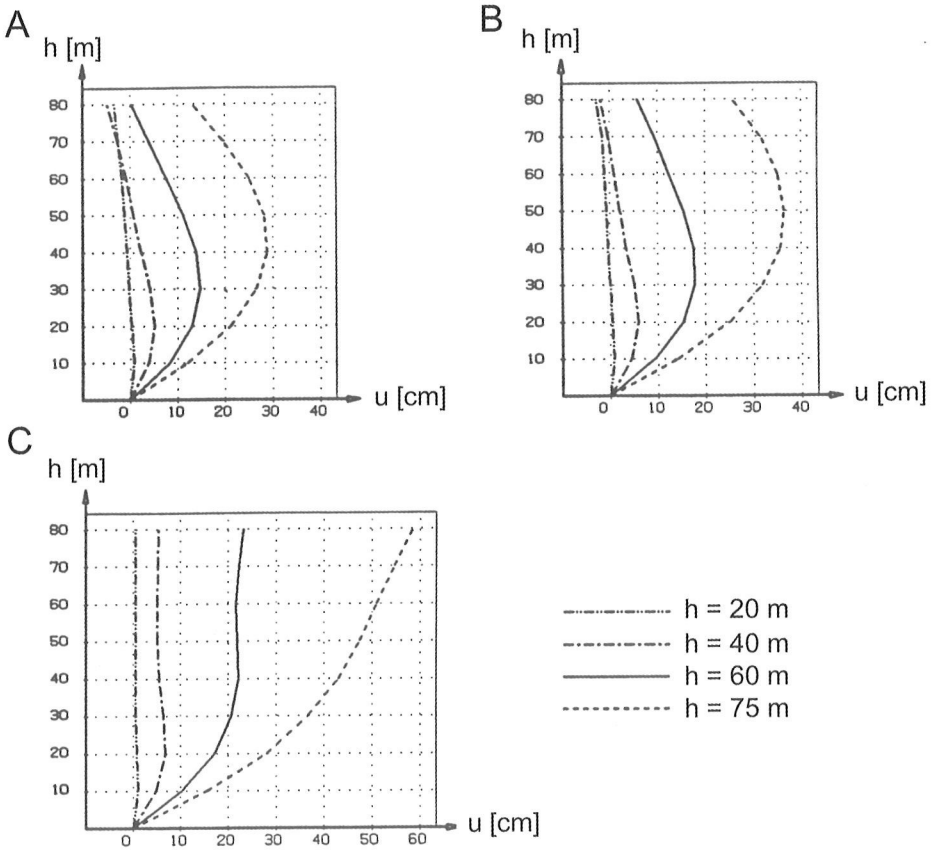

Fig. 18 *from [24]: Research dam of 80 m height (see Fig. 41) Horizontal displacements of the cement concrete core at partial and full reservoir level h*

A: Wall surface rough
B: Slip layer on both sides
C: Completely smooth

- Another effect at the end of the construction period is to increase earth pressure and thus shear prestress in the shell zones by 35.5 %. Settlements in the shell zones along the core wall faces increase at 40 % of wall height by 50 %, from 20 cm to 30 cm.
- As can be seen in Fig. 18, the use of slip layers leads to an increase in horizontal crest deflection but a slight decrease in wall bending. Maximum horizontal crest deflection increases by 24 %, from 29 cm to 36 cm, while bending (as defined in 1/R) decreases slight from 2.7 . $10^{-4}m^{-1}$ to 2.6 . $10^{-4}m^{-1}$. According to Fig. 14, they are therefore in the admissible range for 1 m thick walls, too.
- In either case, no horizontal displacement occurs at the wall footing.
- On impounding, as mentioned above, the upward movements in the downstream shell zone reduce the contact stresses at the core wall footing. This effect is dealt with below with reference to Dam no. 17.

5.1.2 Bearing behavior of Austrian embankment dams with membrane seals

Group A1: dams with surface membranes

Bearing behavior can be assessed on the basis of deformations of the dam body and seepage flows.

As bearing capacity for the hydrostatic load is not a problem with this type of dam, we are primarily interested in the capacity of the diaphragm to respond to deformation strains without cracking. Cracks in the surface diaphragm and consequent seepage can be caused by differential settlements and displacements. The connections between the upstream facing and the concrete structures, especially with the plinth (frequently connected to cutoff walls and containing inspection galleries) on steep slopes, are particularly at risk. As mentioned in section 4.1, in the case of Dam no. 12, the connection between the facing and a steep abutment required extensive remedial works to obtain a reliable seal [6].

As the surface diaphragm ties in with the foundations at the upstream toe of the dam, there is no overload from the dam fill. Even with appropriate anchorage for the concrete structures (cutoff walls or inspection galleries), therefore, grouting in the contact area is only possible at low pressures (up to 3 bar). This disadvantage is particularly acute on steep slopes, which may have been loosened by valley erosion and subsequent stress relief.

The above mentioned blistering in the upstream facing caused by vapor pressure in a number of dams does not lead to the formation of continuous cracks and thus does not cause seepage. The fact that all Austrian reservoirs have bottom outlets for complete drawdown facilitates monitoring and remedial work on upstream facings.

Dam no. 11: Oscheniksee

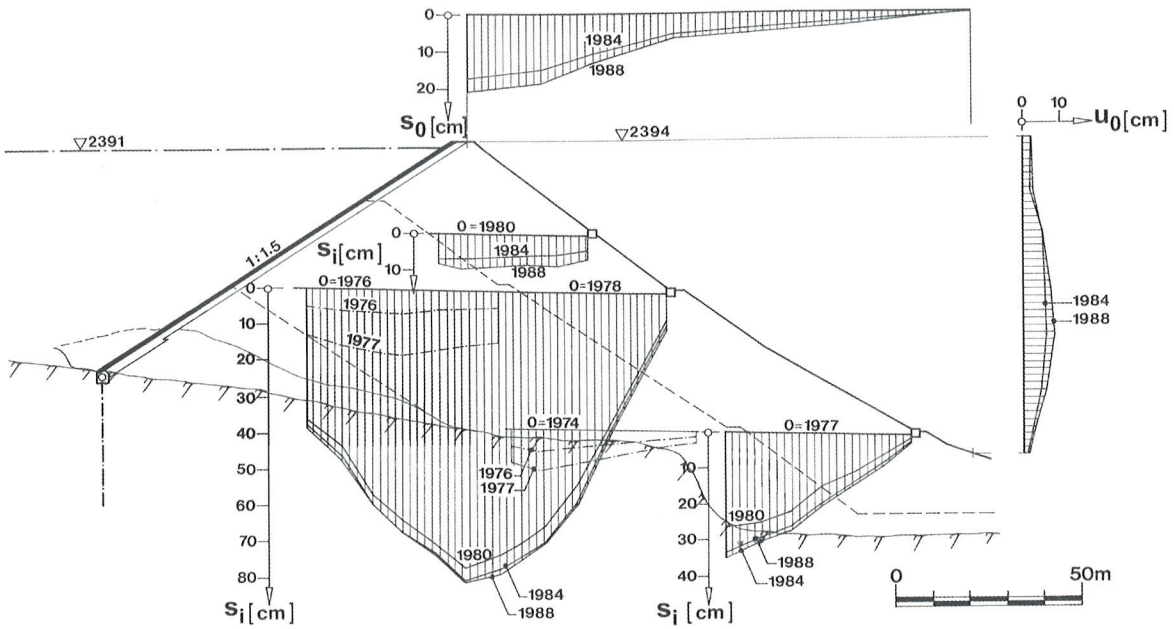

Fig. 19 *from [9]: Dam no. 11*
Settlement and horizontal displacements at different times

s_i: Interior settlements
s_o: Surface settlements
u_o: Surface horizontal displacements

This dam is the outstanding Austrian example of its type, with a height of seal of 61m and a dam height of 116 m from the downstream toe. The dam has been raised three times, and the facing from the first stage of construction reinforced to a final thickness of 20 cm. Fig. 19, which is taken from [9], shows the measured settlements and displacements in the various stages of construction. It is interesting to see that, following initial settlements up to a maximum of approx. 85 cm at the center of the dam, the deformations in the dam body, which comprises talus and quarry-run rock material, largely stabilized in just a few years.

Group A2: dams with core membranes

As can be inferred from section 5.1.1, the bearing behavior of dams with core membranes must be seen as a complex process involving the interaction of three main elements: the upstream shell, the downstream shell and the core. The upstream shell serves to support the sealing element, and it must also remain stable on rapid drawdown. The sealing element is designed to respond to movements in the dam without cracking and to withstand seepage without suffering erosion. It must also have adequate material strength. The downstream shell zone has to be capable of absorbing the deadweight of the dam, the earth pressure from the upstream shell zone and the hydrostatic pressure in the foundations. At the contact with the core wall, it also serves to drain the seepage and filter out the solids. All these functions must also be fulfilled in the presence of seismic activity.

Dam no. 1: Bielerdamm

Built in 1948, this concrete core dam - with a core height of 25 m - is founded on a ground moraine over 60 m deep. The core is built of reinforced concrete elements 18 m in length and 3 m in height, with the contraction joints sealed with copper sheet and asphalt. Core thickness decreases from 2.0 m at the base to 0.6 m at the crest. The core extends downward into a cutoff wall and upward into an upstream parapet wall. Shafts were incorporated for visual inspection of the forty vertical core joints, with wire pendulums installed in three of them. After 54 years of operation, there are no settlements at the top of the core and maximum downstream horizontal displacements of only 3 cm. Their elastic range between high and low reservoir levels is approx. 0.5 cm. Seepage from the 10,000 m² of diaphragm totaling approx. 3l/sec at top water level is channeled in sections to four gauging weirs. Impounding has not caused any springs to emerge downstream of the dam. Decrease of the piezometric pressure in the foundations is not measured [33b].

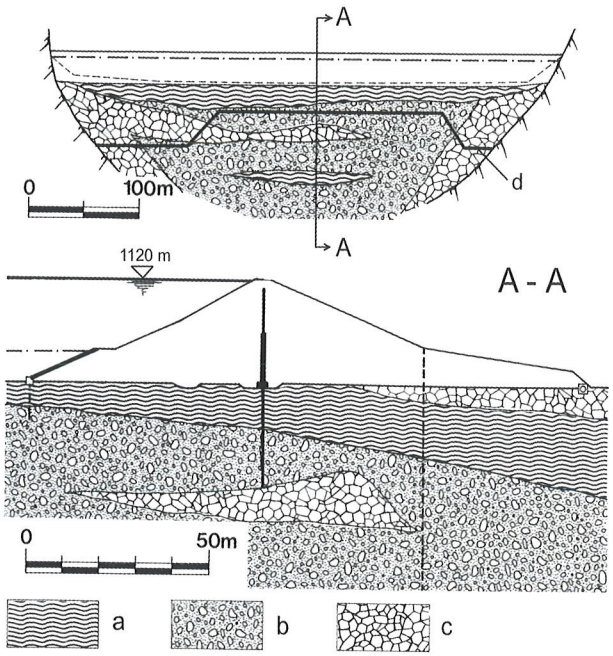

Fig. 20 *from [9]: Dam no. 6 Geology*

a: Silt and sand
b: Sand and gravel
c: Talus material
d: Boundary of cut-off wall

Dam no. 6: Eberlaste

Completed in 1968, Eberlaste was the first dam to be built in Austria with a central asphaltic concrete core [36]. As mentioned above, the innovative character of the solution related primarily to the construction of the asphaltic concrete core on highly compressible foundations comprising heterogeneous sediments and talus materials extending to a depth of well over 100 m. Fig. 20 shows the foundation geology and Fig. 21 the grain gradation curves for the individual foundation zones. As a logical solution, the foundations were sealed with a clay concrete cutoff. The lower limit of the cutoff is marked in Fig. 20. In the particularly permeable zones of talus material at the foot of the valley flanks, it reaches a maximum depth of 52 m and is 60 cm thick. According to the report in [34], monitoring of the two sealing elements on completion of the construction works showed maximum abso-

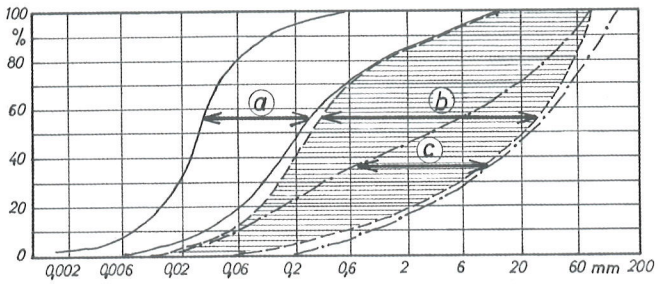

Fig. 21 *from [33]: Dam no. 6*
Grain graduation curves of the different zones of deposits in the foundation; a, b and c, see Fig. 20

lute settlements of 2.2 m and maximum relative settlements of 1.8 m over a length of only 35 m. In the dam's 34 years of operation, settlement has continued, reaching a maximum of 2.7 m. Downstream crest deflection to date shows a maximum of approx. 16 cm and has now reached a largely elastic state with 2.5 cm fluctuation. The main problem encountered was seepage through the foundations. According to [33] and [34], extensive investigations performed with the help of electric and hydraulic models showed that foundation seepage water flows could be brought under control through structural measures such as an asphaltic concrete membrane on the downstream foundation contact area (zone 7 in Fig. 4) and relief wells at the downstream toe of the dam (no. 4 in Fig. 4). As a result of the fine-grained layers near the surface in the middle of the valley, and the deep clay concrete cutoff at the valley flanks, a decrease in piezometric pressure of approx. 57 % of full water pressure has occurred according to [33a] in the deep permeable layer immediately downstream from the core wall. The relief wells further reduce the pressures in the deep layer to a safe 20 % of full water pressure at the end of the toe weight. Suspended solids measured in the seepage waters vary considerably but are generally in the range of the suspended load of the impounded water, i.e. a maximum of 5 mg/lt. After five years of operation, seepage losses rose by 50 l/s and the piezometric levels in the right half of the dam also increased. The remedial works required are described in section 8.2 of this report. Since completion of the remedial works, measurable seepage has returned to the original level, i.e. a maximum of 125 l/s. In 1998, after 32 years of operation, a relief well had to be replaced due to a fractured filter pipe.

Dam no. 15: Finstertal

With a height of seal of 96 m, the Finstertal Dam - as mentioned in section 4.1 - is one of the highest dams ever built with an asphaltic concrete core wall. The design of the dam was innovative insofar as the core membrane, which is 70 cm thick at the base and 50 cm thick at the crest, was placed with an inclination of 1 (vertical) to 0.4 (horizontal) by successively staggering the 25 cm layers. The core membrane was thus located at a distance from the center of the dam and thus from the zone where the highest levels of transverse strain occur during construction. Core wall deformations are monitored with the help of the magnetic deformation gauge shown in Fig. 22, which was also an innovation in that the system is installed without mechanical penetration of the asphaltic concrete core. The gau-

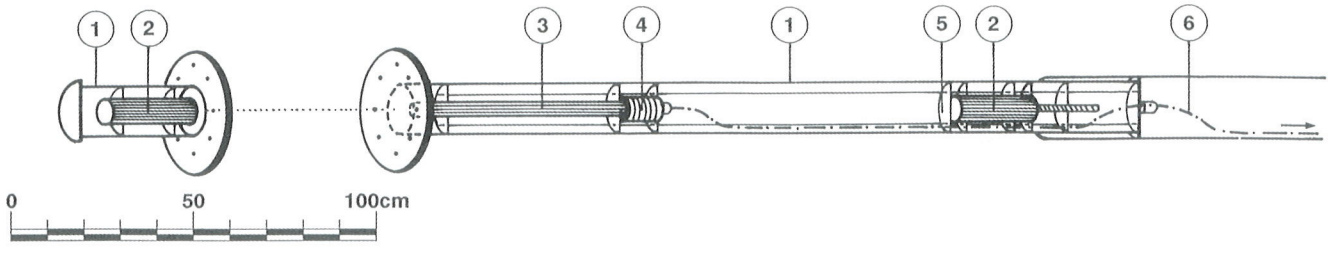

Fig. 22 *from [9]: Dam no. 15*
Magnetic measuring device for asphaltic concrete core wall deformations.

(1) Antimagnetic tube of stainless steel.
(2) Permanent alnico magnet.
(3) Probe for measuring variations in the magnetic field.
(4) Temperature measurement.
(5) Teflon rings.
(6) Measuring cable with 12 cores.

ge was developed by the physicist Professor F. Brandstätter of the University of Innsbruck, who also oversaw the installation process and evaluated the recorded data. As can be seen from Fig. 23,

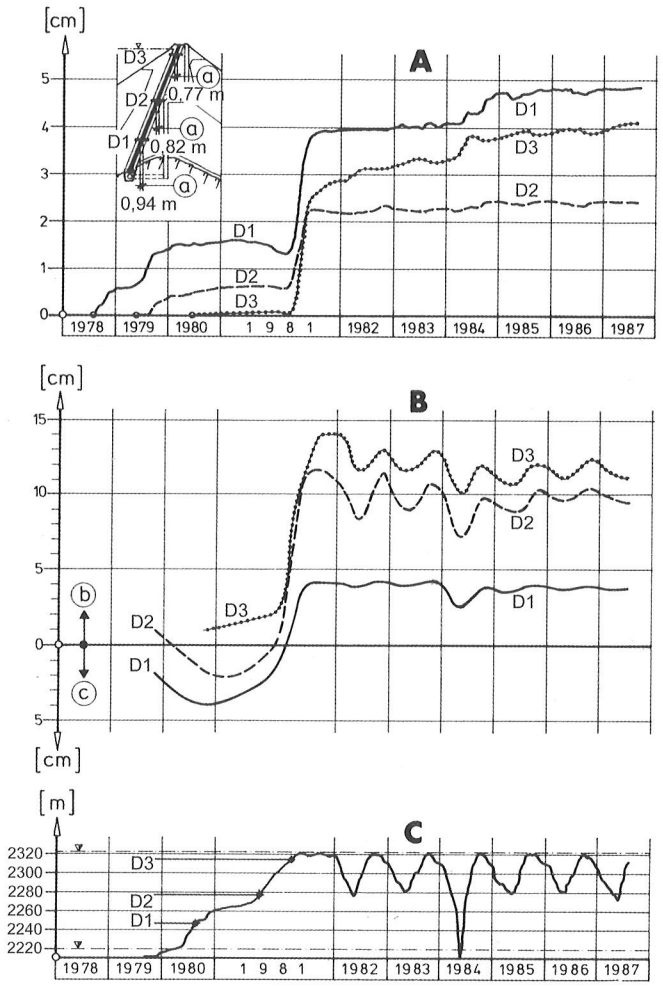

Fig. 23 *from [39]: Dam no. 15*
Observed widening of the asphaltic concrete core wall.
(A) Development of horizontal widening at D1, D2, D3
(B) Development of horizontal displacement of the downstream face of the core wall at D1, D2, D3
(C) Variation of reservoir level
(a) Reference length (distance between the plates of the thickness measuring device).
(b) Displacements towards downstream.
(c) Displacements towards upstream.

the deformation gauge was installed at three levels, with gauge lengths of 77 cm (D3), 82 cm (D2) and 94 cm (D1). At D3 the data obtained with the magnetic system are additionally monitored from the upstream and downstream faces using extensometers. In view of the good agreement obtained between the two independent systems [40], it can be assumed that D1 and D2 also provide reliable data. Based on these redundant measurements, the behavior of the asphaltic concrete core can therefore be described as follows:

- As shown in Fig. 23/A, core widening was detected at D1 and D2 during the construction period up to 1980, namely 1.8 % of gauge length at D1 and 0.9 % at D2. The horizontal upstream displacements measured at the downstream face of the core membrane with the help of extensometers from the plumb-line shaft (Fig. 23/B) were approx. 4 cm at D1 and 2.5 cm at D2.
- Maximum core widening was observed at first full reservoir level in 1981 simultaneously with downstream core displacement. Whereas core widening at D1 and D2 stabilized in the following two years of operation up to 1983, a further increase was observed at D3. A significant increase in core widening occurred at D1 and D3 on complete drawdown in 1984. This was followed by more or less complete stabilization at all three monitoring levels in the following years of impounding up to 1987. In 1987 core widening at D1 was approx. 4.8 cm = 5.2 %, at D2 2.3 cm = 2.8 % and at D3 4.1 cm = 5.3 %. Downstream core displacements decreased continuously up to 1987, approaching elastic behavior with reversible displacements of approx. 2 cm between high and low water levels following a maximum displacement of 14 cm at D3 after first filling in 1981. Fig. 24 shows measured horizontal displacements at three points 3.8 m upstream from the core wall and at three points on the downstream core face for levels D1, D2 and D3 at first filling in 1981 and complete drawdown in 1984. The following relative displacements can thus be derived:

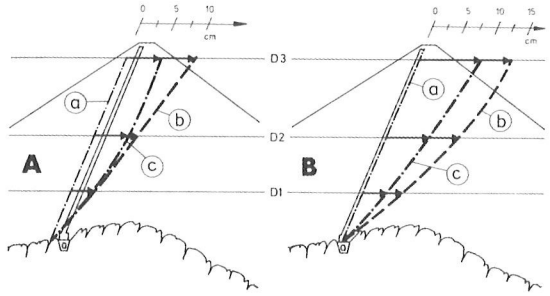

Fig. 24 *from [39]: Dam no. 15*
(A) Horizontal displacements of the upstream transition zone.
(B) Horizontal displacement of the downstream face of the core wall.
(a) Reference line.
(b) Maximum storage, 1981.
(c) Complete drawdown, 1984.

	Relative displacement		Core widening	
Level	First filling 1981 (cm)	Drawdown 1984 (cm)	First filling 1981 (cm)	Drawdown 1984 (cm)
D1	2.8	0.3	4.0	4.8
D2	5.2	1.4	2.2	2.3
D3	3.8	4.7	2.8	4.1

A comparison between relative displacements and core widening shows that the latter was higher at D1, lower at D3, and in the case of D2 lower in 1981 and higher in 1984. It can therefore be concluded that the core must have caused compaction in the upstream transition zone at D1 in 1981 and 1984, and at D2 in 1984, whereas there was still loosening at D2 in 1981 and at D3 in 1981 and 1984.

- Fig. 25 gives the data for core seepage. From an initial volume of approx. 9.2 l/s, seepage decreased by over 50 % to approx. 4.2 l/s through self-sealing after six years of reservoir operation. For a total core area of 37.000 m^2, seepage is therefore 1.1 . 10^{-4} l/sm^2.

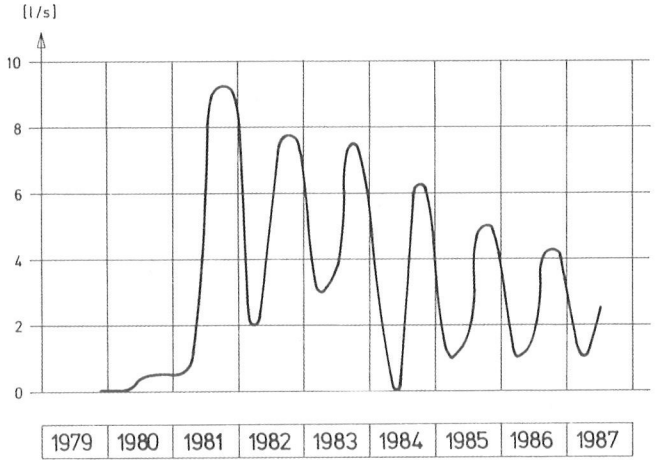

Fig. 25 *from [39]: Dam no. 15*
Seepage through the asphaltic concrete core

The deformation behavior of the dam in the maximum cross-section is presented in Figs. 26 and 27 in the form of isolines of settlement and horizontal displacement. Due to the ridge shape of the foundation rock, the maximum values lie outside of the central zone in both cases. For a dam of this height, the observed deformations were extremely slight. It can be seen that first complete drawdown in 1984 (d) led to a 60 % increase in settlement in the upstream shell zone, from 25 cm to 40 cm, as a result of saturation and downstream displacement of the core membrane, and that the 0-line of horizontal displacement shifted under impounding from downstream of the core at the end of construction to well into the upstream shell zone.

The isolines of measured settlements and horizontal displacements in Fig. 28 reflect dam deformation behavior in a longitudinal section. The influence of the shape of the bedrock is clearly reflected in the pattern of horizontal displacements.

A stress and strain analysis performed using FEM

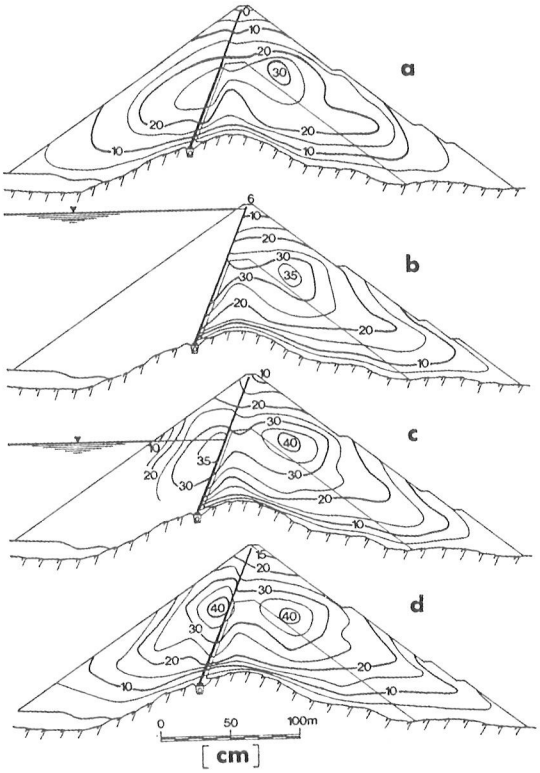

Fig. 26 *from [41]: Dam no. 15*
Settlements of the central cross-section.
(a) End of construction, 1980.
(b) First impounding to maximum storage level, 1981.
(c) Partial drawdown, 1983.
(d) First complete drawdown, 1984.

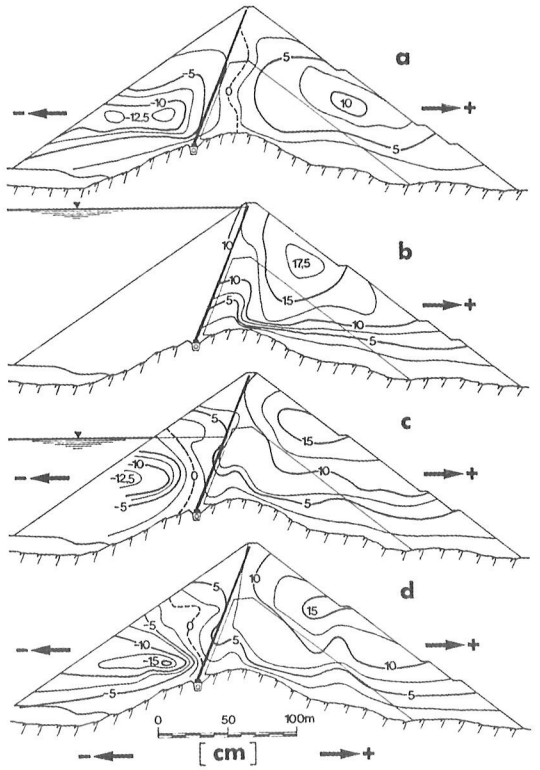

Fig. 27 *from [41]: Dam no. 15*
Horizontal displacement of the central cross-section.
(a) End of construction, 1980.
(b) First impounding to maximum storage level, 1981.
(c) Partial drawdown, 1983.
d) First complete drawdown, 1984.

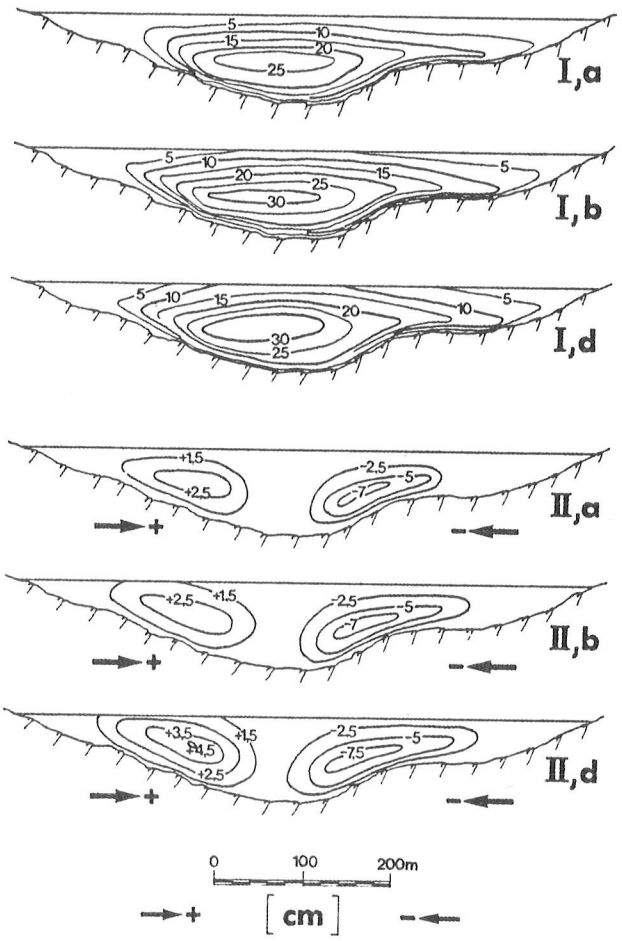

Fig. 28 *from [41]: Dam no. 15*
Deformations along the longitudinal section of the dam.
I) Settlements.
II) Horizontal displacements.
(a) End of construction, 1980.
(b) First impounding to maximum storage level, 1981.
d) First complete drawdown, 1984.

was in good agreement with measured bearing behavior [22]. On the basis of these results the following conclusions can be drawn:

- In the construction phase, the convex shape of the bedrock led to significant transverse deformations in the lower levels of the dam. These deformations possibly contributed to the measured widening in the asphaltic concrete core.
- First filling in 1981 led to downstream deflection in the asphaltic concrete core. The movement was not followed by the upstream shell zone, which was relaxed as a result of uplift pressure. This relaxed space permitted core widening to take a number of forms. At the lower level of the dam (D1), core widening probably caused compaction of the loosened upstream transition zone. At the highest level (D3) there was still expansion space in spite of the considerable degree of core widening, presumably as a result of upstream relief movements. Given the high shear strength of the construction materials, vertical cracks could be as deep as 10 to 30 m. The middle level (D2) was probably subjected to slight loosening upstream of the core in 1981 and slight compaction in 1984.
- In view of the pattern of seepage flows, the decisive question whether the measured widening in the asphaltic concrete core (if it occurred at all) was detrimental to the effective functioning of the seal can definitely be answered in the negative, although the mechanism of the decrease of piezometric level with core seepage remains unknown.
- The above mentioned analyses [22] confirm that a plastic state has developed in the upstream transition zone (see Fig. 28a).
- It is reasonable to assume that the asphaltic con-

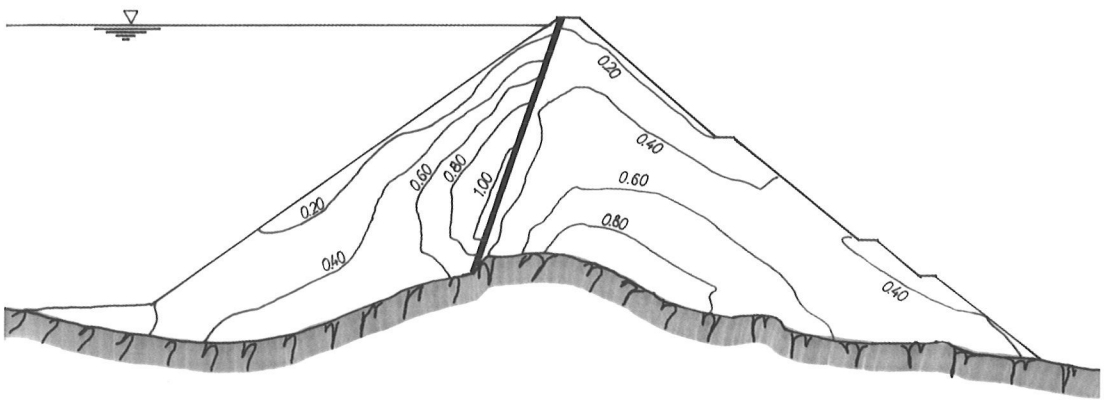

Fig. 28a *from [22]: Dam no. 15*
FEM calculations
Isobars of material utilization at LC full reservoir level

Dam no. 17: Bockhartsee

crete connects to the downstream shell zone without relative displacements. At constant volume deformation, 1 cm of core widening would be enough to induce well over 1 m (!) of settlement at the crest of the core. The magnetic deformation gauges can also be used to measure relative displacements in the core, but none in fact occurred. The core must therefore be connected to the downstream shell zone without permitting shearing. The relative settlements resulting from impounding presumably therefore only occurred in the plastic transition zone located upstream from the core (see Fig. 28a).

It was a felicitous coincidence that the research project into the reduction of skin friction with cement-concrete core membranes [21] was completed as work on this dam began. With the help of Chief Engineer H. Neururer and the approval of the Austrian supervisory authority, the original plan for a 31 m high asphaltic concrete core was replaced with a 60 cm thick cement-concrete core with the newly developed bitumen slip layer applied to the upstream face only. Fig. 29 shows the design of the core with the sealing types used for the core wall elements, which are 7.5 m long and 4.3 m high.

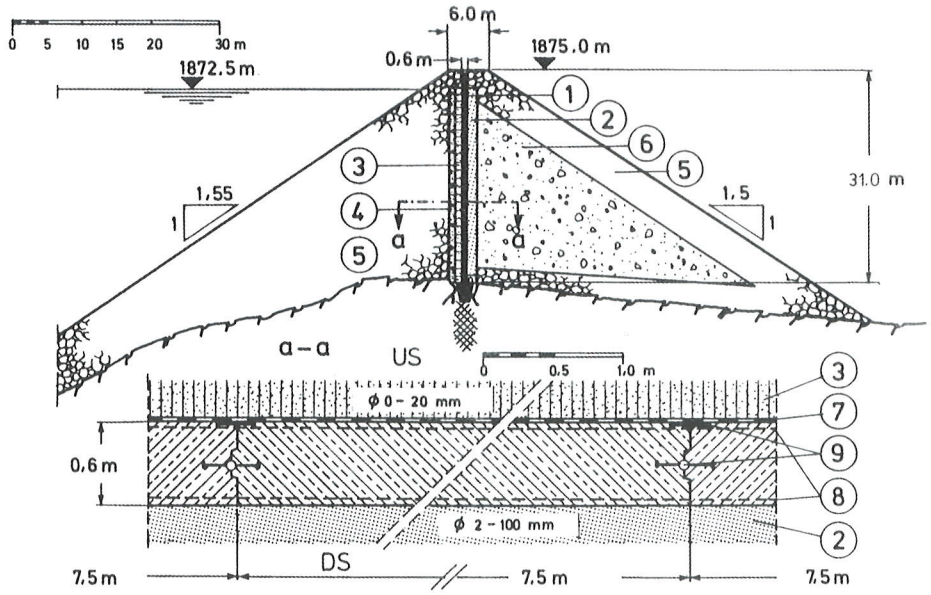

1) Concrete core wall.
2) Drainage zone.
3) Fine grained zone.
4) Transition zone.
5) Rockfill (max. diameter = 1.0 m).
6) Moraine (max. diameter = 1.0 m).
7) Slip layer.
8) Skin reinforcement.
9) Waterstop
US/DS – Upstream/Downstream.

Fig. 29 *from [15]: Dam no. 17 Main cross-section.*

The surveillance equipment installed in the dam served primarily to monitor the following aspects:

- the effectiveness of the slip layer, and
- deformations of the concrete core.

With regard to the slip layer, Fig. 30 shows the vertical pressures σ_{b1M} in the concrete core dam during the construction phase. The stress measured at elevation 1845.70 m is comprised of σ_E = deadweight of the concrete, σ_{Tr} = skin friction downstream and σ_{Tg} = stress deriving from the shear load of the 3 mm thick upstream slip layer of B95/25 bitumen.

Calculations in [15] show that σ_{Tg} is only approx. 50% of σ_{Tr}. According to [21], the use of a softer type of bitumen would have reduced σ_{Tg} to as much as 90% von σ_{Tr}. The curve for σ_{b1M} shows that the stresses decreased during the interruptions in filling operations Δt_2 as a result of relaxation in the bitumen. These results again confirm the effectiveness of the slip layer.

The question of deformations of the concrete core is addressed in Fig. 31. Diagram A shows the vectors of movement of gauge points in the contact zones of the concrete core. As a result of downstream deflection of the core and saturation settlements, settlements occurred upstream of the core until 9.6.1986, increasing from the base to the crest up to a maximum of 35 cm. Downstream of the core, settlements for the same period were only 5 cm. Thirteen years later, in 1999, the upstream settlements had reached 45 cm compared with 8 cm downstream. Diagram B shows the horizontal movement of the core wall as measured with a plumb-line in the third year of reservoir filling to top water level on 9.6.1986. The main displacements of approx. 3.2 cm occurred in the lowest third of the core. At the base of the core wall, twisting occurred without horizontal displacement. The plastic displacements increased by a further 0.5 cm approximately by 1999.

In Fig. 32, movements at three core wall measuring points (plumb-line nos. 1, 4 and 7) are plotted along the time axis. The curves indicate more or

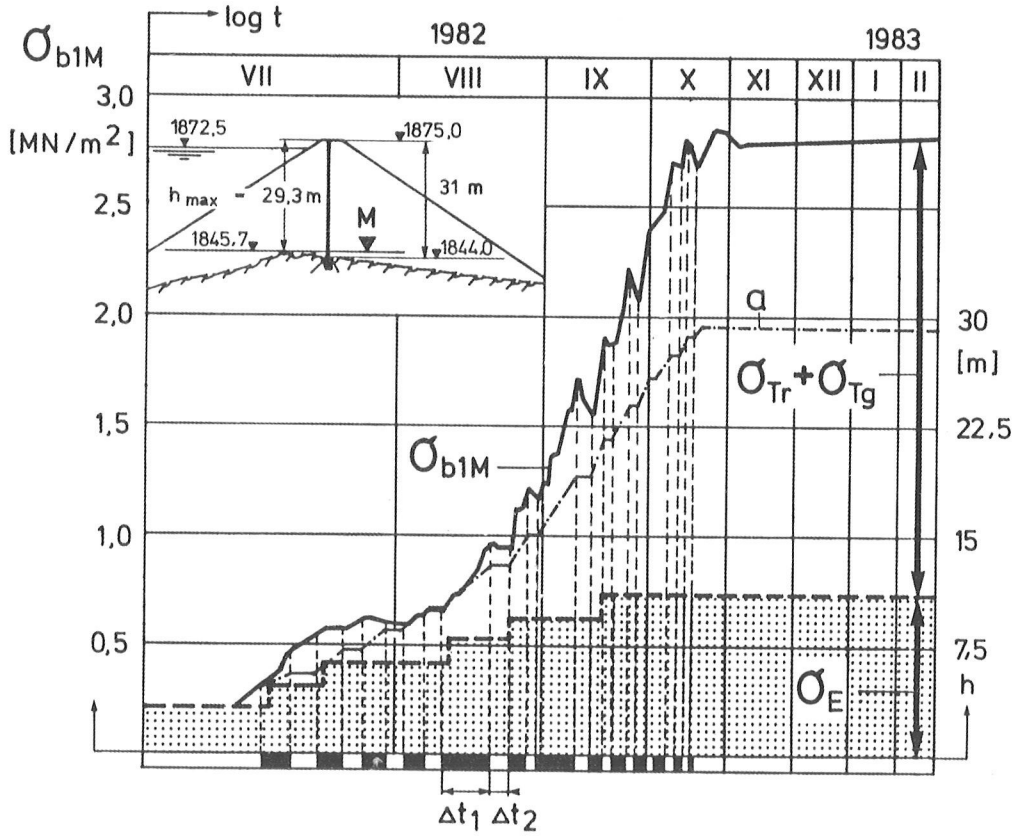

σ_{b1M} *Value of measurements (average of 4 gauges)*
σ_E, σ_{Tg}, σ_{Tr} *... are explained in the text*
M ... Measuring level
t ... Time
Δt_1 *Periods of fill*
Δt_2 *... Periods of interruption*
a ... Fill progress

Fig. 30 *from [15]: Dam no. 17*
Results for stress measurements during construction of the concrete core .

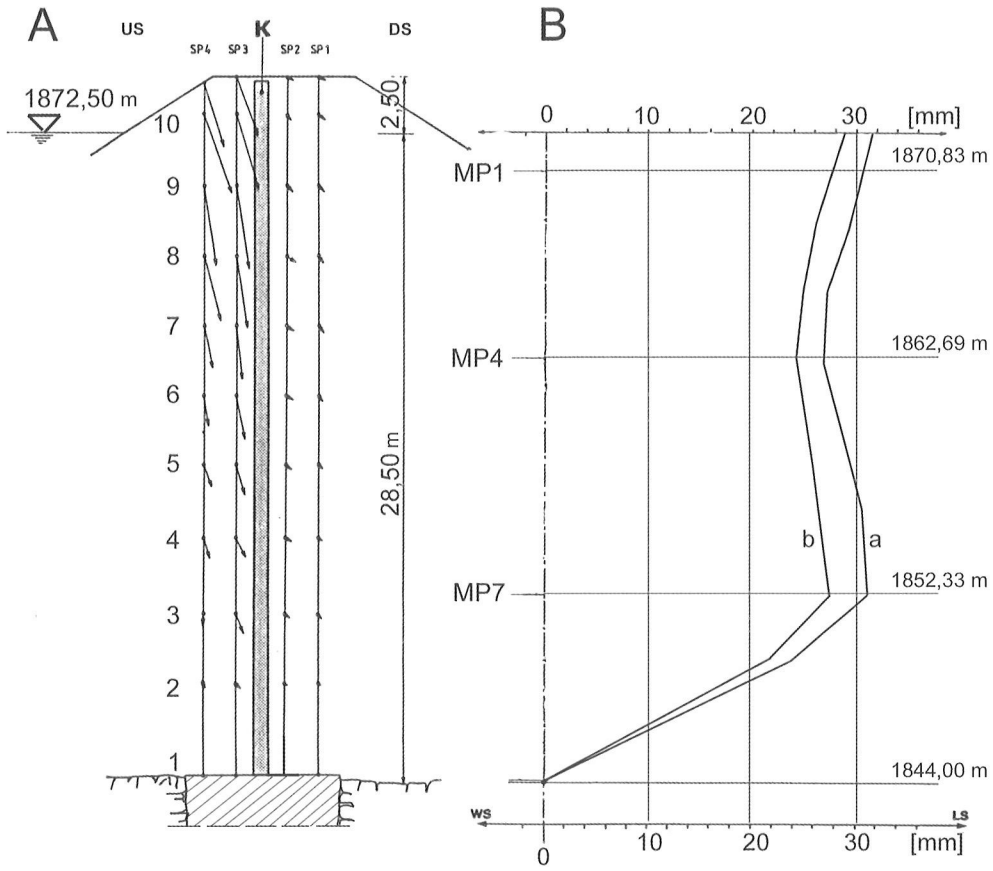

Fig. 31 *from [23]: Dam no. 17*
Results of deformation measurements

A: Deformation vectors of zones on both sides of the cement concrete core at full reservoir level 1986
SP 1,2,3,4: Measuring tubes
B: Horizontal displacements of the core; a/b at full/low reservoir level
MP 1, 4 and 7: Measuring points for Fig. 32

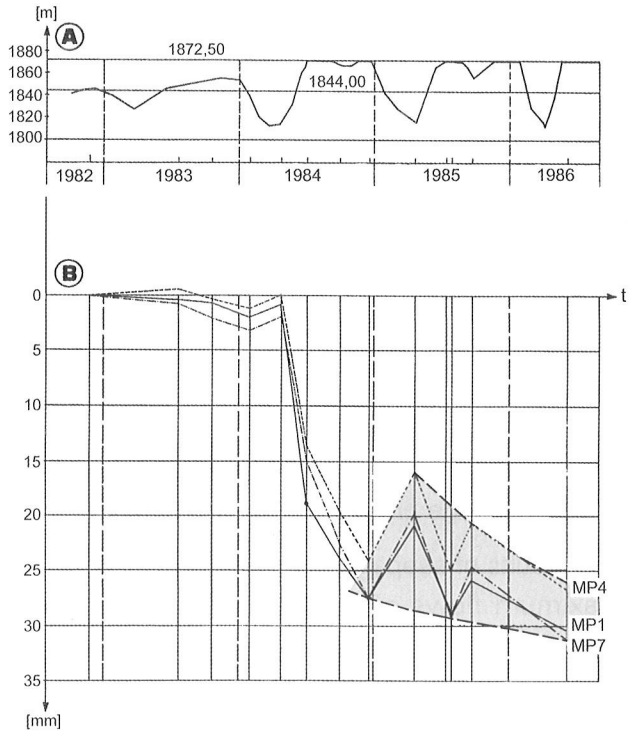

Fig. 32 *from [23]: Dam no. 17*
A: Reservoir level
B: Time-displacement curves of cement concrete core; MP 1, 4, 7: Measuring points, see Fig. 31/B

less complete stabilization after three years of reservoir operation, with elastic movements between high and low water levels of approx. 4 mm. Upstream displacement of the core wall following drawdown on 5.3.1987 can be seen in Fig. 31/B.

In Fig. 33 the measured vertical concrete pressures are plotted over time for measuring level 1845.70 m. On 29.6.1984, with the impounded water still 4.75 m below top water level at 1872.50 m, a dramatic loss of pressure was indicated by the downstream sensors accompanied by a drop in the mean compressive stresses. This can be explained as follows: As the results of FE calculations for LC top water level show in Fig. 33a, right-handed rotation movements occur in the downstream shell zone, which - as shown in Fig. 13 - activate upward frictional forces along the downstream face of the core wall and reduce the vertical pressures in the core. These processes are also confirmed by the relief movements (uplift) at the base of the core wall measured in the plumb-line shaft and by the decrease in the measured vertical soil pressures downstream of the core wall [23].

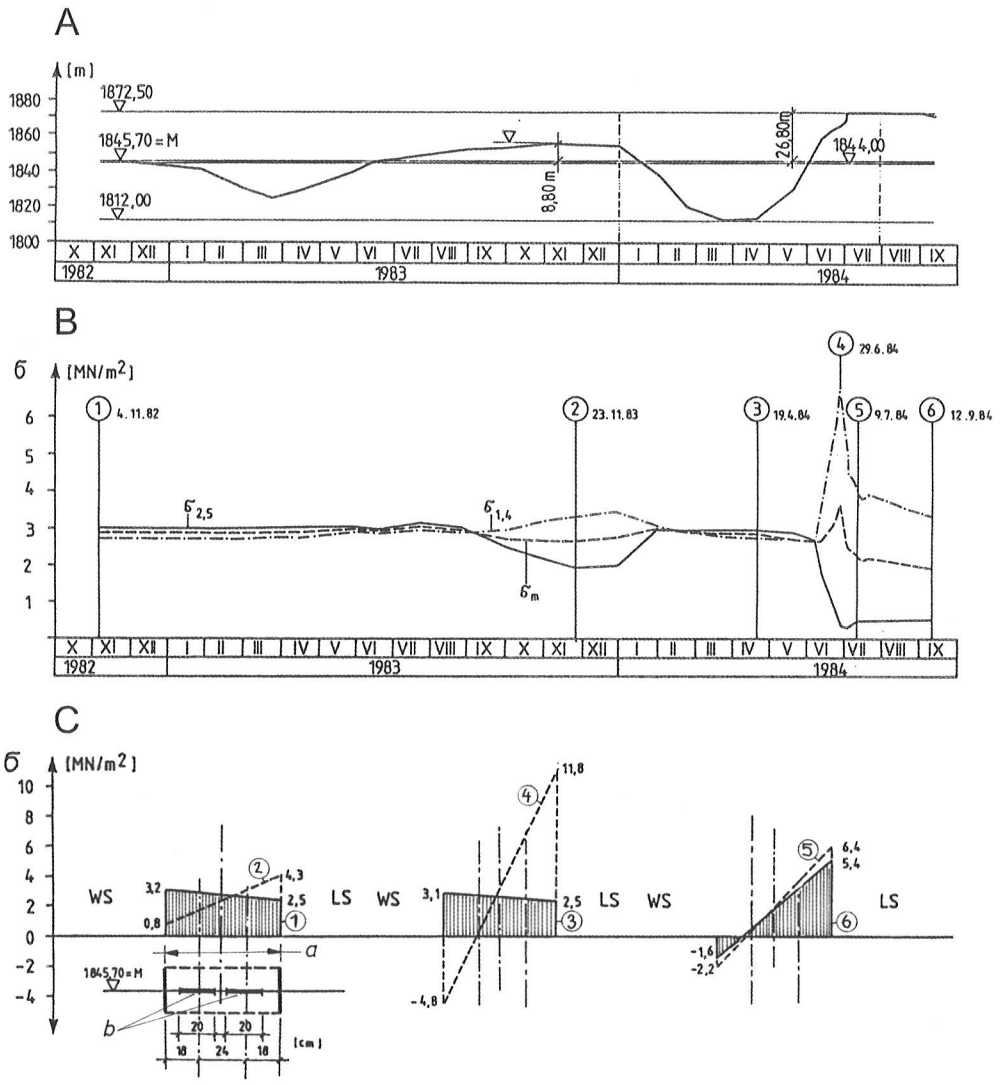

A: Reservoir level
B: Measured stresses at elevation M = 1845.70m
C: Theoretical stress distribution of wall section
a: Wall thickness = 60cm
b: Pressure cells no 2 and 5 US (σ 2,5) and No 1 and 4 DS (σ 1,4)
1 to 6: Times of stress distribution

Fig. 33 *from [23]: Dam no. 17*
Results of stress measurements of the cement concrete core

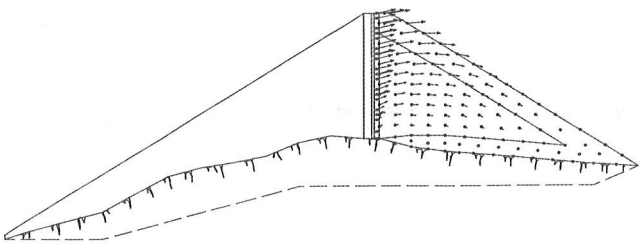

Fig. 33a *from [23]: Dam no. 17*
Result of FEM calculations – LC full reservoir level; deformation vectors of the downstream shell

On the basis of the measured data, bearing behavior can be summarized as follows:

- The thrust of the impounded water causes downstream movements, leading to deflection in the core wall and twisting without horizontal deflection at the base of the wall.
- At top water level, negative skin friction effects from the downstream shell zone lead to upward movements in the core wall. This reduces the vertical pressures and avoids damage to the concrete at the downstream toe of the wall deriving from excessive edge pressures.
- The results of seepage monitoring show, that with maximum flows of 0.02 l/s, the concrete core dam can be considered technically impermeable. This can be explained by vertical wall pressures that are well in excess of hydrostatic pressure and the sealing effect of the bitumen slip layer applied to the whole of the upstream face. Seepage through the foundation rock is max. 0.4 l/s.

Dam no. 19: Feistritzbach

With an 85 m height of seal (87 m core height), Feistritzbach Dam is one of the world's highest dams with an asphaltic concrete core. The core tapers from 70 cm at the base to 50 cm at the crest. Unlike Dam no. 15 (Finstertal), the core diaphragm is vertical for the first 70 m, and only the remaining 17 m are inclined downstream at 1 (vertical) to 0.25 (horizontal). As a result, the vertical section of the core is offset 4.25 m upstream from the dam axis, thus increasing the volume of the downstream shell. The core is located between an upstream impermeable zone and a downstream filter zone. Consulting services were again provided by Professor H. Breth. On the basis of the measured data [46, 47 and 48], bearing behavior can be described as follows:

Fig. 34 shows the vectors of movement for some of the measuring points and also the points H5/8, V3/6, H3/38 and V1/7. As can be seen from Fig. 35, settlements at these four points increased at first impounding to over 1 m on the upstream side (points V1/7 and H3/38). The impounding settlements at point H3/38 accounted for 24 % of total settlements. There are no indications that the core diaphragm has settled independently of the adjoining zones. From the inclinometer readings from two vertical tubes located approx. 6 m upstream (tube V1) and 17 m downstream from the core diaphragm (tube V3), the greatest downstream movement resulting from the thrust of the impounded water occurred in September 2002 after ten storage cycles, namely 10.4 cm at V1 and 11.0 cm at V3 at roughly the same elevation, i.e. approx. 1058 m or 72 % of dam height. The difference of 0.6 cm is extremely small and is indicative of a good contact with the asphaltic concrete core. That might be due to lateral deformations in the adjoining zones rela-

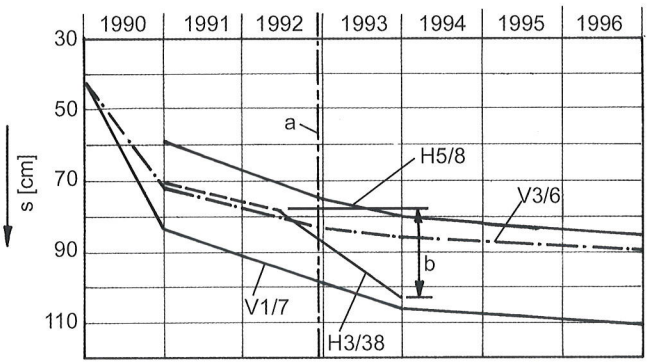

Fig. 35 *from [46a]: Dam no. 19*
Time-settlement curves of points in Fig. 34
a: Time of first full reservoir level
b: Impounding settlement at point H3/38

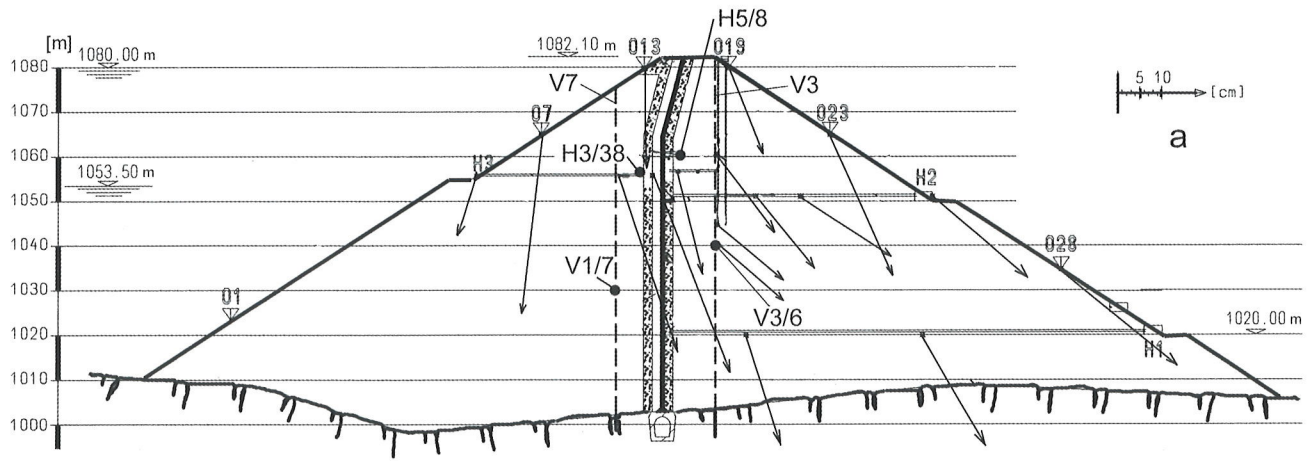

Fig. 34 *from [47]: Dam no. 19*
Deformation vectors of points inside and on the surface of the dam

a: Scale of deformation
V/H: Vertical/horizontal measuring tubes
0: Surface points

ting to the relatively pronounced settlements. Extensometer readings for the thickness of the asphaltic concrete core at elevation 1061 m gave no indication of core widening as a result of impounding. Fig. 36 shows the deformation curve for the downstream tube V3 at high and low water levels. Elastic movements of approx. 2 cm can be derived from the diagram.

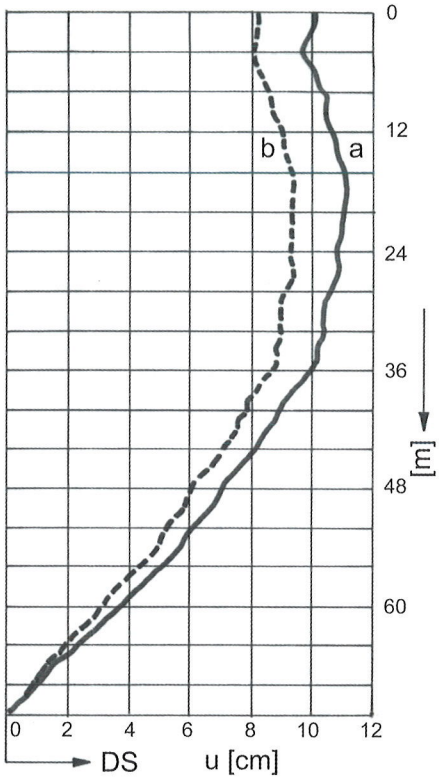

Fig. 36 *from [48]: Dam no. 19*
Displacement of measuring tube V3 in Fig. 34
a/b: Full/low reservoir level 2002
DS: Downstream side

According to [47], striking results were obtained for the vertical pressures measured in the asphaltic concrete core. With just one exception, the pressures measured by eleven sensors are well above hydrostatic load. Together with the vertical earth pressures measured downstream of the core diaphragm, they are indicative of load transfers from the upstream to the downstream side as a consequence of impounding settlements. This aspect will be dealt with reference to Dam no. 20 below.

From the core seepage measured it can be concluded that the core is completely impervious. Total seepage varies between 15 l/s and 30 l/s depending on water level in the reservoir and occurs exclusively in the foundation rock and especially on the right flank, where extensive grouting was required. No solids were detected in the seepage water.

Dam no. 20: Rotgüldensee

The vertical asphaltic concrete core of this dam is 45 m high and varies in thickness from 70 cm at the base to 50 cm at the crest. As such it was not therefore subject to any special engineering requirements. What makes this dam interesting instead is its heterogeneous foundations, with the upstream shell zone founded on a thick overburden, and the core diaphragm, inspection gallery and downstream shell zone on bedrock. The toe of the downstream shell zone was constructed from the old dam mentioned above [49], with its inclined asphalt core constructed according to the technology of 1956/57.

From the monitoring report for the dam [51], bearing behavior can be described as follows:

As in the case of Dam no. 17, different degrees of settlement occurred upstream and downstream from the core at first filling in 1992. In Fig. 37 the settlements for measuring points DF 3.2 and 4.2 at elevation 1730 m are plotted along the time axis. Fig. 38 shows displacement of the downstream measuring tube DF 4.2. A maximum downstream displacement of approx. 6.3 cm was measured on 23.10.1997 with water level at an elevation of 1731.70 m, i.e. 1.3 m below top water level. Subsequent drawdown to an elevation of 1699.70 m, which can also be seen in the diagram (Fig. 38), caused an upstream movement of approx. 1 cm. The larger upstream settlements that occurred on impounding can be explained on the basis of downstream core displacement and saturation settlements.

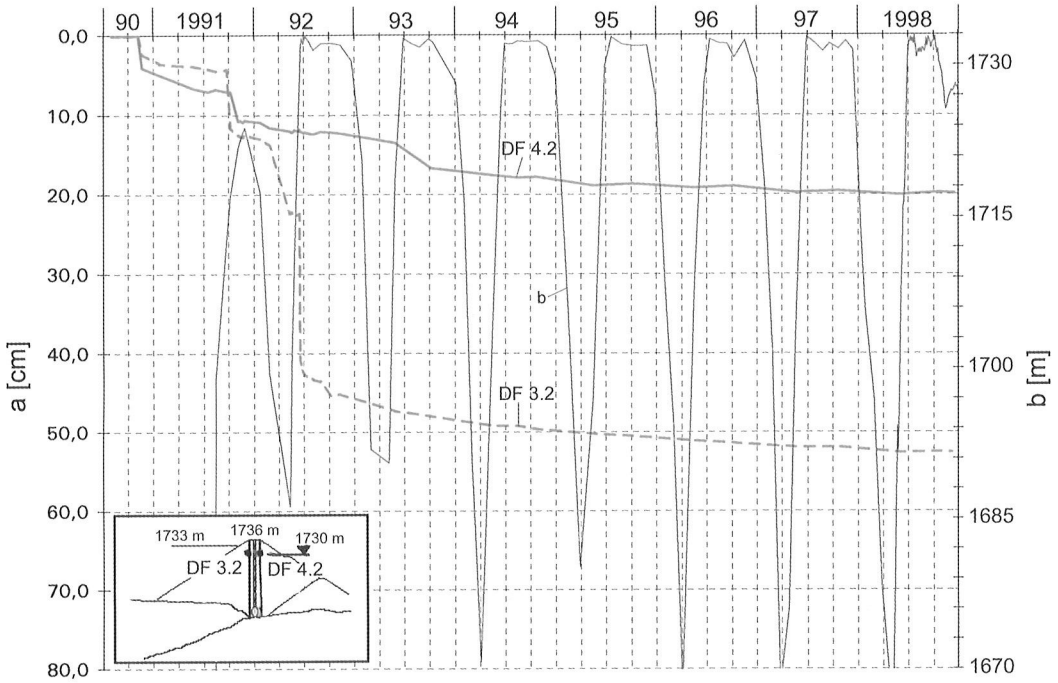

Fig. 37 *from [51]: Dam no. 20*
Time-settlement curves of points DF 3.2 and DF 4.2 US/DS of the asphaltic concrete core at elevation 1730 m

a: Settlement scale
b: Reservoir level

A number of interesting questions are raised by the earth pressures measured downstream from the core, and the following conclusions can be drawn:

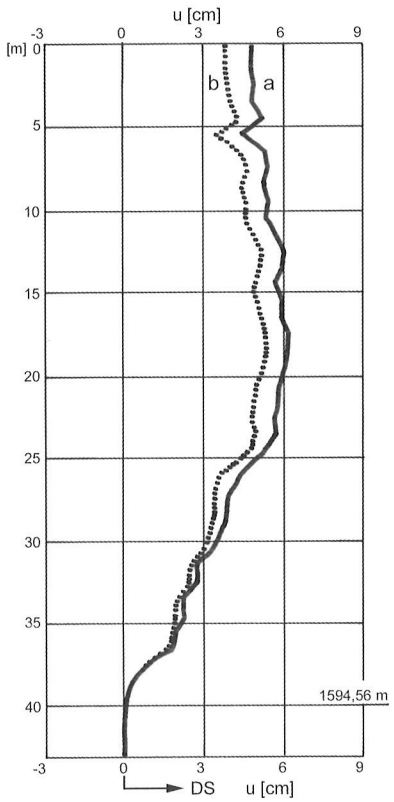

Fig. 38 *from [51]: Dam no. 20*
Displacement of measuring tube DF 4.2
a/b: High/low water level 1997/1998

In Fig. 39 pressures from three vertical and three horizontal earth pressure cells installed at an elevation of 1714.34 m are plotted together with reservoir level. As was to be expected, first impounding led to a pronounced increase in the earth pressures. A similar pattern was observed with fluctuations in reservoir level in the following years. Average measured vertical pressures at top water level in 1992 were approx. 30% above theoretical $\gamma \cdot H$. (γ = specific weight = approx. 23 kN/m³, H = dam height above measuring point = 21.6 m). The measured horizontal stresses at top water level correspond to hydrostatic pressure plus active earth pressure E'_a on the upstream side under uplift pressure effects.

Unlike the case of Dam no. 17 with its concrete core, the data obtained from this asphaltic concrete core would suggest load transfers from the upstream to the downstream side as a result of impounding settlements (see also Fig. 10). The constant fluctuations in vertical pressures in the subsequent years are also probably due to load transfers.

Among the very full monitoring results presented in [51], it is interesting to note that, despite the overburden on which it is founded, settlements in the upstream shell are generally below 20 cm - like those in the downstream zone - with the exception of the upstream zone immediately adjoining the

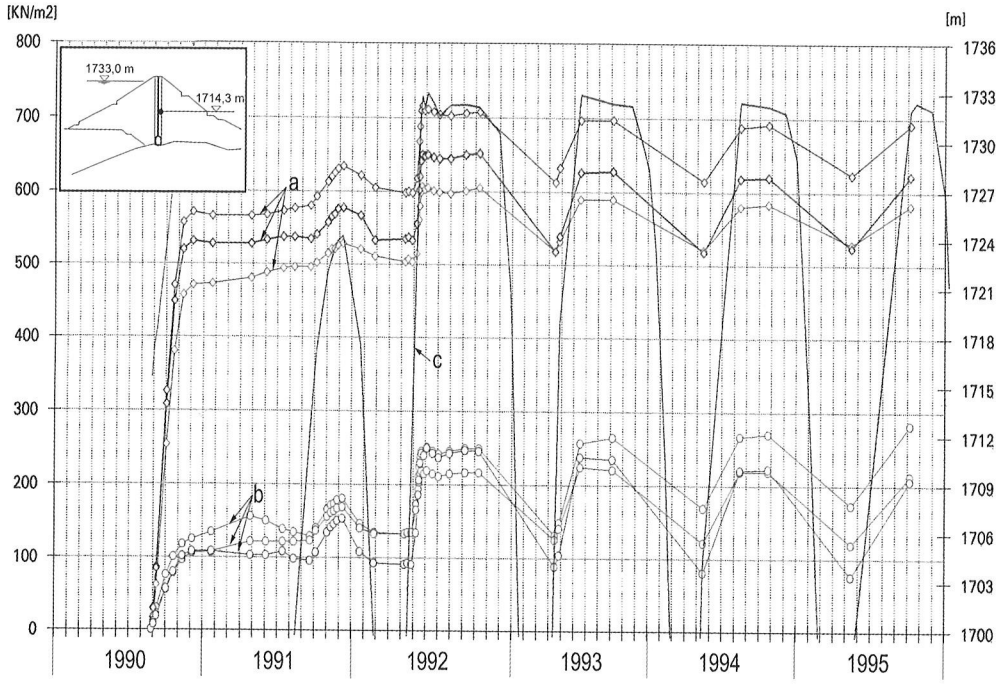

Fig. 39 *from [51]: Dam no. 20*
Result of earth pressure measurement in vertical (a) and horizontal (b) directions at elevation 1714.34 m DS of the asphaltic concrete core
c: Reservoir level

core. The horizontal movements towards the faces of both shell zones are limited to a few cm. Another significant aspect involves the pore water pressures measured in the overburden. They show that pore water pressures correlate with hydrostatic load so that no overpressure can build up in the foundations on drawdown. Seepage through the core diaphragm at top water level is approx. 0.1 l/s. For a total core area of approx. 7000 m^2, core seepage can thus be expressed as 1.4 . 10^{-4} l/sm^2, which is roughly equivalent to the situation at Dam no. 15 (Finstertal). Seepage through the foundation rock is approx. 1 l/s.

5.2 Bearing behavior of embankment dams with earth cores

5.2.1 Research results relating to 5.2

Although every embankment dam is designed individually to meet the requirements of the site, they also have common features that permit some comparisons and general conclusions to be drawn. In a research project that was central to the work done at the BFG Institute on „The bearing behavior of embankment dams relative to the type of seal" [24], eleven types of seal were studied for a fictitious 80 m high dam (Figs. 40 and 41) with the help of FEM analysis. The characteristic values employed for the analysis are presented in tabular form below. Embankment dams with membrane

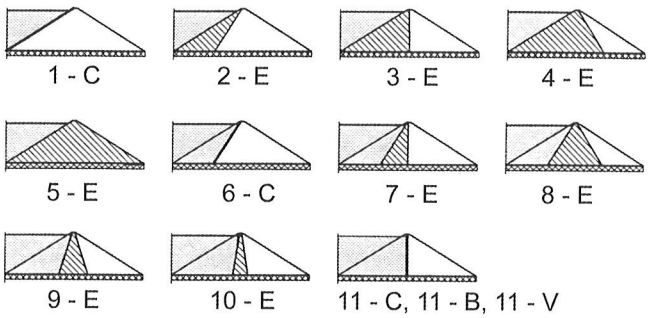

Fig. 40 *from [24]*
Variants of seals for research
E: Earth seals
B: Concrete Membrane
C: Asphaltic concrete Membrane
V: Membrane seal of prestressed dam

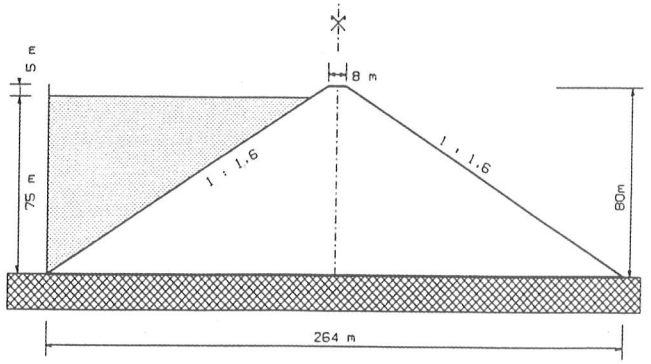

Abb. 41 *from [24]*
Geometry of the research dam

seals (variants 1, 6 and 11) were also included in the analysis. (For the results, see section 5.1.1.)

A) Load case deadweight

SHELL ZONES

			normal case	alternative
Stress-dependent loading modulus $E_b = 50000 + 25\ \sigma_{oct}$	E_b	kN/m²	50000 – 80000	-
Unloading modulus (const.)	E_e	kN/m²	150000	-
Poisson's ratio	POIS		0.30	-
Specific weight	GAMMA	kN/m³	21	-
Internal angle of friction	PHI '	degrees °	44	-
Cohesion	COHE '	kN/m²	10	-

EARTH CORES

			normal case	alternative
Stress-dependent loading modulus $E_b = 50000 + 25\ \sigma_{oct}$	E_b	kN/m²	50000 – 80000	16666 – 26666 / 25000 – 40000
Unloading modulus (const.)	E_e	kN/m²	150000	50000 / 75000 / 300000
Poisson's ratio	POIS		0.30	0.20 / 0.40
Specific weight	GAMMA	kN/m³	21	-
Internal angle of friction	PHI '	degrees °	44	-
Cohesion	COHE '	kN/m²	10	-

CONCRETE CORE

			normal case	alternative
Modulus of elasticity	E	kN/m²	30000000	-
Poisson's ratio	POIS		0.30	-
Specific weight	GAMMA	kN/m³	24	-

CONTACT between CONCRETE CORE and EMBANKMENT

			normal case	alternative
Bituminous slip layer	COHE '	kN/m²	10	-
Angle of friction of untreated core face	DELTA	degrees °	25	

B) Load case top water level

UPSTRESM SHELL ZONES

			normal case	alternative
Mod. of elasticity (const. in part)	E_W	kN/m²	12500 – 27500	-
Specific weight	GAMMA	kN/m³	12	-

EARTH CORES

			normal case	alternative
Mod. of elasticity (const. in part)	E_K	kN/m²	12500 – 27500	16666 – 26666 / 25000 – 40000 100000 – 160000
Specific weight	GAMMA	kN/m³	12	-

Table 4: *Characteristic values of the research dam, Fig. 41*

In variants 2 to 5, the impervious zone extends from the upstream face, while variants 7 to 10 have earth cores located within the dam body. In the case of dams with earth cores, the upstream shell zone does not have a bearing function with regard to hydrostatic load but, as in the case of interior membrane seals, serves to maintain the stability of the core.

The main difference between impervious earth zones and interior membrane seals relates to their role in the reduction of hydrostatic pressure. In the case of dams built with membrane seals on the one hand, the downstream shell zone takes the load, and the role of the membrane with regard to load bearing is largely limited to transmission of the hydrostatic load and earth pressure. In impervious earth zones, on the other hand, pore water flows develop, with the percolation forces always directed downwards. The impervious earth zone therefore plays a role, depending on its size, in load transfer into the foundations.

The main results of the sealing works research project can be summarized as follows:

The influence of location and size of the impervious zone or core was studied in variants 2 to 5 and 7 to 10. The impervious zones in variants 2 to 5 start at the upstream face of the embankment and can therefore be compared with surface diaphragms. As can be seen in Fig. 42 for the load case of top water level 30 m above the foundation contact,

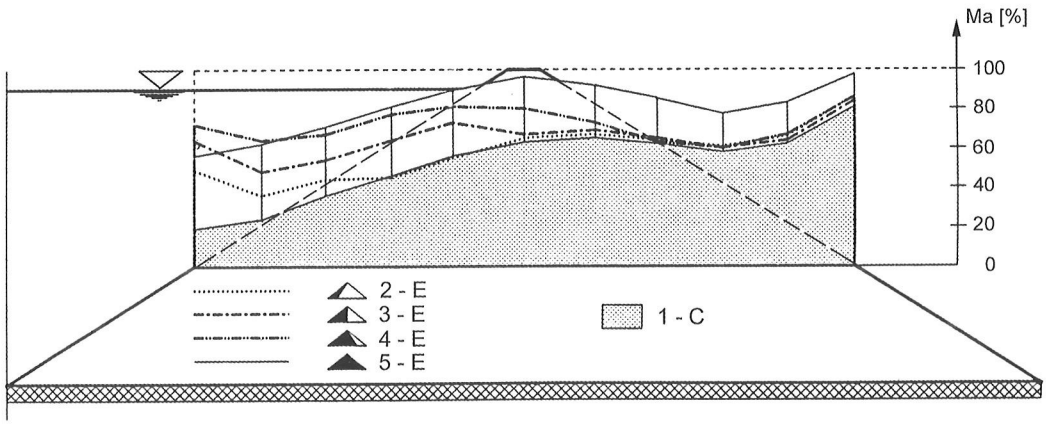

Abb. 42 *from [24]: Research dam*
Material utilization Ma of variants of earth seals 2-E to 5-E in relation to variant 1-C: facing diaphragm

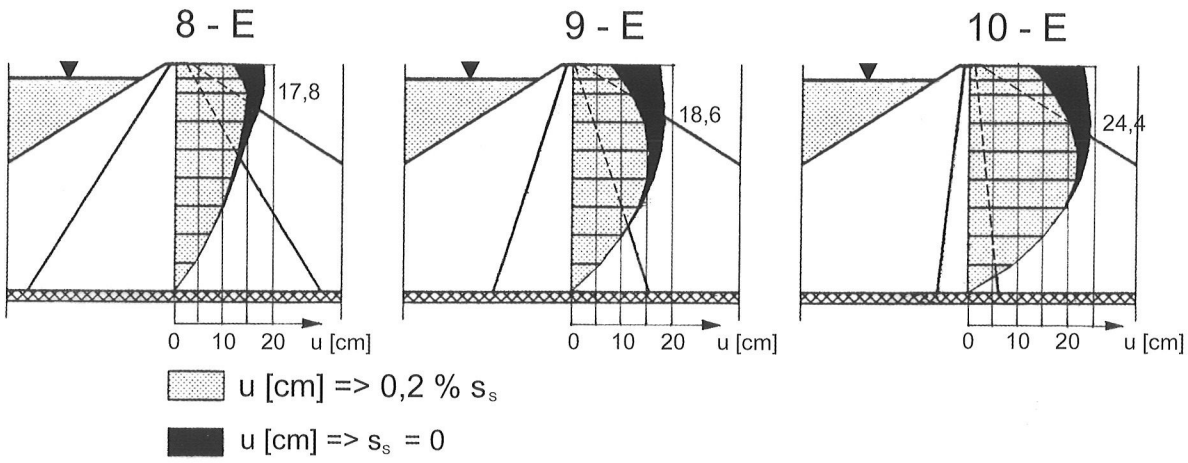

Fig. 43 *from [24]: Research dam*
Horizontal displacement u in the center of earth core dams – variants 8-E, 9-E and 10-E
s_s: Impounding settlements

material utilization in the downstream shell zone increases with increasing size of the impervious zone. The increase is only significant, however, in the case of the single zone dam (variant 5), in which the flow pressure extends well into the downstream side.

The effect of differences in core thickness (variants 8, 9 and 10) on horizontal crest deflection resulting from impounding is illustrated in Fig. 43, which shows a clear increase in crest deflection with decreasing core thickness as well as the influence of impounding settlements on the upstream shell zone.

For variants 8 to 10, the influence of differences in core stiffness on bearing behavior was also studied. As can be seen from Fig. 44/A, the load case deadweight with a stiffness ratio (α = E_{core}/E_{shell} of 0.33 in variant 10 produced a σ_V in the dam axis of

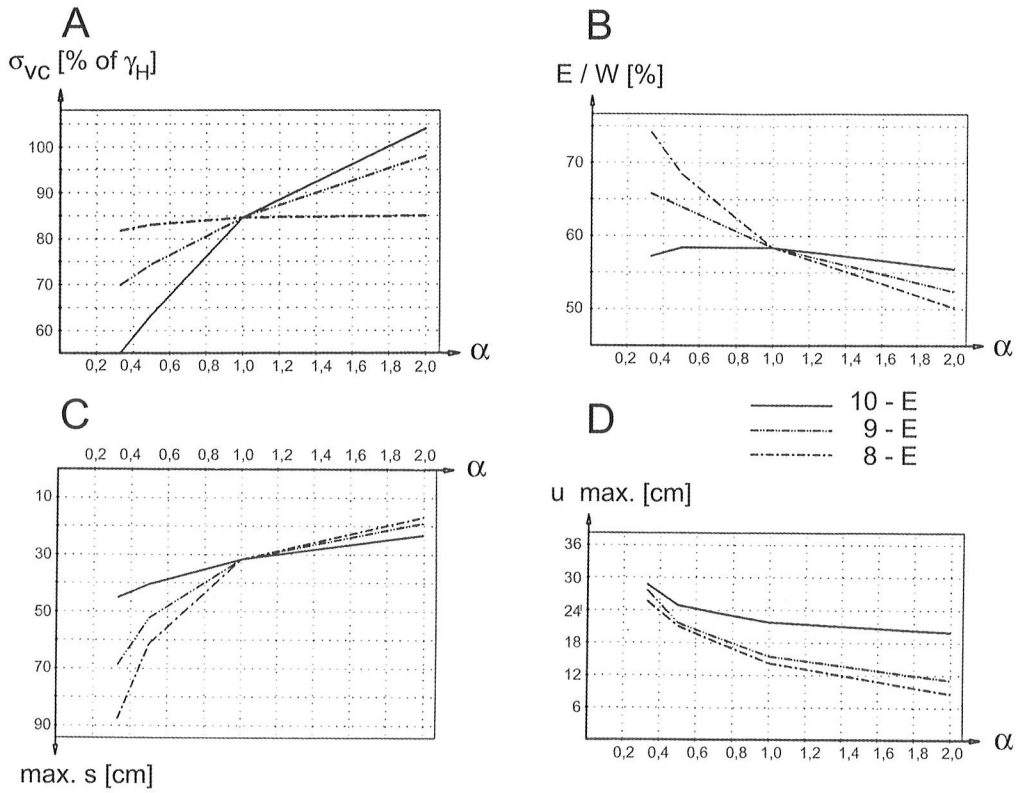

Fig. 44 *from [24]: Research dam*
Relationships with α
A, C: LC deadweight
B, D: LC impounding
α = E core/E shell
E: Earth pressure force
W: Hydrostatic load
σ_{vc}: Vertical earth pressure in the core
s_{max}: Max settlement in the center
u_{max}: Max horizontal displacement
8-E, 9-E and 10-E: Variants

55 % of theoretical vertical pressure γ H (H = height of fill). For α= 1, σ_V = 0.85 γ . H. As shown in Fig. 44/B, earth pressure increases with increasing core thickness in the case of soft cores. That is to say the shear prestress (earth pressure E_V) in the shell zones is increased. In the case of variant 8, calculating with α = 0.33 produced a shear prestress of E_V = 0.74W (W = hydrostatic load) for LC deadweight already, and with α = 1 an E_V = 0.58W. In the case of soft cores with α = 0.33, the displacement-effective load for LC impounding W + E'_a - E_V is therefore reduced considerably to 0.26 W + E'_a. This led to the development of the prestressed dam described in section 6.4. In Fig. 44/C the settlements and in Fig. 44/D the post-construction horizontal movements are plotted against α. The settlements for LC deadweight increase with increasingly soft and thick cores, while the horizontal displacements for LC impounding decrease.

The third factor studied was differences in lateral strain in the impervious cores (variants 8 to 10). A Poisson's ratio of μ = 0.3 was employed for the calculations for the core and shell zones, with variants studied using μ= 0.2 and μ= 0.4 for the core at a constant μ = 0.3 for the shell zones. Fig. 45/A shows the influence of μ on earth pressure E in the axis of the dam for LC deadweight. As can be seen, earth pressure increases with increasing lateral deformation from E = 0.58 W at μ = 0.3 to E = 0.76 W at μ = 0.4. In Fig. 45/B it can be seen that the settlements in the axis of the dam decrease as a result of increasing earth pressures at higher values for μ.

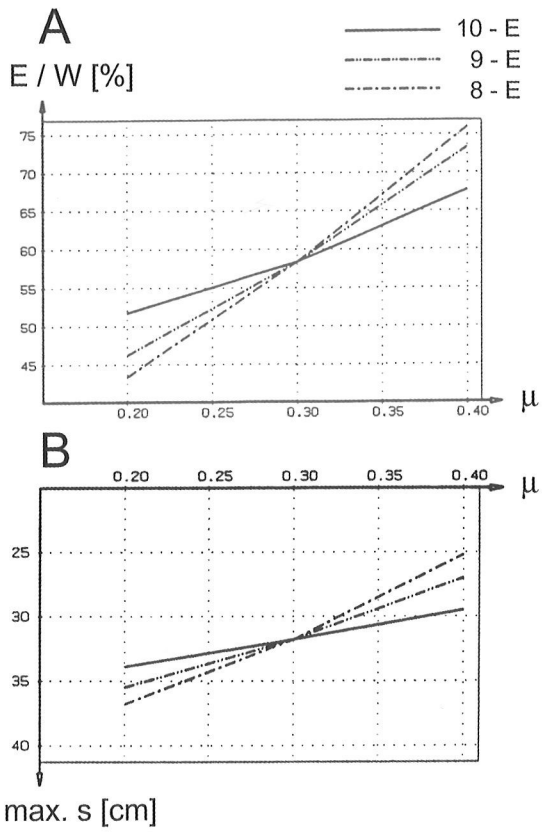

Fig. 45 *from [24]: Research dam Relationship with μ:*
A, B: LC dead weight
μ: Poisson 's ratio of the core
E, W, s_{max}: see Fig. 44

The research project on „The transfer of stresses (loads) in earth bodies with reference to dam construction" [24] was designed to study the problem with the help of physical models and to compare the measured results with the calculations.

Load transfer occurs in all structures. In the case of embankment dams, the horizontal hydrostatic load is transferred to the foundations with the help of the shearing strength of the fill material. The problem considered in this study, however, is not the transfer of the thrust of the impounded water but the transfer of deadweight. In earth core dams,

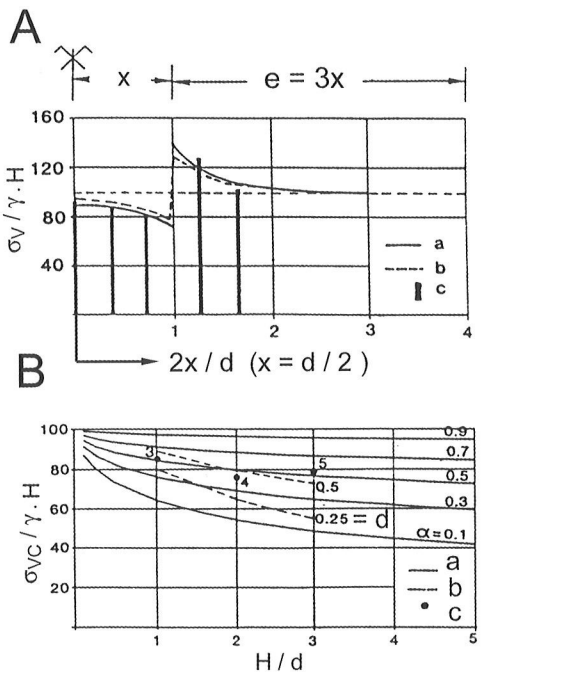

Fig. 46 *from [24]*
Research into load transfer between earth core and adjacent zones with physical models and calculations
Relationships with σ_v and σ_{vc}:
σ_v: Vertical earth pressure general
σ_{vc}: Vertical earth pressure in the core
d: Core width
e: Width of the adjacent zone in the model = 1,5 d
H: Fill height
γ: Unit weight
α, E: see Fig. 4 4
a: Results with the beam calculation model
b: FEM calculation
c: Measured values from test no. 3(A) and no. 3,4,5(B)

transfer from the softer core to the stiffer adjoining zones is normally to be expected. As shown in the above analytical investigations, the magnitude of transfer depends mainly on stiffness ratio α. The geometry of the dam and the shear strength of the materials also have a significant influence. „Arching effect" is now the standard term used to describe this phenomenon. In the experiments performed, it was possible to create this effect through forced relative movements in a test box.

Fig. 46/A shows the results of test no. 3 and Fig. 46/B the evaluation. As can be seen, the simplified calculation model of a beam with high shearing stiffness [52] offers a good approximation for estimating load transfer. However, load transfer is not limited to the cross-section of the dam. In narrow valleys, transfer also occurs transverse to the valley. In the case of earth core dams, a double arching effect can therefore develop. For the design of the Dabaklamm Dam in East Tyrol (a project later abandoned for reasons of environmental policy), the effect of load transfer transverse to the valley was studied with the help of a 1.3 m high plane strain model (Fig. 47). The details are presented in section 9.3.

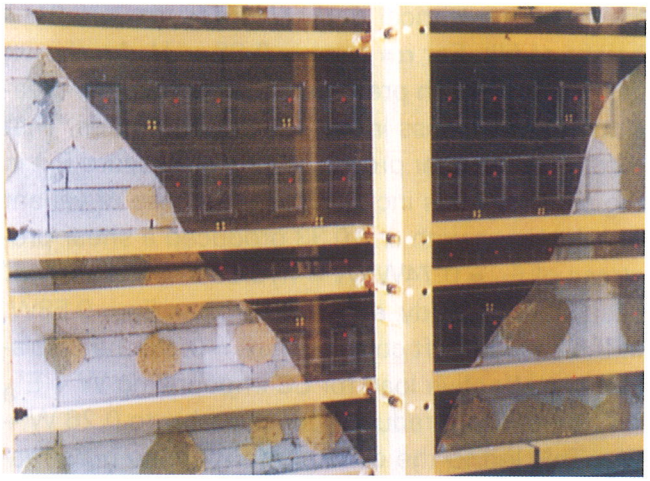

Fig. 47 *from [9]: Dabaklamm Project. Experimental setup with the 2-D model of the valley section.*

5.2.2 Bearing behavior of Austrian embankment dams with earth cores

Dam no. 2: Freibach

With a height of 41 m, Freibach Dam is the smallest earth core dam in Austria. As can be seen in Fig. 5, the central core is continued as an upstream blanket in the foundation area of the upstream shell zone, with a drainage blanket placed beneath the downstream shell zone. Fig. 48/A illustrates the geology of the site in the valley section. The engineering challenge of the site was its foundation on a thick layer of deposits with zones of seepage paths on the left bank. Fig. 48/B shows the foundation sealing works in the contact area, with a concrete cutoff wall, a clay diaphragm and a grout curtain extending deep into the permeable zones. The right slope was also sealed by rock grouting. From the data obtained from the extensive surveillance equipment installed to monitor seepage, dam deformations, and the decrease in the piezometric pressure in the dam and foundations, the bearing behavior of the dam can be described as follows [53], [54] and [55]:

After forty years of operation, dam deformations in the form of up to approx. 20 cm crest settlements have largely abated. Horizontal crest movements caused by annual fluctuations in reservoir level are reversible at an estimated 2 mm between high and low water levels. The decrease in piezometric level in the dam, the dam foundations and the right bank occurs in the central part of the dam. There are differences in the piezometric levels in the various alluvial zones on the left bank downstream from the line of the core area corresponding to the seepage path zones b and d, i.e. gravel on top and red talus below. The piezometric lines in the gravel close to the surface explain the seepage emerging from the left bank immediately downstream from the dam. The springs have been curbed in outlet structures, and some of them are subjected to continuous monitoring. Total measurable seepage at top water level is approx. 40 l/s. Excessive sedi-

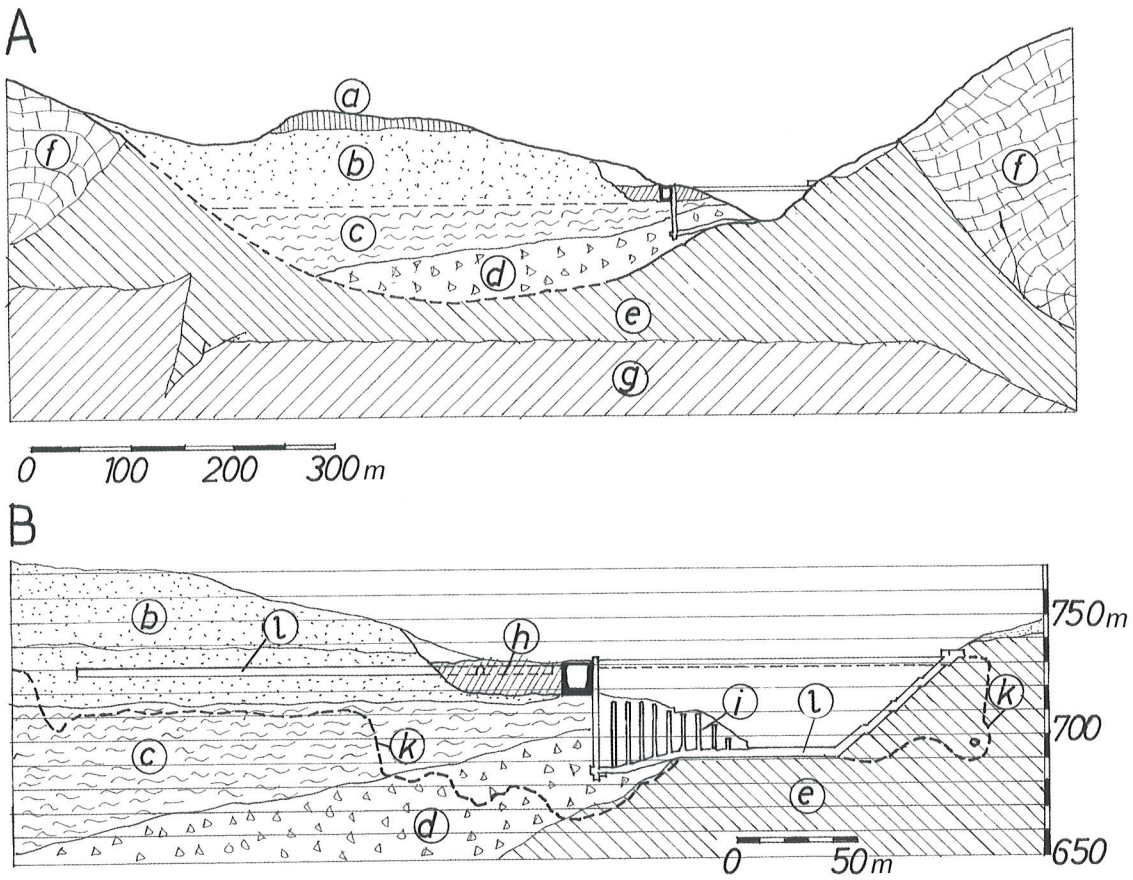

Fig. 48 *from [53]: Dam no. 2 – Valley sections*
A: Geology
a: Moraine
b: Sand and gravel
c: Silt (banded silt)
d: Rockfall material (red talus)
e: Limestone marl with limestone lenses
f: Limestone
g: Conglomerate with clay cementation
B: Sealing measures
h: Clay curtain
i: Cement concrete wall
k: Grout curtain
l: Inspection gallery and shaft

ment load in the seepage has not been observed at any of the gauge points. Additional sealing works involving grouting on the left bank in 1985 and a 145 m long diaphragm wall with a max. depth of 20 m in 1986 failed to reduce the seepage.

Dam no. 4: Gepatsch

With a height of 153 m, the Gepatsch rockfill dam is the highest fill dam in Austria. Its innovative character relates primarily to the placement of quarry-run material with a stone size of up to max. 1 m3 in 2 m lifts for the shell zones and the first ever use of 8 t vibratory rollers for compaction. This triggered rapid developments in the design of extremely powerful heavy vibratory rollers. Simultaneous with developments in embankment dam construction in Mexico, a new standard of dam bearing behavior monitoring was achieved with innovative monitoring equipment. The available documents relating to the dam can be summarized as follows:

Deformation:

- The movements of the monitoring points in the dam profiles in Fig. 49 reflect the influence of the triangular embankment, with the movements generally directed from the inside to the outside. On the upstream side at elevation 1715 m, placement of the shell zone ahead of the core can be clearly identified as the cause of initial movements to the inside. In the comparatively much stiffer natural gravel of the transition zones, the deformations were significantly less pronounced. The extension of the downstream transition zone led not only to a reduction in settlements by approx. 30 % but also, presumably as a result of the increased support thus provided, to more pronounced lateral core deformation towards the less stiff upstream shell zone.

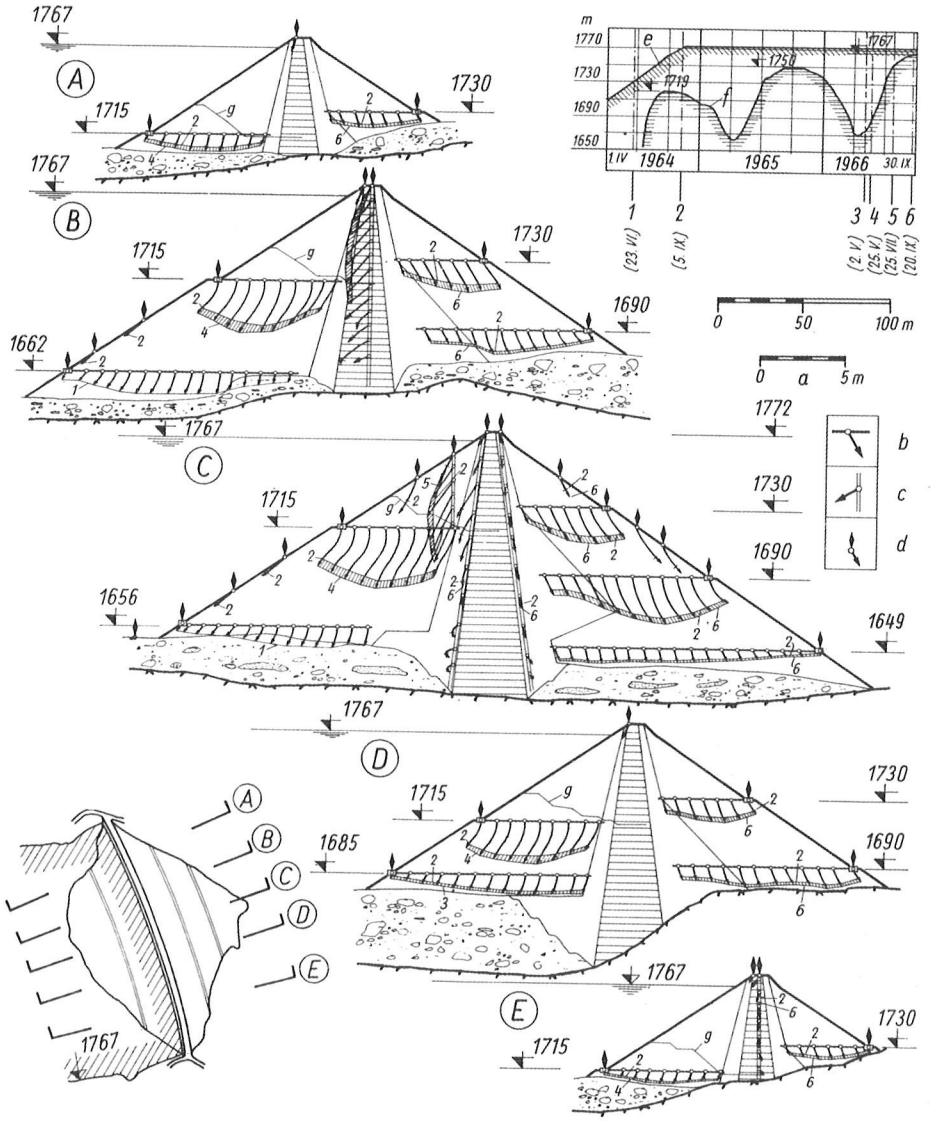

Fig. 49
from [28]: Dam no. 4
Deformations of the dam cross-section.
a) Scale of deformations.
b) Lying tube with vector of movement.
c) Upright tube with vector of movement.
d) Fixed point with vector of movement.
e) Dam fill.
f) Reservoir level.
g) Fill crest in April 1964.
1-6) Measuring dates.

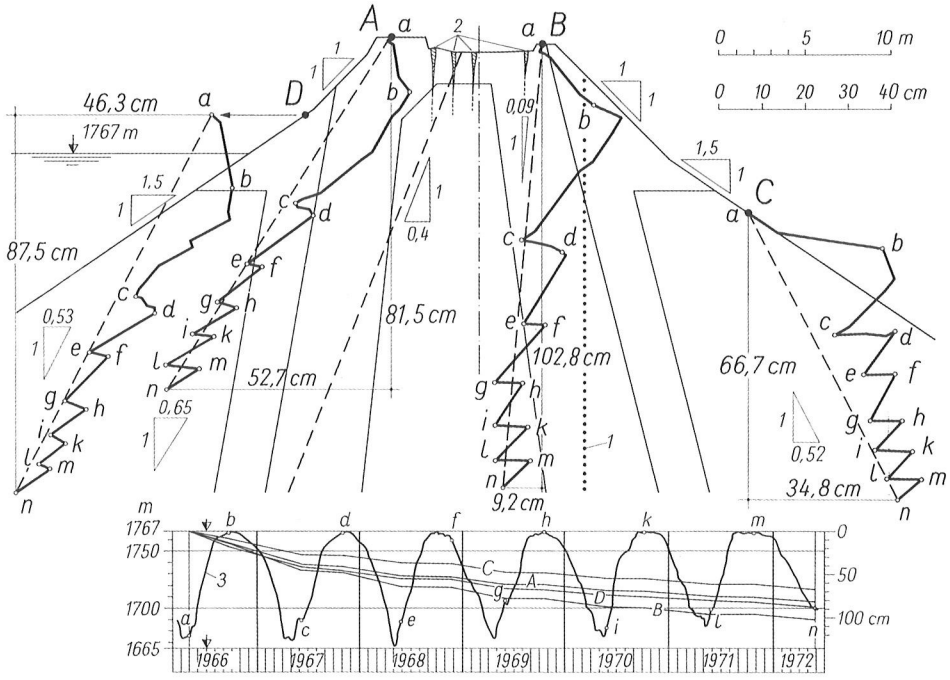

(A) to (D) Time curves of the settlement of points
(a) to (n) Measuring dates.
(1) Zero line of the horizontal movements.
(2) Longitudinal cracks.
(3) Time curve of storage level.

Fig. 50 *from [18]: Dam no. 4.*
Movements of the crown points A to D of the main cross-section 1966 - 1972.

- Fig. 50 shows the effects, reinforced by impounding settlements, of the transverse deformations of the core, primarily on the upstream side, on crest movement in the six impounding periods from 1966 to 1972. The most pronounced settlements, namely 106.8 cm, occurred at downstream crest reference point B, which lies in the immediate vicinity of the zero line of horizontal movements downstream from the crest. The elastic portion of post-construction horizontal crest deflection between high and low water levels at reference point B is an estimated 7 cm.

- As a result of the 40 cm widening in the crest after six years of impounding as shown in Fig. 51, longitudinal cracking and step-like surface irregularities developed at the crest. As can be seen from the diagram, annual increments in crest width only occurred at top water level. The cracks were approx. 3 m deep, which means they extended into the core but remained some 2 m above top water level.

- After 36 years of reservoir operation the plastic deformations in the dam have largely subsided.

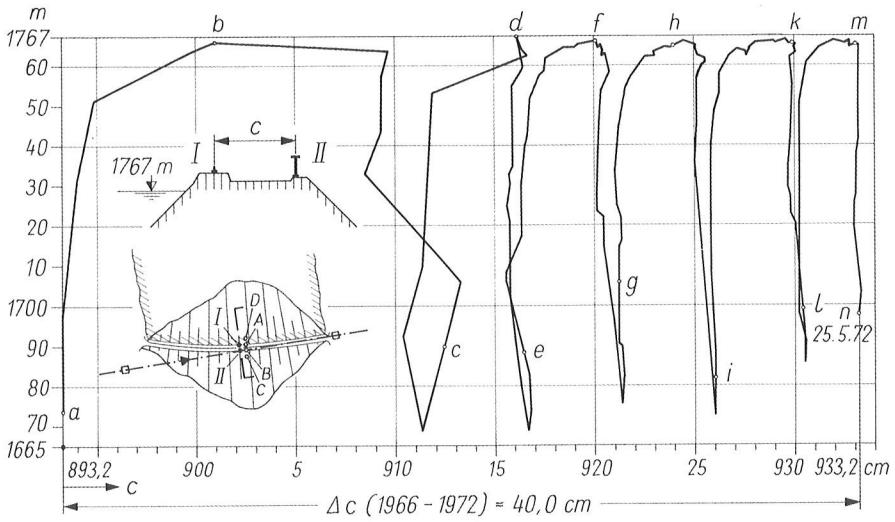

Fig. 51 *from [18]: Dam no. 4*
Extension Δc between crown points I and II 1966 - 1972. The measuring dates a - n are shown in figure 50.

Crest widening reached 78 cm, crest settlement 194 cm, and elastic horizontal crest movements 4.5 cm. Up to 1.1 cm of lift occurs in the upstream shell zone on reservoir filling as a result of uplift pressure. Reloading of the shell zone when water level drops and uplift ceases is still causing additional settlements of up to 1.5 cm at the upstream crest reference point [58].

- It should also be noted that strain zones have developed in the flank areas of the dam crest (Fig. 52), while compression in the central section has led to a reduction in settlements there. That is indicative of an arching effect transverse to the valley.

Pressures and seepage

- Fig. 53 shows the time curve for pore water pressures in the core at elevation1660 m in the first few years of reservoir operation. It is interesting to see that, as a result of compaction with 40 t pneumatic-tired rollers, pore water pressures at placement rose to approx. 100 % of vertical soil pressure $\sigma_V = \gamma \times h$. Within six months, the pressures fell to approx. 20 % of $\gamma \times h$. The 1 % bentonite added to the upstream core zone 1a did not affect the reduction of hydrostatic pressure in the core.

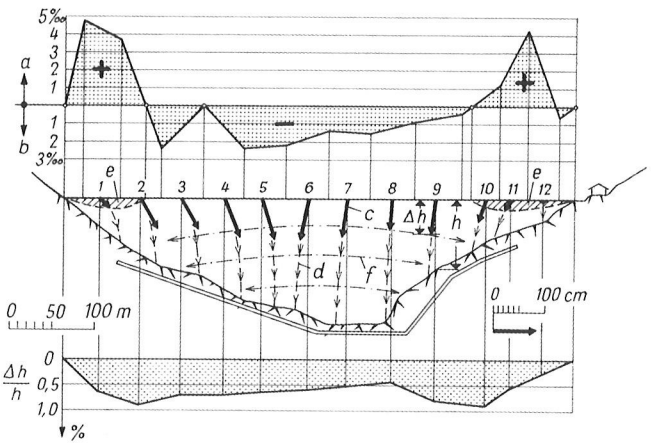

Fig. 52 *from [18]: Dam no. 4*
Crown movements in the longitudinal section 1966 – 1972
a/b: Extension/compression
c: Vectors of movement
d: Arching effect
Δh/h: Relative settlements (%)

- Interesting results were obtained for the horizontal earth pressures measured at four levels downstream and one level upstream from the core (Fig. 54). As the downstream pressures measured at top water level correspond approximately to hydrostatic load σ_W, the load from active earth pressure from the upstream shell

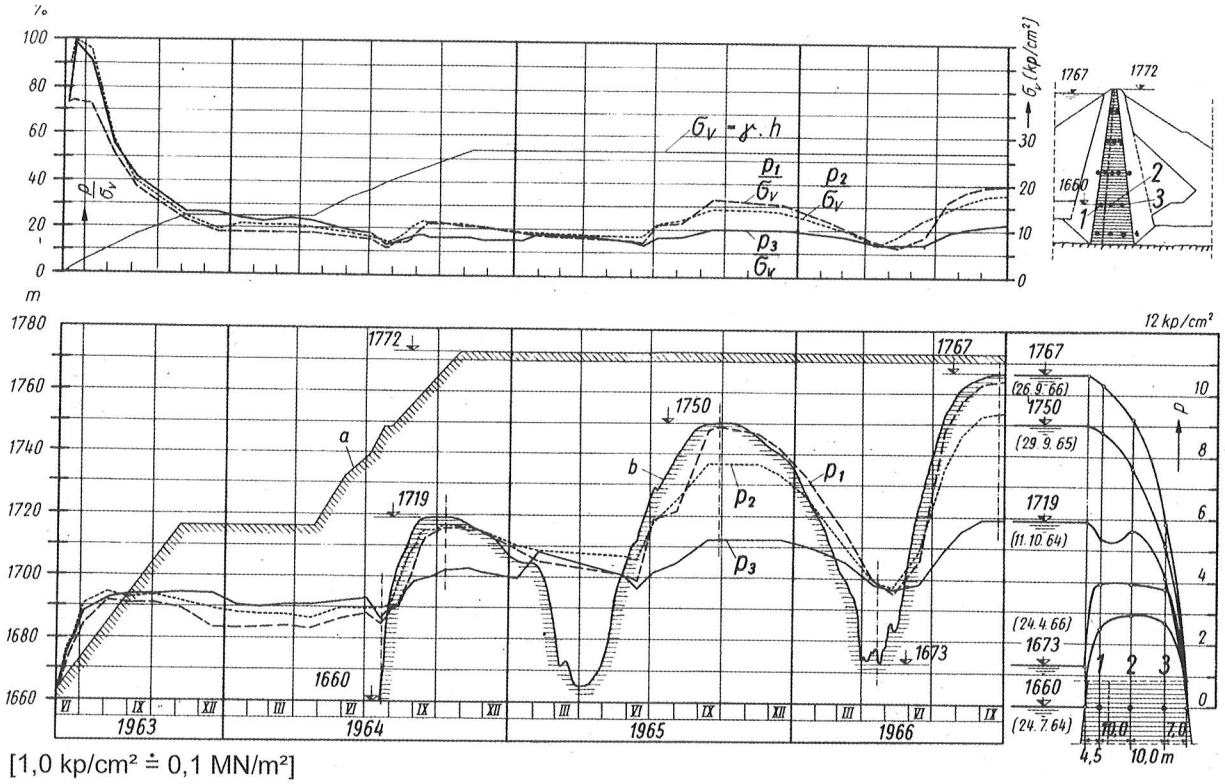

Fig. 53 *from [28]: Dam no. 4*
Pore water pressures and pore water pressure factors at elevation 1660 m.
1-3: Pore water pressure cells.
p_{1-3}: Pore water pressures at cells 1-3.
$\sigma_V = \gamma.h$ = Vertical pressure calculated (γ: Density at the moment of placing, h: Relative fill height)
p/σ_V: Pore water pressure factor.
a: Dam fill.
b: Reservoir level.

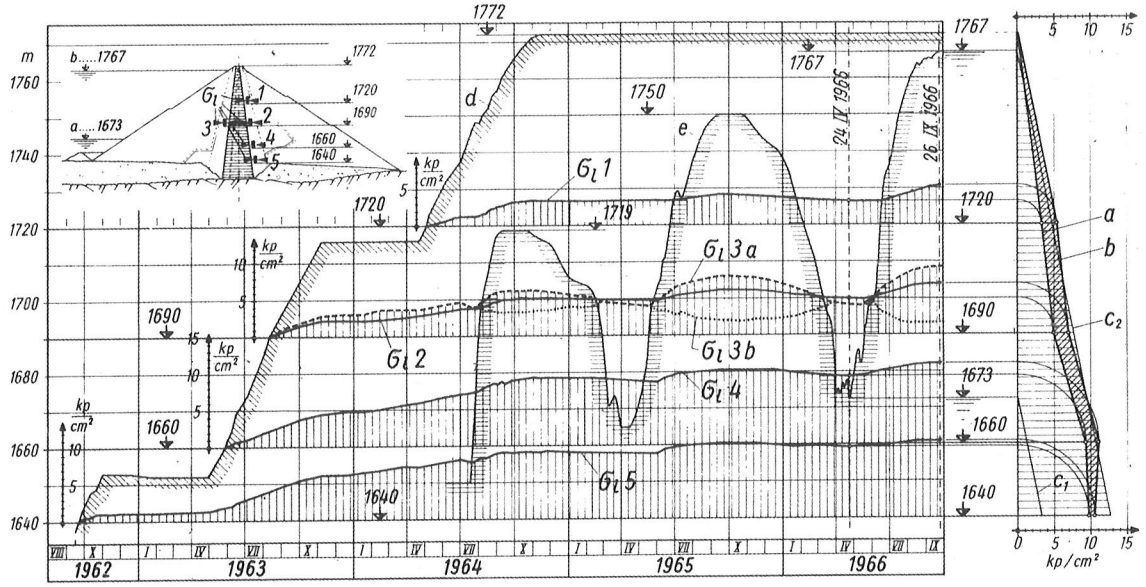

Fig. 54 *from [28]: Dam no. 4*
Side pressures on the core surface.
1-5: Soil pressure cells.
σ_l 1-5: Side pressures at cells 1-5.
σ_l 3a, 3b: Side pressure at cell 3 with and without pore water pressure.
a, b: Side pressure on the downstream side for reservoir level at 1673m and full level at 1767m. c1, c2: Water pressure for reservoir level at 1673m and full level at 1767m.
d: Dam fill.
e: Reservoir level.

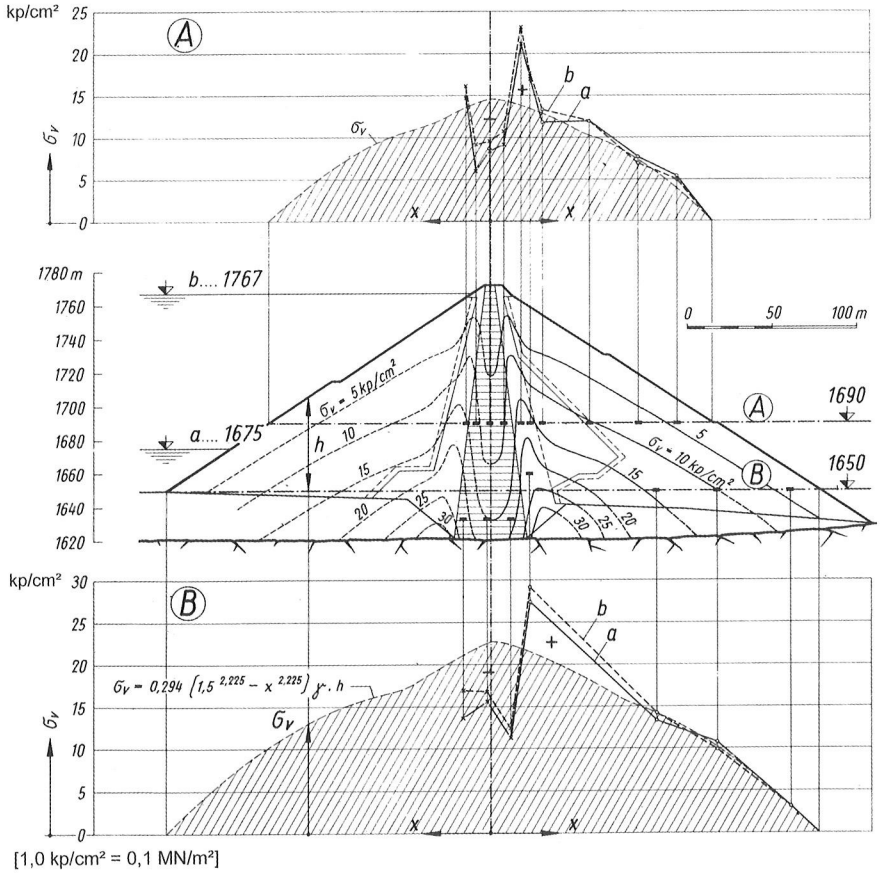

Fig. 55 *from [28]: Dam no. 4*
Vertical soil pressures at elevation 1690m (A) and 1650m (B), and isobars in the main dam cross-section.
a, b: Pressure distribution measured for a reservoir level at 1675m and 1767m (measured values marked with a cross are the average of the readings for 2 cells).
σ_V: Vertical pressure calculated.

zone under uplift conditions E_a' must already have been transmitted through the core to the foundations. At periods of low water level, measured core side pressure is between 0.6 σ_W and 0.8 σ_W. That is indicative of a high shear prestress in the shell zones exerted by the plastic core for LC deadweight.

- As with the above measured data for core side pressure, the data obtained for vertical pressures in the dam body (Fig. 55) made it possible for the first time ever to demonstrate a further characteristic of soft central earth cores in the form of the above-mentioned arching effect, which was first discussed by D. M. Trollope in 1957 [60]. From the measured data in Fig. 55 it can be seen that, as a result of the more pronounced settlements in the core, load transfer has developed from the core to the stiffer adjoining transition zones. For top water level at 1767 m, the pressures measured in the core at elevation 1690 m are approx. 900 kN/m² and at elevation 1650 m approx. 1250 kN/m², which is well above the corresponding headwater pressure of 770 kN/m² and 1170 kN/m² respectively. Hydraulic fracturing deriving from the thrust of the impounded water can therefore be ruled out.
- In [28] the author describes the decrease in piezometric level in the bedrock and seepage. Peak seepage flows through the dam and foundations of 18 l/s in the first year of impounding to top water level in 1966 have fallen to 8 l/s after 36 years of operation as a result of self-sealing effects.

Dam no. 5: Durlassboden

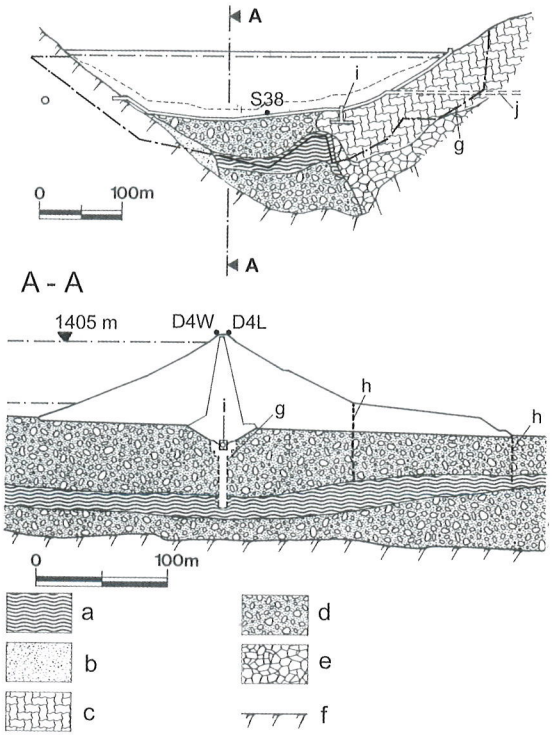

Fig. 56 *from [9]: Dam no. 5*
Geology and structural measures
a: Silt
b: Moraine
c: Landslide
d: Sand and gravel
e: Talus material
f: Bedrock
g: Grout curtain
h: Relief wells
i: Inspection gallery and shaft
j: Exploration gallery

The 85 m high Durlassboden Dam is a highly complex structure [61]. It is founded on a heterogeneous mass of gravels and silt extending to a depth of up to 136 m, and on the right valley flank it ties in with a creeping slope. Like Dams nos. 2 and 6, it is an example of the achievements possible in dam engineering on extremely difficult foundations. As can be seen in Fig. 56, the up to 60 m deep

grout curtain beneath the central earth core extends into a lower-level silt layer and into the creeping slope.

The structural measures selected to cope with headwater pressure comprise an upstream blanket, a downstream filter zone as a combined chimney and base drain, and a drainage blanket under the toe weight in connection with pressure relief wells (see Fig. 5). As in the case of Dam no. 6, particular importance was attached to the question of seepage water flows.

Deformations:

Deformation monitoring is performed by measuring the settlements and in some cases horizontal displacements of gauge points on the dam crest, in the inspection gallery, in the exploration gallery on the right bank and on the downstream face of the dam. Figs. 57A and 57B show the time/settlement curves of the three points in Fig. 56, i.e. D4L and D4W on the crest and S38 in the inspection gallery after the first year of impounding to top water level. By 9.7.1970, as can be seen in the figure, the inspection gallery had already settled by 108 cm under the load of the dam. Whereas inspection gallery settlements of up to approx. 131 cm have largely ceased after 32 years of reservoir operation, slight crest settlements are still occurring. The fact that settlements at the crest reference points are greater upstream than downstream, by approx. 45 cm to 38 cm, is indicative of the influence of impoundment. Elastic lift of approx. 1 to 2 cm deriving from uplift pressure occurs both at the dam crest and in the inspection gallery. At the level of the exploration gallery in the creeping slope, settlements in the dam contact area have totaled up to

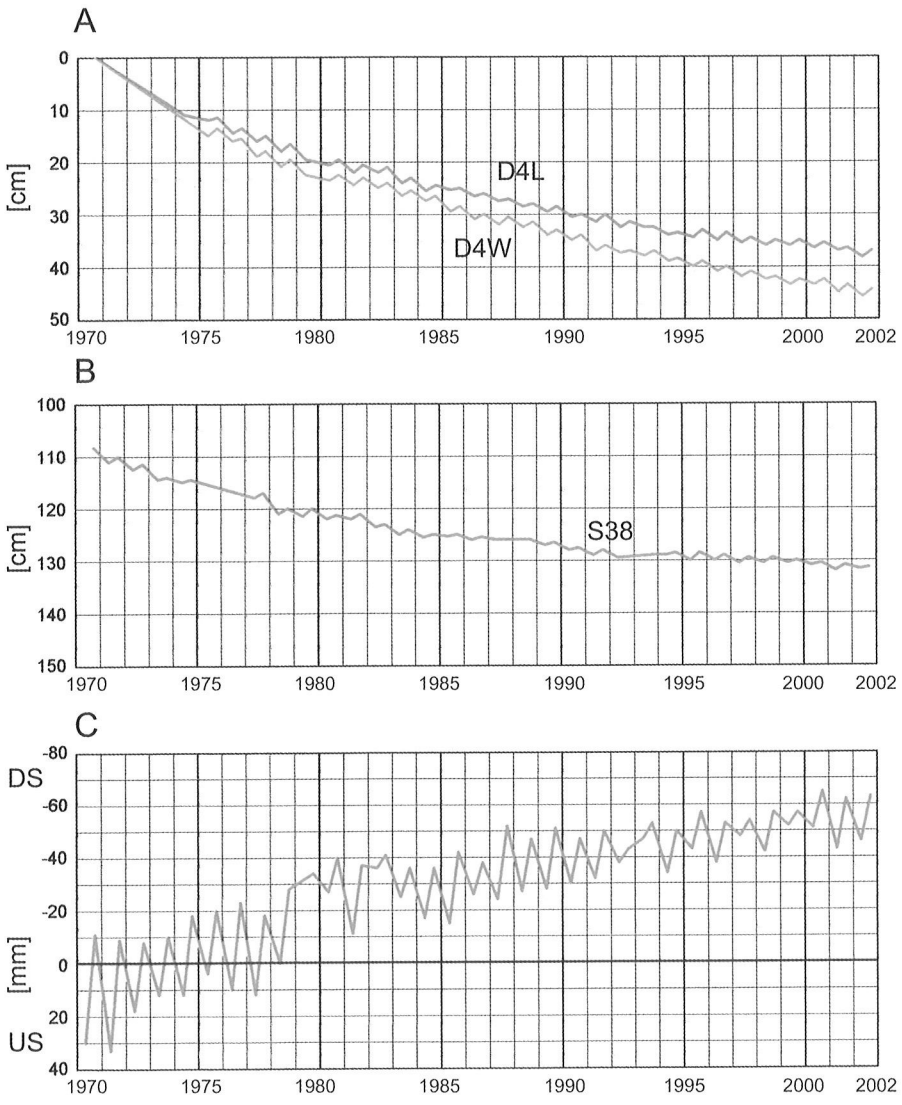

Fig. 57 *from [61a]: Dam no. 5*
A,B: Time-settlement curves of crown points D4W and D4L and point S38 in the inspection gallery
C: Time-displacement curve of a crest point near D4W

approx. l6 cm since 1970. Horizontal movements at a crest reference point near D4W (see Fig. 57/C) have measured up to approx. 4 cm plastic plus approx. 2 cm elastic movements since 18.9.1969, and at a corresponding point in the inspection gallery up to 2.5 cm plastic and also approx. 2 cm elastic movements between high and low water levels since 8.5.1969. This result is surprising and suggests that impoundment affects the foundations down to a considerable depth.

In the exploration gallery, the horizontal movement of the creeping slope in the direction of slope has so far measured approx. 1.5 cm plus 3 mm elastic movement as a result of fluctuating reservoir level. The plastic deformations are still continuing.

Plumb-line readings in the shaft of the inspection gallery (see Fig. 56) show reversible post-construction movement in the creeping slope of up to 3 mm at a height of approx. 15 m.

As can also be seen from Fig. 58, at a deep level below the silt layer downstream from the dam a piezometric line has formed which is higher than the toe weight surface and which can only be lowered to below ground level with the help of relief wells downstream from the toe weight. Control of the seepage water flows in the creeping slope of the right bank is performed largely with the exploration gallery, which is located approx. 33 m downstream of the dam axis at elevation 1351.50 m where it extends 192 m into the creeping slope.

Seepage and suspended solids:

As shown in Fig. 58, core seepage water is diverted to the inspection gallery at the toe of the downstream chimney drain. Together with seepage in the inspection gallery, total seepage is a maximum of 2.5 l/s. In the exploration gallery located at

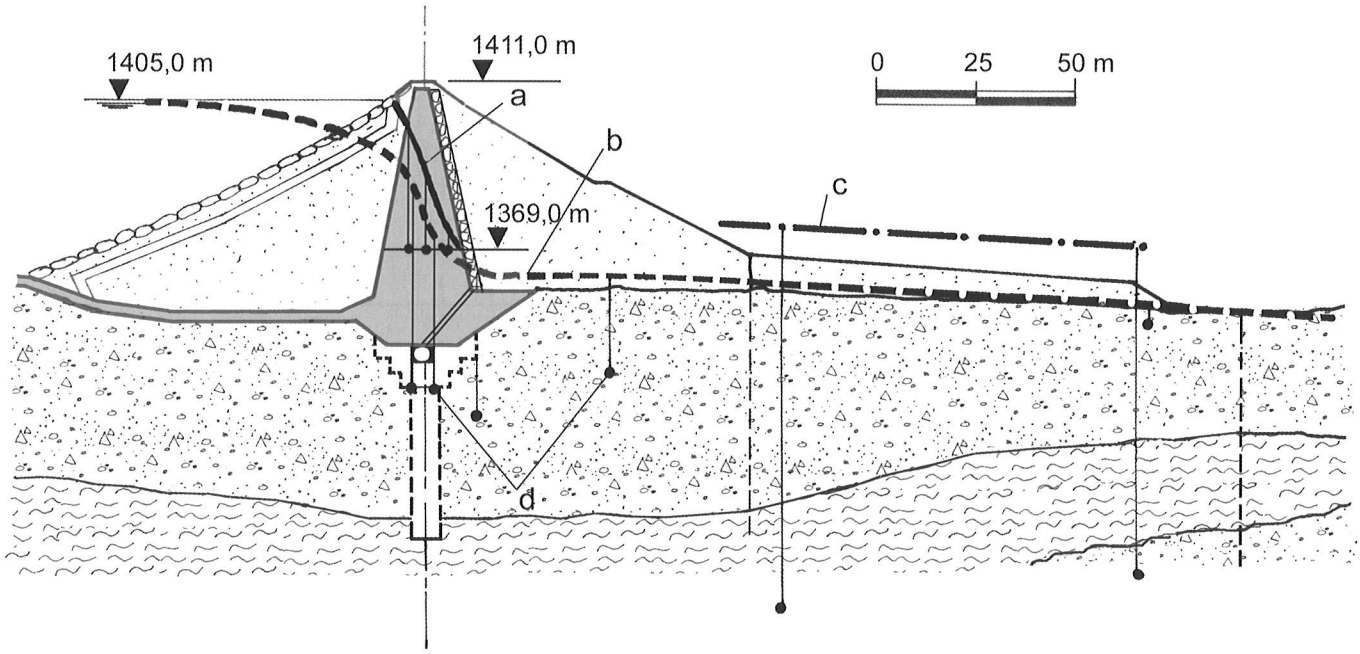

a: Earth core at elevation 1369m
b: Upper foundation zone
c: Deep zone
d: Measuring points

Fig. 58 *from [61a]: Dam no. 5*
Dissipation lines of reservoir water pressure

Decrease of piezometric level:

The piezometric level across the core as monitored in two profiles with three pore pressure cells each shows an approximately linear decrease. The piezometric line at elevation 1369 m is plotted in Fig.58 for a profile located approx. 45 m to the right of the geological section in Fig. 56. The reduction in pressure in the upper foundation zone occurs primarily at the grout curtain.

elevation 1351.50 m in the creeping slope, seepage only starts to respond to reservoir level at approx. 1384 m, which is 21 m below top water level. The piezometric level in the slope thus decreases by 32.5 m before the pressure in the gallery starts to rise. Seepage water flows in the exploration gallery reach a maximum of 7 l/s. Seepage in the left rock slope, which is measured at the end of the bottom outlet and spillway conduit, is dependent on reservoir level, peaking at 17 l/s.

At top water level, the six relief wells discharge up to 32 l/s. The weirs on the various relief wells are activated at different reservoir levels. The first weir starts to discharge water at an elevation of approx. 1377 m, which is some 28 m below top water level. The relief wells and the central seepage measuring weir located at the downstream footing of the toe weight show a linear correlation between seepage and reservoir level. The central measuring weir discharges a maximum of approx. 60 l/s. Linear correlations with reservoir level between top water level and drawdown level are also to be found in the case of the seven relief wells downstream of the central seepage weir, which discharge up to approx. 30 l/s. Spring discharge is also monitored.

Extensive monitoring for solids at 34 gauge points have given no indication of permanent sediment loads in the seepage; the variations in the readings can be largely explained by precipitation and/or local events. Moreover, the values are frequently in the same range as those for the impounded water.

Dam no. 16: Bolgenach

The topography of the site of the 102 m high Bolgenach Dam is complex. As indicated by Fig. 59, which shows the shape of the dam on plan relative to the abutments at three levels (680.0 m, 700.0 m and 720.0 m), the valley flanks where the central core connects form natural embayments on both sides. According to [63] and [64], this is the result of surface erosion in the soft strata of marl that strike across the valley between hard layers of sandstone and dip steeply in the upstream direction. As can be seen from maximum cross-section in Fig. 5, they form the seal for the foundations.

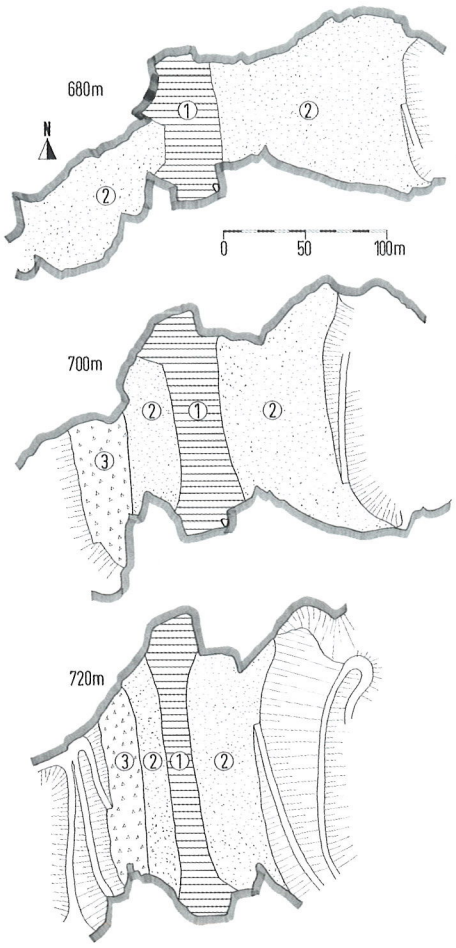

Fig. 59 *from [66]: Dam no. 16*
Valley elevations 680m, 700m and 720m
1: Earth core
2: Shell zone of gravel
3: Shell zone of rockfill

The slight downstream curvature of the axis of the dam and upstream inclination of the central moraine core below elevation 700 m made it possible to connect the core to the marl strata with some involvement of the sandstone ribs. The downstream shell zone is constructed of bench gravel, while the upstream shell zone is a combination of gravel and quarry-run material. The extent to which the valley is narrowed by the projecting sandstone ribs upstream and downstream of the dam core is shown in the following table :

Elevation (m)	**Narrowing to % of core length** upstream	downstream
665	20%	41%
680	25%	55%
700	35%	65%
720	57%	63%

Table 5: *Narrowing of the valley*

The relationship between height H of the levels above the riverbed and width W of the valley at those levels, as shown in Table 6, gives an indication of load transfer transverse to the valley.

Elevation (m)	Upstream shell zone	Core	Downstream shell zone
665	H/W = 0.90	0.18	0.48
680	1.09	0.28	0.49
700	0.93	0.35	0.55
720	0.94	0.36	0.57
748.60 (crest)		0.39	

Table 6: *Relationship between height H and width W of the valley*

As can be seen, the sandstone ribs upstream from the core form a gorge-shaped valley section.

From [66] the bearing behavior of the dam can be summarized as follows:

Deformations:

Monitoring has produced some surprising results. Given the topography of the site, one would have expected the upstream constriction of the valley to have had a barrier effect and movements to have occurred in a mainly downstream direction, but in fact the opposite is the case. As can be seen from Fig. 60, the most pronounced movements in the surface monuments have been upstream of the axis of the dam. The zero line of horizontal movement lies well into the downstream shell zone. There is thus significant upstream movement in the whole of the upper part of the dam. The settlements at the crest reference points shown in Fig. 61 also indicate an upstream tendency. This contradictory pattern of dam behavior could be due to the influence of impounding operations, with frequent changes in storage level in the top reservoir zone of approx. 15 m. The continual fluctuations in uplift pressure could have caused the redistribution of grain accompanying the movements in the dam, especially in the upstream shell zone with its quarry-run rock material. This is clearly the dominant factor, as the monitoring data offer no evidence of downstream deflections in response to horizontal hydrostatic pressure. A further possible explanation is to be found in the results of earth pressure monitoring described below. The vectors of movement for the upstream crest reference points are shown for the longitudinal

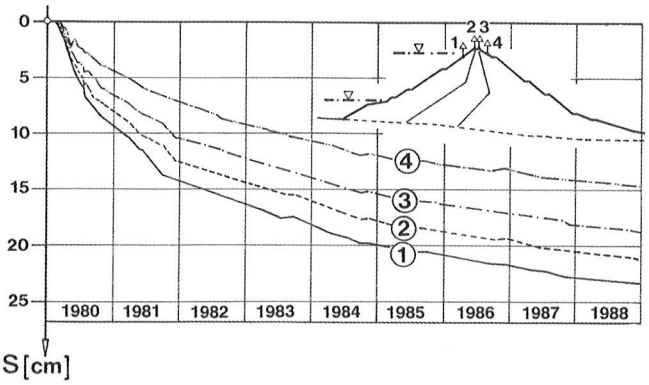

Fig. 61 *from [9]: Dam no. 16*
Time-settlement curve of crown points up to 1988

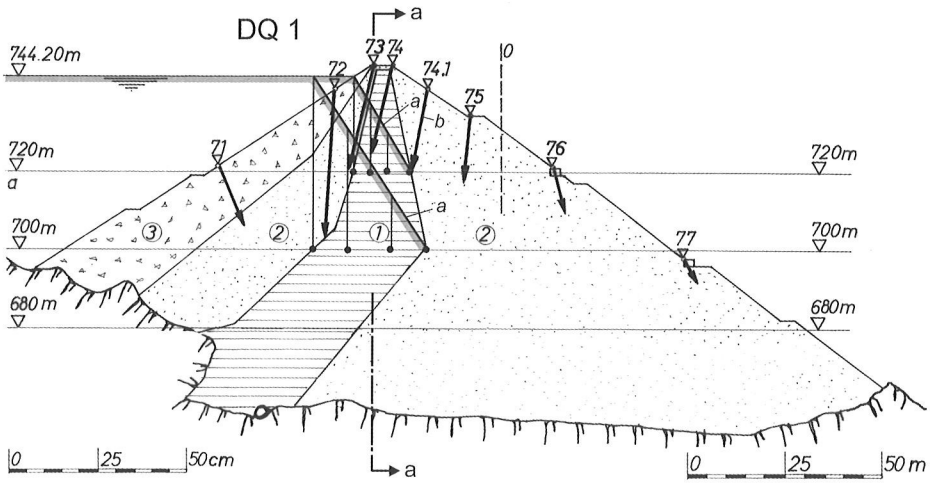

Fig. 60 *from [66]: Dam no. 16*
Dam section DQ1
a: Dissipation lines of reservoir water pressure at elevations 700m and 720m
b: Vectors of movement of surface points up to 1998
0: Zero line of displacement
Zones 1,2 and 3, see Fig. 59
a-a: Longitudinal section – Fig. 62

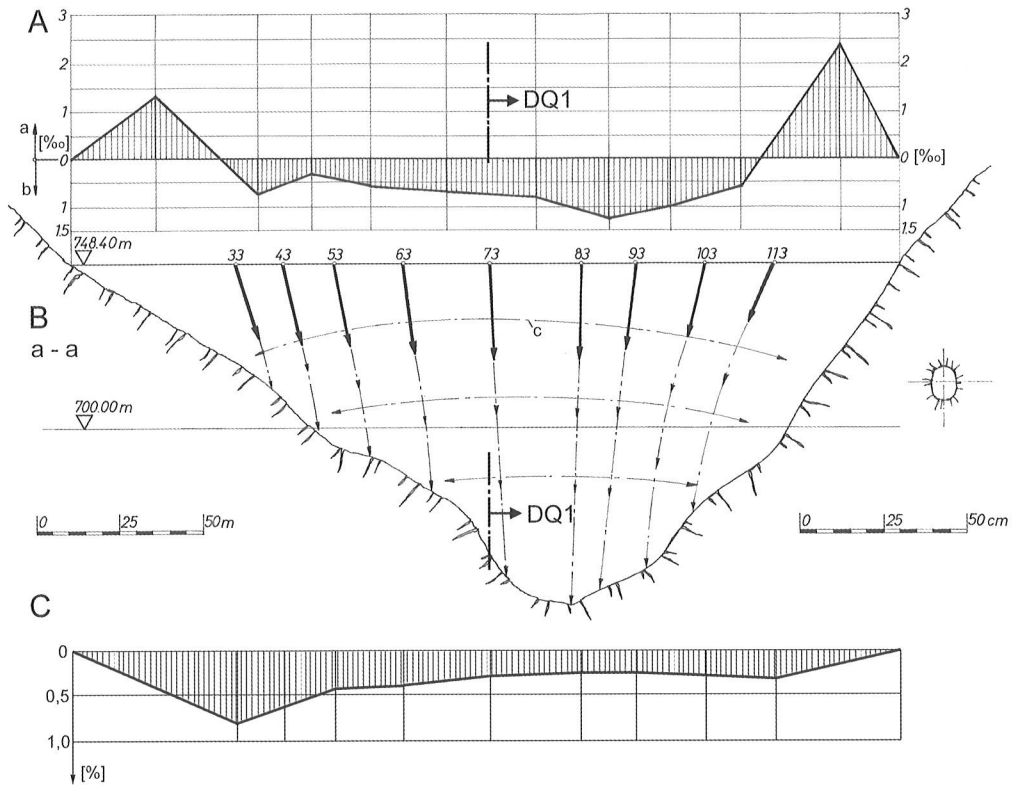

A: Tension (a) and compression (b) along the crest
B: Vectors of movement of US crown points up to 1998
C: Δh/h: Relative settlements (%)
c: Arching effect (see Fig. 52)

***Fig. 62** from [66]: Dam no. 16*
Longitudinal section a-a:

section in Fig. 62. Along the crest of the dam there are expansion effects at the edges and compression effects in the middle. As a result of relative movements, an "arching effect" transverse to the valley has developed (see Fig. 52).

Pore water and earth pressures:

The pore water pressures can be used to describe the decrease in piezometric level in the dam. According to Fig. 60, the earth core alone is responsible for the decrease in piezometric level at elevations 700 m and 720 m. As only the sensors located upstream from the axis of the dam indicate an impounding effect, it can be assumed that the readings from the downstream sensors relate to residual pore water pressures. At level 700 m the readings are less than 10 % of theoretical vertical pressure γ x h, and at level 720 m approx. 20 %. That suggests that the process of core consolidation is largely complete.

Extensive earth pressure monitoring was used in combination with pore water pressure data to determine the magnitude of load transfers from the softer core to the stiffer adjoining zones. Table 7 below shows the effective vertical earth pressures $\sigma'_V = \sigma_V - u$ (u = pore water pressure) measured for LC deadweight and top water level at elevations 700 m and 720 m of cross-section DQ1. The load case of deadweight is taken from the data obtained during lowering of the reservoir to drawdown level at 695 m from October 1997 to April 1998. Where duplicate measuring points were available, the arithmetical average of the two values was calculated. The location of the measuring points is shown in Fig. 63. For comparison the table also indicates, for every measuring point, the effective vertical earth pressures σ_V' theor. = γ . h - u converted to dam height using γ= 23 kN/m³.

Elevation (m)	Load case	σ_V' and (σ_V' theor.) at the measuring points (kN/m²)			
		1	2	3	4
700	deadweight	500 (724)	530 (789)	720 (939)	1090 (724)
700	top water level	320 (324)	270 (689)	720 (939)	1090 (724)
720	deadweight	650 (506)	450 (461)	330 (501)	750 (506)
720	top water level	520 (306)	260 (401)	330 (501)	750 (506)

***Table 7:** Effective vertical earth pressures σ_V' and (σ_V' theor.) at elevations 700 m and 720 m*

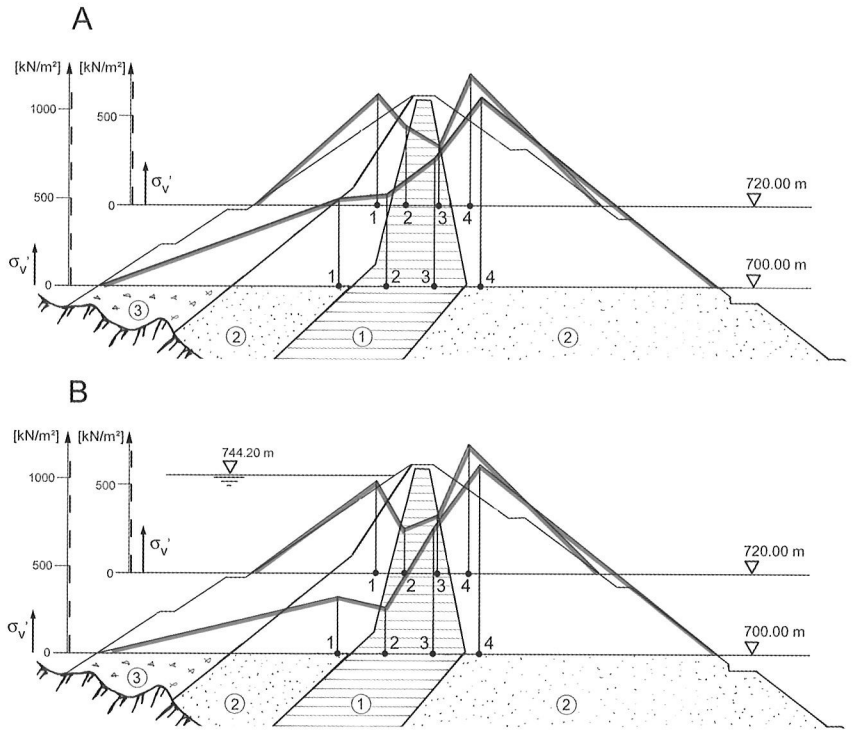

Fig. 63 *from [66]: Dam no. 16*
Distribution of effective vertical earth pressure σ_V' *at elevations 700 m and 720 m*

A: LC dead weight
B: LC max. reservoir level
1, 2, 3, 4: Measuring points
Zone 1,2 and 3, see Fig. 59

Notes:

- At both elevations, the measured effective pressures σ_V' at point 4 downstream from the core are higher than the theoretical values σ_V' theor.
- At upstream point 1 for elevation 720 m, too, σ_V' is higher than σ_V' theor.
- For all other measuring points at both elevations, the theoretical σ_V' theor. values are higher than the measured effective pressures σ_V'.

From these results it can be concluded that a part of core load is transferred to both shell zones at elevation 720 m but only to the downstream shell zone at elevation 700 m. Measuring level 700 m would therefore seem be relieved of vertical load by a load transfer transverse to the valley (arching effect) in the narrow gorge-shaped section of the valley located upstream from the dam. That is suggested by the lower measured values for σ_V'at elevation 700 m compared with elevation 720 m at point 1. No such load-relieving effect can be detected at elevation 700 m downstream from the core, where the narrowing of the valley is much less pronounced, as can seen from Table 5.

Another significant point is that, in spite of load transfer all measured effective pressures σ_V' in the core are higher than hydrostatic pressure, so that no hydraulic fracturing could occur. For measuring points 4 downstream from the core, the readings for σ_h can also be used to calculate the share of reservoir water pressure. It is much higher at elevation 700 m than at elevation 720 m, namely $\sigma_h = 0.9\sigma_W$ compared with $\sigma_h = 0.83\sigma_W$. The load bearing role of the core is thus considerable and is higher than in the case of the Gepatsch rockfill dam where $\sigma_h \doteq \sigma_W$.

The shielding effect on the lower part of the dam upstream from the core deriving from load transfer transverse to the valley suggests that the greater downstream earth pressure needed to achieve the necessary equilibrium for LC deadweight has caused upstream movement, which has obviously not been compensated by the subsequent thrust of the impounded water and the deformations in the inclined moraine core.

Seepages and the decrease in piezometric pressure in the foundations:

For all seepage flows, the influence of hydrostatic load is slight or negligible. With total seepage flows in the inspection gallery of between 0.2 l/s and 0.4 l/s, Bolgenach is technically an impervious dam. The decrease in piezometric level in the marl strata in continuation of the earth core correlates with reservoir level. Reservoir water pressure is completely drained in the sandstone layers of the core foundation area.

6. Additional problems

6.1 Shear resistance of loose material on foundation rock

In one of the research projects conducted at the BFG Institute [11] and [68], various potential sliding bodies were studied with reference to the roughness of the surface of the bedrock (see Fig. 64). The decisive factor was micro-roughness in the case of sliding bodies A and macro-roughness for sliding bodies B. Tests to determine surface roughness were performed using large-scale shear apparatus with a shear surface of 1 m² (Fig. 65). The specimen materials were obtained from the natural terrain by drilling and placed in a sturdy concrete container. Fig. 66 shows the result of a test with the effective shear angles φ_S for natural roughness I and engineered roughness II and III, which is obtained by cutting grooves in the rock. The internal angle of friction φ of the fill was also measured. According to [68], a roughness coefficient can be determined that permits effective shear angle φ_S to be read off from a nomogram for every bedrock surface shape. Where necessary, it is then possible to take the appropriate measures to artificially roughen the rock surface. The principle of engineered roughness based on the results of the above test method was first applied in the case of Dam no. 15 for a steep rock surface abraded by glacial action (Fig. 67). The method was also used to study the roughness of the bedrock for Dam no. 11.

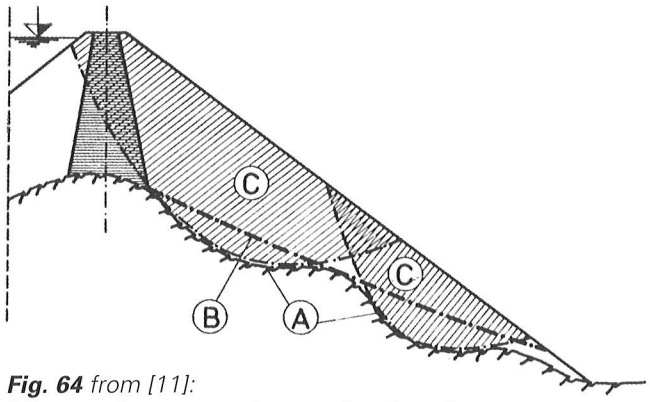

Fig. 64 *from [11]:*
Micro- and macro-roughness of rock surface
(A) Decisive micro-roughness.
(B) Decisive macro-roughness.
(C) Potential sliding bodies.

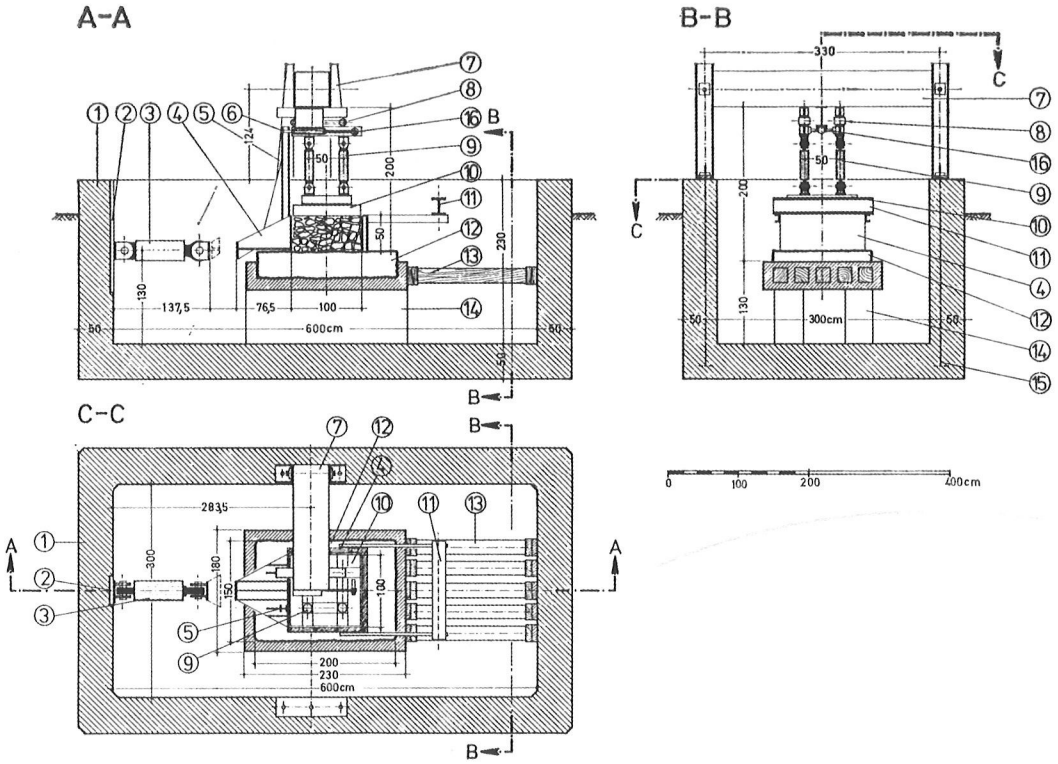

Fig. 65 *from [11]:*
Large-scale shear apparatus.

(1) Test concrete trough.
(2) Lateral thrust plate.
(3) Horizontal hydraulic jack, 1300 kN.
(4) Shear box.
(5) Engaging bar for roller cage (8).
(6) Coupling piece.
(7) Yoke for the vertical jacks (9).
(8) Roller cage.
(9) 4 vertical hydraulic jacks, 250 kN each.
(10) Pressure transfer plate of the vertical jacks (9).
(11) Balance weight.
(12) Rock slab under test in concrete envelope.
(13) Horizontal thrust bars.
(14) Concrete bed.
(15) Anchors prestressed for the yoke.
(16) Hydraulic jack for advancing the roller cage (8), as an alternative to the engaging bar (5).

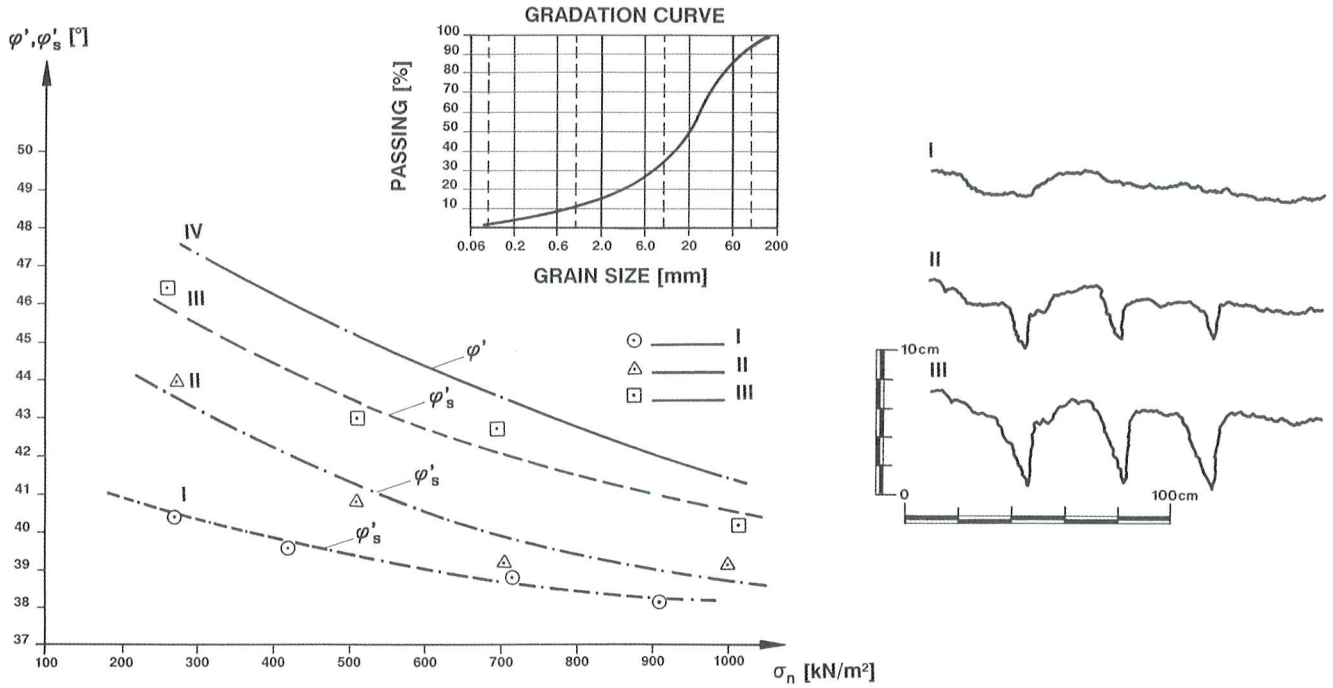

I: Natural roughness of rock surface
II, III: Engineered roughness
σn: Normal stress at shear plane
φ': Effective angle of internal friction of the fill
φs': Effective shear angle

Fig. 66 *from [9]: Dam no. 15*
Results of the large-scale shear tests.

Fig. 67 *from [9]: Dam no. 15*
Cut groove in the smooth rock.

6.2 Filter criteria for geotextiles

Resistance to erosion in a sealing element is one of the key requirements in fill dam construction. For some decades now it has been possible to satisfy this requirement through the use of synthetic filters (geotextiles made of woven and non-woven fabrics). Dam engineers have often been hesitant to use geotextiles, however, as they feel that too little is known about their aging stability relative to the long service life of an embankment dam. The objective of one of the research projects conducted at the BFG Institute [12] and [69] was to develop criteria for geotextiles comparable to those applied to natural filters on the model of the Cistin - Ziems criteria [70]. The relevance of these criteria derives from the relatively good comparability of the pore channels to be found in natural filters with mesh size M_W of woven fabrics and pore size O_{90} of non-woven fleeces. According to Ogink, O_{90} is the grain diameter of a 50 g specimen that corresponds to a 90 % residue on the screen of a non-woven fabric. Fig. 68 shows the example of the criteria developed for laminar flows up to a non-uniformity of the soil to be protected of U = 5. [69] also includes criteria for $U_I > 5$ and for turbulent flows ($U_I = d_{60}/d_{10}$).

In the case of Dam no. 16 (Bolgenach), the gravel

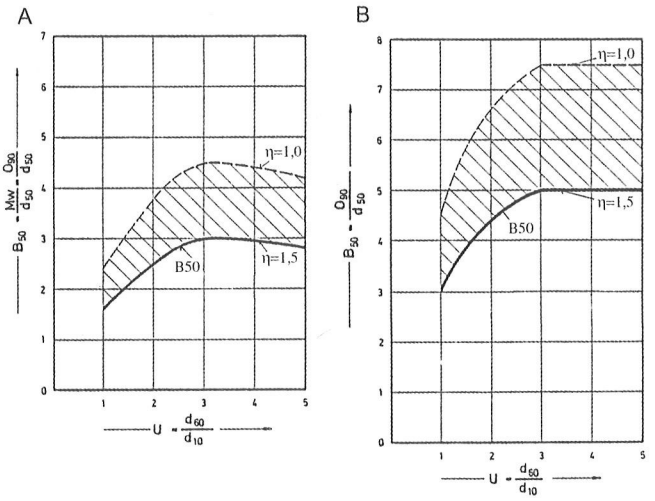

Fig. 68 *from [69]*
Filter criteria for geotextile with laminar water through - flow.
A: Criteria for nets or thin fleeces
B: Criteria for thick fleeces
η: Safety factor
B50: Design value

filter in the downstream shell zone was wrapped in fabric. A possible application would be a chimney drain installed downstream from an earth core using the dry slotted wall process [71] and protected with a non-woven geotextile on both sides.

6.3 Determination of loads on embedded rigid structures

In Austrian embankment dams, rigid structures in reinforced concrete in the form of galleries and shafts are primarily constructed as part of the dam monitoring system but may also play a role in drainage during construction, for grouting the foundations independently of fill placement, and in routing pipes for bottom outlets. As a result of the considerable fill heights involved, such structures differ significantly from those to be found in highway and canal construction. In a research project at the BFG Institute [25], the standard methods employed to calculate loads on underground pipes were modified with the help of four correction factors $f_{1 \text{ to } 4}$ for vertical loads and four factors $g_{1 \text{ to } 4}$ for horizontal loads. Each factor relates to a load case that can apply in an embankment dam. These factors make it possible to correct the results of FEM analysis for a normal case to take account of the real loads involved in fill dams. The proposed method is easy to use and covers every conceivable combination of the relevant parameters. The reliability of the method was verified with the help of the measured values available in the literature for ten examples, and the results are presented in [25]. In eight cases, agreement with the measured data varies between -5 % and +6.2 %. In the other two examples, the result was a deviation of -33.3 % and +23.3 %, which suggests that the measured data are doubtful.

6.4 The prestressed embankment dam

Fill dam research at the BFG Institute terminated with the development of a new approach to safety for embankment dams [19] [75]. In order to reduce the risk of a negative reaction to the thrust of the impounded water on first filling, the concept of the prestressed dam was developed to obtain full loading and a reliable check on the sealing works with the reservoir still empty. Fig. 69 shows in diagrammatic form how the method works.

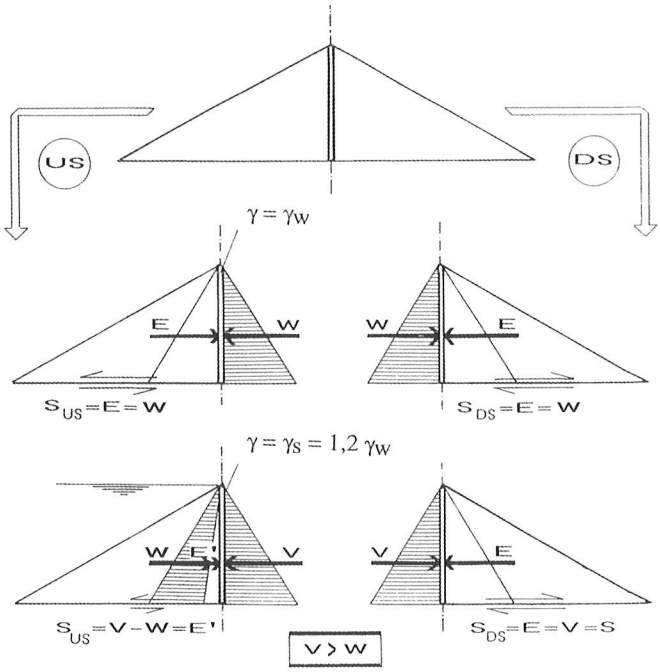

Fig. 69 *from [19]:*
Prestressed embankment dam.
US/DS: Upstream/Downstream.
W: Water pressure force.
E: Earth pressure force.
S: Shear force.
γ_w: Specific weight of water.
γ_s: Unit weight of clay concrete.
V: Horizontal pressure force of clay concrete before hardening.
E': Earth pressure force under uplift.

Construction stage:

In the course of fill placement, two synthetic membranes are installed together at the center of the dam with an impervious connection to an inspection gallery or cutoff wall. During or on completion of fill placement, the space between the two membranes is filled with water so that full hydrostatic

load is applied to the center of the dam. As can be seen in Fig. 70/A, this produces a shear prestress in the two shell zones and thus activates earth pressure E = W. When the lateral movements in the shell zones have subsided, the water in the space created between the two membranes is replaced by a suspension of powdered clay, cement and water with a specific weight of about $\gamma = 1.2\ \gamma_W$. That increases the prestress to E = V.

Impounding stage:

At reservoir filling, only minor additional horizontal loads are produced as the sum of hydrostatic pressure W and earth pressure under uplift E' roughly corresponds to the increased prestress V. Fig. 70

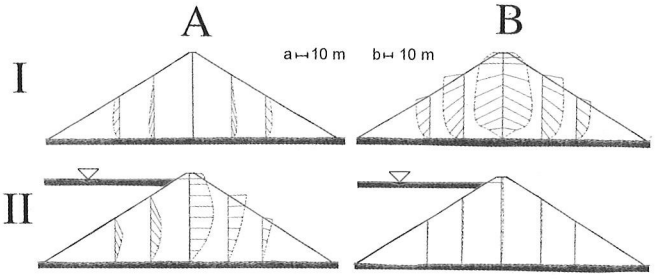

Fig. 70 *from [19]:*
Prestressed embankment dam. Results of 2-D FEM calculations of a research dam.
(A) Conventional dam.
(B) Prestressed dam.
(I) Load case: deadweight.
(II) Load case: maximum reservoir level.
(a) Geometric scale of dam.
(b) Scale of displacement.

presents a comparison of the bearing behavior of a research dam with an interior membrane seal without prestressing (A) and with prestressing (B). As can be seen, horizontal deformations deriving from the thrust of the impounded water are anticipated during the construction phase in the case of a prestressed dam. Similar behavior was observed in the 61 m high Mauthaus earth core dam, in which the plastic core material developed high lateral pressures during the construction phase and thus had a prestressing effect on the shell zones [74].

To confirm the validity of the concept, tests were performed on 1.3 m high plane strain models and the measured data verified with the help of FEM analysis. As can be seen from Fig. 71, the results were in good agreement. Fig. 71a shows the excavated clay concrete core following testing with a plane strain model.

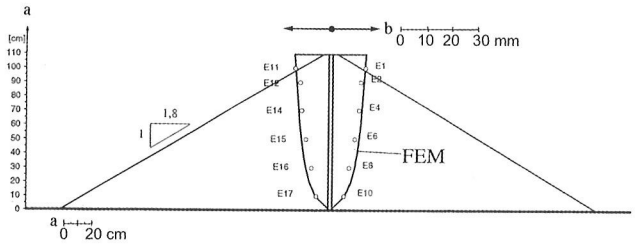

Fig. 71 *from [19]:*
Prestressed embankment dam. Deformations of the 2-D physical model.
Load case: prestressed with clay concrete suspension
FEM: Results of FEM calculations
E1-E17: Results of extensometer measurements
a: Geometric scale.
b: Displacement scale

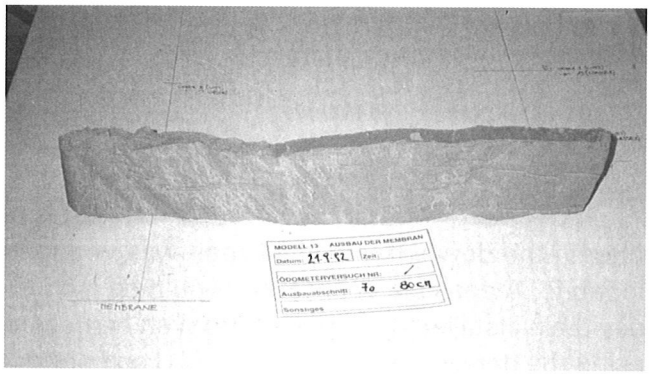

Fig. 71a *from [19]:*
Prestressed model dam. Excavated part of the hardened clay concrete between the two membranes after the test.

7. Construction

7.1 Investigations and choice of materials

As mentioned above with regard to Dam no. 2 (Freibach), Professor Breth was responsible for the introduction of soil mechanics for investigations in the field of fill dam construction in Austria in the mid 1950s. One of the developments that resulted from the differences between the requirements of dam construction and those of conventional soil engineering was an increase in the size of the test equipment. The construction of Proctor cylinders with a diameter of 30 cm for testing materials with a grain size of up to 50 mm is a case in point. The same applies to the sample diameters of triaxial cells. Similarly, to determine the shear strength of coarse-grained material like quarry-run rock for Dam no. 3 (Gepatsch), French large-scale shear testing equipment measuring 1.2 m x 1.2 m was used for the grain fraction up to 200 mm. In 1972 the BFG Institute commissioned the large-scale shear testing equipment shown in Fig. 65, and numerous large-scale shear tests were performed in addition to the research project discussed in section 6.1. Fig. 72 shows the shearing curve from a test with shell zone material of quarry-run Koralpen gneiss for Dam no. 19 (Feistritzbach).

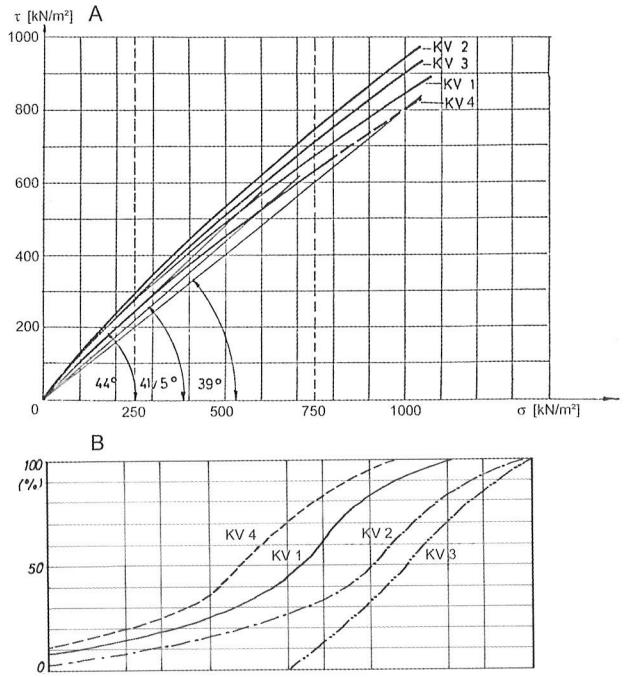

Fig. 72 *from [47]: Dam no. 19*
A: Results of large shear tests and triaxial tests with rockfill material
B: KV 1, 2 and 3: Grain graduation of material for direct shear test
KV 4: Grain graduation of triaxial tests

The above mentioned large-scale Proctor cylinders were also used for permeability testing [26]. In the case of the Gepatsch rockfill dam, for example, they were employed to measure the reduction in permeability in core material resulting from the addition of 1 % bentonite. As can be seen in Fig. 73, which is taken from [76], roughly the same improvement is achieved with widely varying grain fractions < 0.2 mm in the core material.

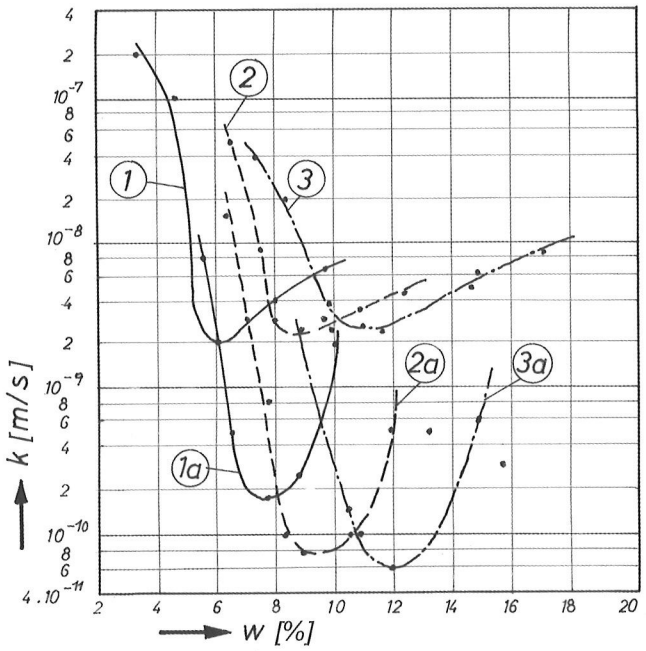

Fig. 73 *from [76]: Dam no. 4*
Result of permeability test with core material – Grain fraction up to 50 mm diameter
(1), (2) and (3): Grain fraction lower 0.2 mm: 13%, 27% and 36%
(1a), (2a) and (3a): With addition of 1% bentonite

The BFG Institute was also the first to investigate the question of changes in permeability in the course of triaxial testing. Well graded core material with a 17 % grain fraction < 0.06 mm and a maximum grain size of 30 mm was placed in the equipment shown in Fig. 74, which has a sample diameter of 15 cm. Horizontal seepage occurred at the middle level of the sample. The result in Fig. 75 shows a decrease in initial permeability throughout the deformation process.

Fig. 75 illustrates the wide range of construction materials used, taking Dam no. 4 Gepatsch as an example. The materials selected for Austrian dams are primarily well graded soils in their natural composition such as talus material, moraine or alluvial deposits and quarry-run rock. In the case of earth core materials, it is normally necessary to screen out the larger stones and rocks (grain fraction > 80 mm) in order to reduce segregation tendencies at placement and to increase the fine-grained fraction.

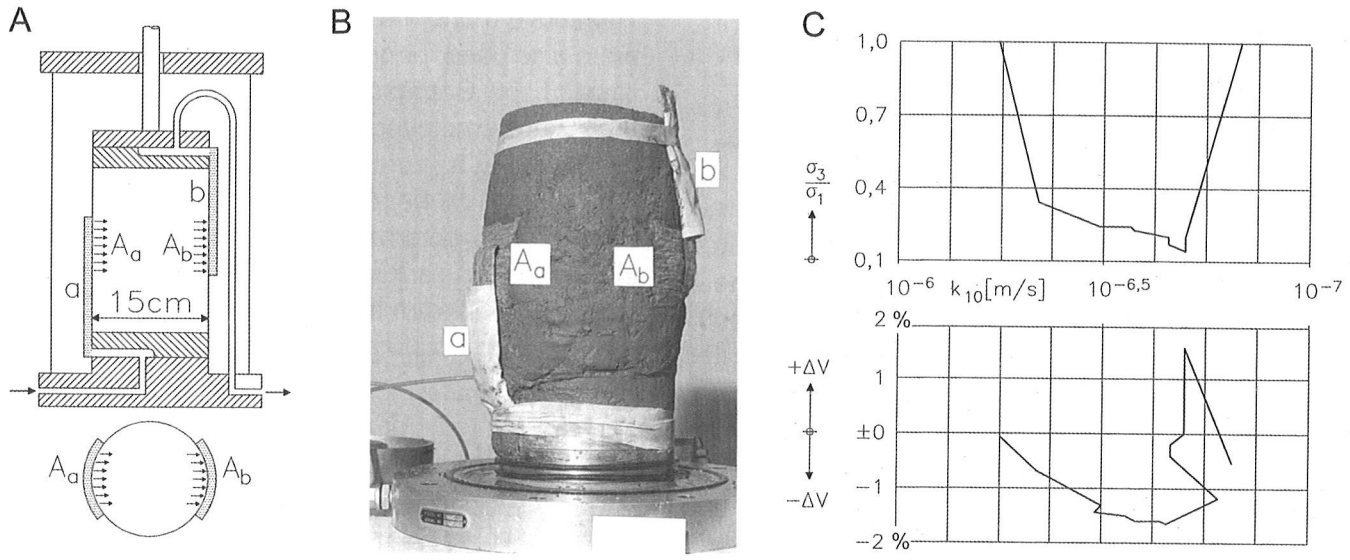

Fig. 74 *from [20]: Dabaklamm project*
Triaxial permeability test with core material
A: Triaxial cells
B: Specimen after test
C: Results

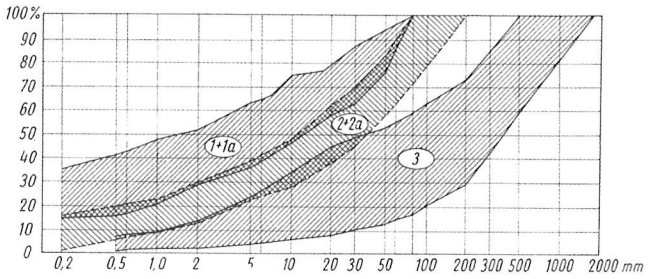

Fig. 75 *from [27]: Dam no. 4*
Grain graduation of dam materials – Dam zones, see Fig. 5.
(1) Impervious core (talus and moraine material).
(1a) Core with addition of 1% bentonite.
(2) Transition zones (gravel).
(2a) Extension of the transition zone (gravel).
(3) Shell zones (quarry-run rock and oversize).

The material of choice for filter and transition zones is alluvions in their natural composition. The high permeability of quarry-run rock makes it particularly suitable for upstream shell zones.

7.2 Excavating, processing, placement

Excavating: Whereas dam materials can normally be excavated from the valley flanks without much risk of slope water problems working from the upper to the lower levels, pits located at the valley bottom often have to contend with groundwater. In the case of dams built using quarry-run rock, the stability of the excavation face remaining after quarrying is an important consideration. In the case of the 230 m high wall at Versetz quarry (Fig. 76), which was used to obtain the shell zone material for Dam no. 4 (Gepatsch), for example, six extensometers were installed to monitor stability. In the graphs plotting deformations over time, every major round of blasting is indicated by a step in the plots.

Processing: Fig. 77 shows the processing plant for the core material used for Gepatsch rockfill dam. A wobbler (a) was used to screen the grain fraction > 80 mm. The material was then dried to reduce the water content by a maximum of 3 % in four rotary kilns (b) with a capacity of 100 t/h each. The material was loaded onto trucks at (c), in some cases after mixing with 1 % bentonite in pan mixers and intermediate storage in silos. The heat absorbed during drying permitted placement in sub-zero temperatures and thus extended the construction season. In the case of Dam no. 16 (Bolgenach), the core material on the conveyor belt leading from the screening plant was sprayed with water to raise the water content to the required level. For Dam no. 5 (Durlassboden), the core material also required drying prior to improvement with bentonite (like Dam no. 4). Special plant of the type used in road surface construction was employed for asphaltic concrete.

Placement: For all Austrian embankment dams, the fill material was placed in layers and compacted with rollers in line with standard international practice [2]. In the case of Dam no. 4 (Gepatsch), as mentioned above, this procedure was also adopted for the first time ever with quarry-run rock material with a maximum grain size of 1 m. The 8 t vibratory rollers employed for the purpose, however, achieved inadequate compaction in the 2 m lifts. In subsequent dams, the lifts were accordingly reduced to 1 m and less and maximum grain

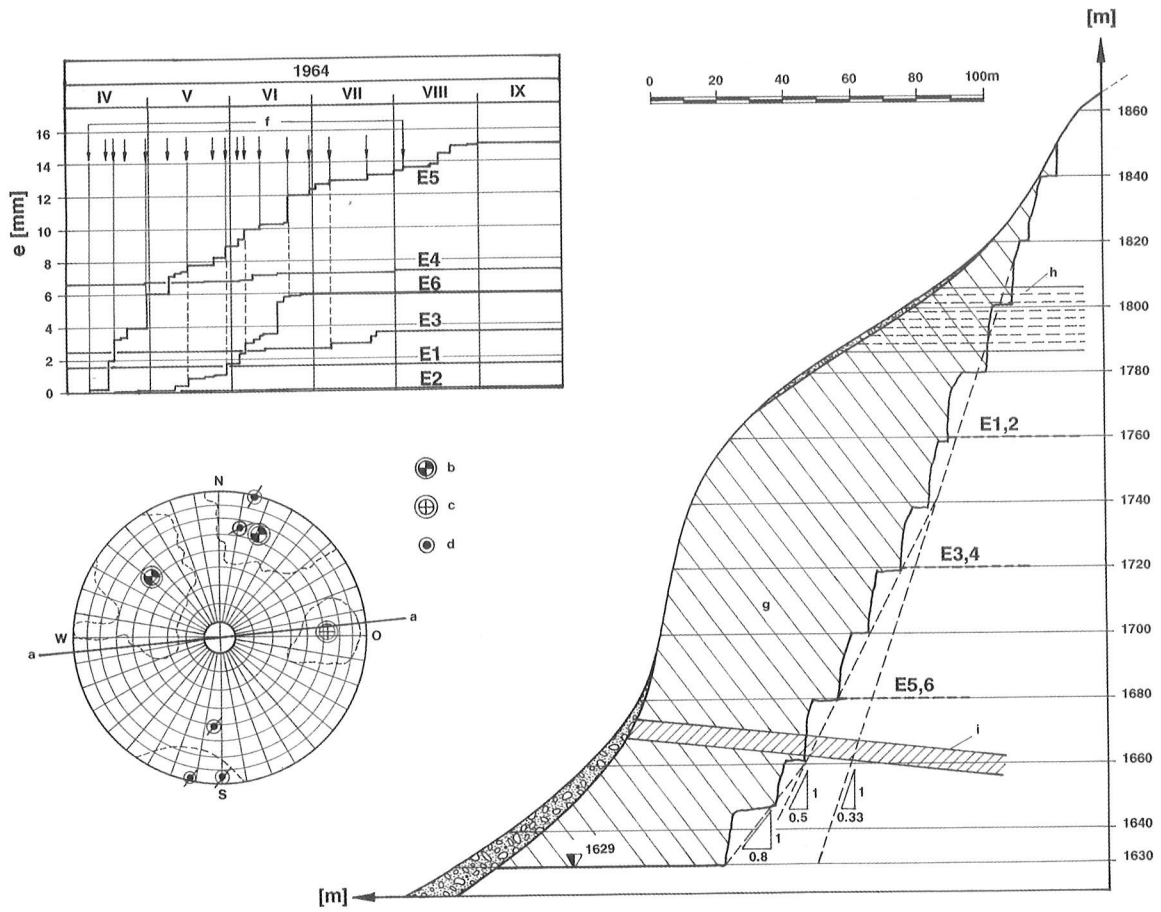

Fig. 76 *from [9]: Dam no. 4*
Versetz quarry.
a-a) Direction of quarry face.
b) Main joint poles.
c) Secondary joint poles.
d) Poles of the schistosity planes.
e) Horizontal face displacement.
f) Blastings.
g) Eye gneiss.
h) Squeezed zone.
i) Diabas.
E1-E6) Extensometer.

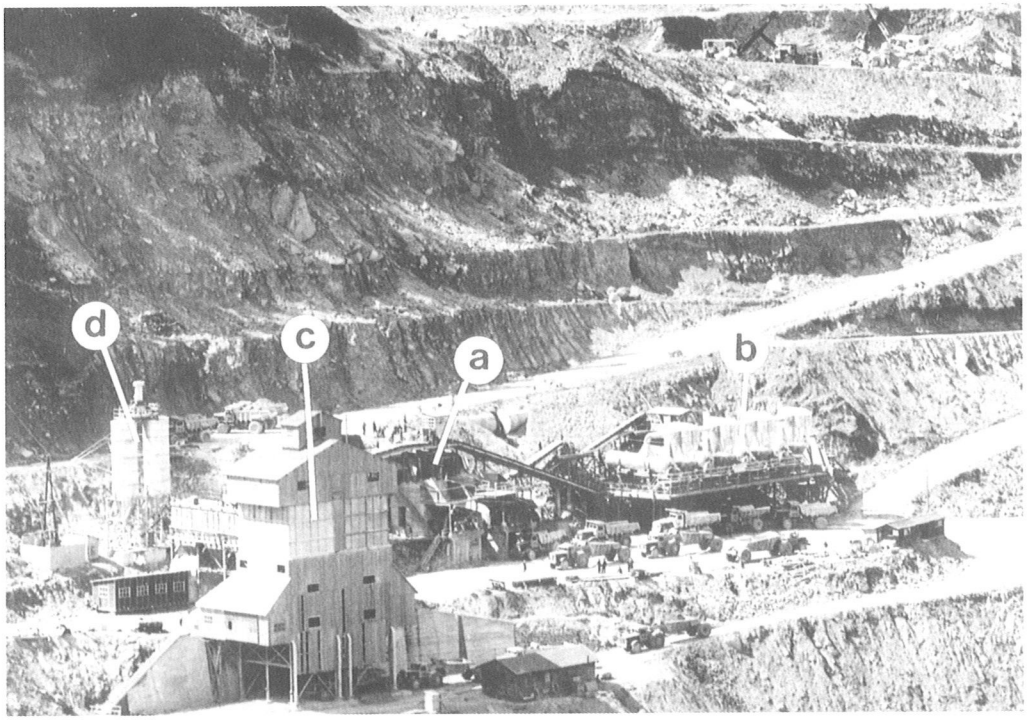

Fig. 77 *from [9]: Dam no. 4*
a) Screening-, b) Drying-, c) Mixing plants. d) Silos for bentonite.

size to 75 cm and less, while the compaction capacity of the rollers was greatly increased. With regard to the problem of segregation in quarry-run rock, good results have been achieved by dumping the fill material on the surface of a new lift and dozing it over the edge onto the previous layer. To reduce saturation settlements, water jets were used to spray quarry-run rock materials for upstream shell zones with approx. 0.5 m^3 of water per m^3 of fill.

The use of rockfill material for the shell zones of Gepatsch Dam had advantages with regard to the shorter construction period resulting from the possibility of winter placement [29] and also with regard to continuous operation of the quarry. As can be seen from Fig. 78, some 50 % of the rockfill was actually placed in the winter half year, using deicing salt to melt the snow on the fill surfaces. The higher lateral pressure generated by the placement of the shell zone ahead of the core in spring reduced the rate of consolidation settlement in the earth core.

Standard highway engineering technology was employed for the asphaltic concrete facings, which were placed using facing machines controlled from winch trucks on the dam crest and then compacted with rollers. Asphaltic concrete core walls, on the other hand, required the development of special finishers capable of placing the asphaltic concrete core together with the adjoining zones in one combined operation. Fig. 79 shows a finisher of a type used at the time by the Strabag company. It served to place approx. 25 cm thick layers and to compact them to about 20 cm with a porosity of 2 % to 3 %.

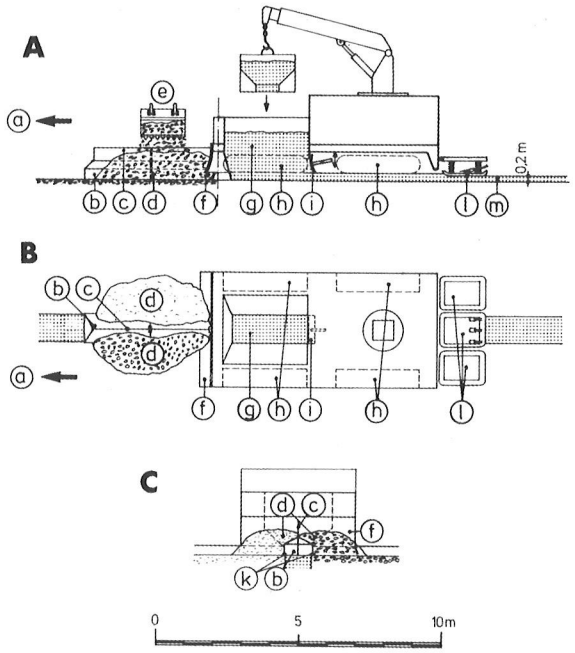

Fig. 79 *from [39]: Dam no. 15:*
Finisher for placement of the asphaltic concrete core:
(A) Side view.
(B) Plan view.
(C) Front view.
(a) Direction of core wall placement.
(b) Protruding bill covering the core wall.
(c) Separation plate.
(d) Transition zone material.
(e) Road loader for transition zone material.
(f) Front shield for leveling the transition zones.
(g) Storage and feeder shaft for asphaltic concrete.
(h) Track-type undercarriage.
(i) Control valve for asphaltic concrete
(k) Skids.
(l) Group of three vibrating plates for asphaltic concrete and transition zones.
(m) Layer of asphaltic concrete.

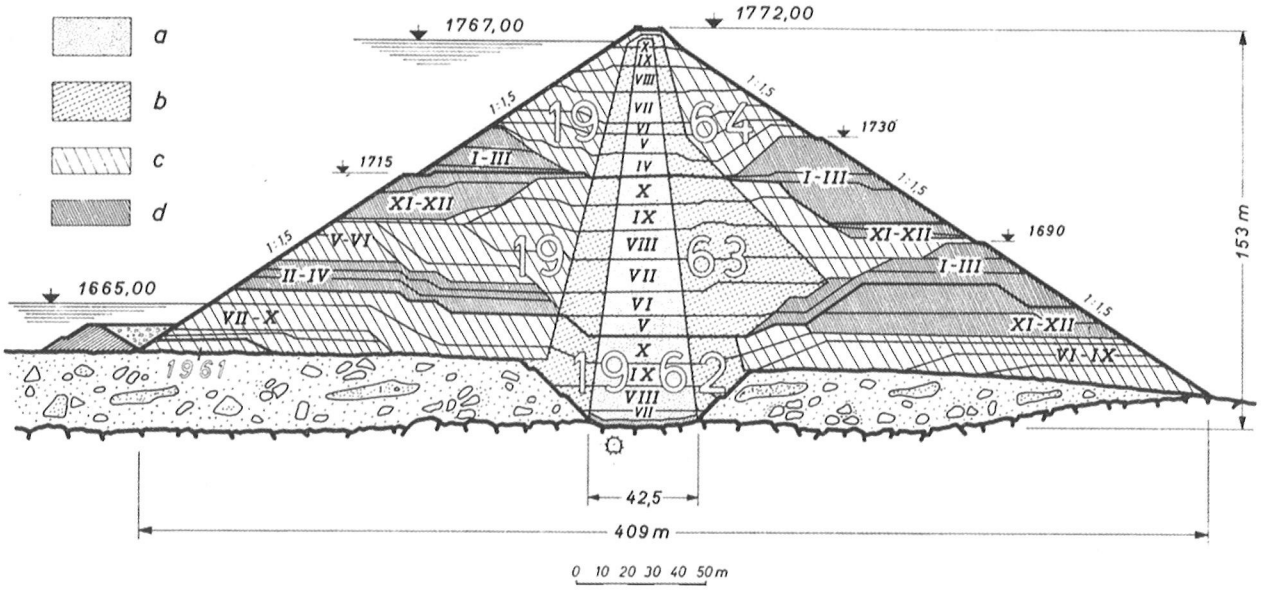

(a) Zone 1, core.
(b) Zone 2, transition zones.
(c) Zone 3, shell zones, summer fill.
(d) Zone 3, shell zones, winter fill.

Fig. 78 *from [29]: Dam no. 4*
Cross-section with monthly fill volumes.

A highly innovative solution was adopted for placement of the connection part of the core material at Dam no. 16 (Bolgenach). Shotcreting equipment was used to spray the core material, screened for a maximum grain size of 30 mm and improved with 3 % bentonite, onto core foundation areas smoothed with the help of roadheader machines. In the case of the Gepatsch rockfill dam, an approx. 10 cm thick clay layer was placed manually. For the treatment of core foundation areas, see [2].

7.3 On-site testing

An important factor in the successful construction of any embankment dam is effective on-site testing. This applies above all to the embankment, where post-construction rehabilitation would be a very challenging and costly task. Of all the indispensable tests for soil mechanical parameters, carried out with different frequencies for each dam zone, densimetry in the field has a special role to play. Fig. 80 illustrates the test body method for fine-grained material which is also provided for in Austrian standard ÖNORM B4412 T2. A test body comprising approx. 10 kg of local material wrapped in PVC film is first compacted and then excavated so that it can be weighed and the volume determined by dipping and weighing.

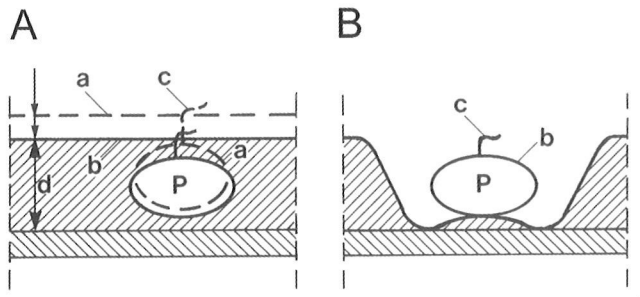

Fig. 80 *from [9]: Dam no. 4*
Density field test using the test body method in accordance with ÖNORM B 4414, T2
A: Compaction stage: a/b before/after compaction
c: Marker wire
d: Thickness of compacted layer
P: Specimen wrapped in PVC film
B: Removal of specimen

For density tests on coarse-grained material as discussed in [9] and [78] (see Fig. 81), fill material is first placed to form a test pit, which is carefully measured. The pit is then filled with weighed material and the settlements measured at the surface of the fill and the bottom of the pit. The volume of the compacted specimen and thus its specific weight can thus be calculated.

Even with the dynamic compaction monitoring methods that are in routine use today, such tests still have a useful role to play for calibration purposes, but they no longer need to be applied so frequently.

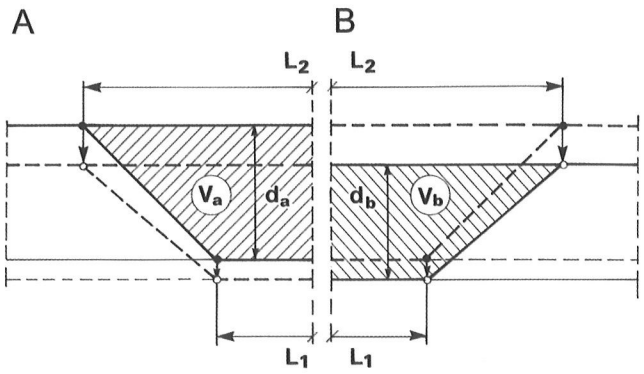

Fig. 81 *from [78]: Dam no 15*
Density field test with coarse-grained material
A/B: Condition before/after compaction

7.4 Foundation treatment

The Austrian approach to foundation treatment is no different from the rest of Europe [2]. In the case of rock grouting with a cement slurry, single-line curtains are normally constructed with repeated rounds of grouting working upwards in approx. 5 m borehole sections until a Lugeon value of 3 or 1 l/min and linear meter is reached depending on the expected water pressure from the reservoir. Curtain depth is assessed on the basis of the discontinuities in the rock. Grout curtains beneath earth cores can be executed prior to core placement and in some cases during construction of the dam, using inspection galleries and working at higher pressures.

The sealing works for the permeable deposits (e.g. alluvion) in the case of Dams nos. 2, 5 and 7 took the form of multiple-row grout curtains injected with suspensions of cement, bentonite and Algonit gel using the sleeve pipe method. As a result of the grouting, the working plane of Dam no. 5 rose by approx. 50 cm. At Dam no. 2, foundation grouting also caused lift in the already completed spillway chute. As described above, sealing works for the permeable deposits in the foundation area of Dam no. 6 (Eberlaste) took the form of the first ever clay concrete cutoff wall with a depth of up to 52 m.

Although the industry has been working for some time to establish agreed quality standards in the field of foundation treatment, the success of such works still depends very much on the experience of the engineers and crews involved. What is important is to keep continuous records of all measures taken so as to permit effective quality assurance work.

8. Monitoring dam behavior and incidents

8.1 Monitoring equipment

In addition to visual inspections, data from monitoring systems are an essential tool in dam surveillance, and the devices used for monitoring dam behavior in Austria have reached a very high standard. The innovations introduced in this field relate not only to the quality of the equipment but also to the data recording practices developed over the last few decades as well as the data transmission and alarm systems for continuously manned control rooms [77]. The result is year-round monitoring of all high embankment dams in Austria and a high standard of dam safety.

In addition to deformations and stresses, seepage flows and the decrease in piezometric level in the dam and its foundations, monitoring in some cases also covers the solid content of the seepage as well as seismic activity.

Table 8 presents a summary of the monitoring equipment to be found in Austrian fill dams over 25 m high. As can be seen, Dam no. 4 (Gepatsch) plays a particularly prominent role in this respect. It was the first dam in which 2D earth pressure measuring was performed [59] and the first to have a new type of horizontal tubes installed for monitoring vertical and horizontal movements in the interior of the dam [27]. These innovations have since spread around the world. Changes in the soil pressure ellipses in Fig. 82 reflect the influence of reservoir water pressure. Guided by the experience gained at Gepatsch Dam, extensive earth pressure monitoring was also performed at Mauthaus Dam in Germany [72]. An exemplary array of monitoring devices is also to be found at Dam no. 15 (Finstertal) as shown in Fig. 83. The installation of two plumb-lines connected by an extensometer in the center of the dam has made it possible to increase the accuracy of crest movement monitoring tenfold to obtain exact data in the mm range and also to establish a continuous monitoring regime. In combination with continuous seepage recording, the Finstertal dam thus features two primary indicators for dam safety. The individual devices are described and discussed in detail in [9], [44] and [45]. Monitoring systems for the reservoir banks are dealt with in section 9.4.

As far as earth pressure monitoring is concerned, it is necessary according to [10a] to determine a calibration factor in the initial placement period. This procedure was developed for the construction of the Mauthaus Dam [72] and was employed at the BFG Institute for all stress measuring on the physical models used [10] and [10b].

No.	Name of dam	Number of measuring stations							
		Deformations				Stresses		Seepage	Piezo-meters
		Dam surface		Internal		Pore water pressure	Earth pressure		
		Settlements	Deformations	Settlements	Deformations				
1	Bielerdamm*)	24	7	3	3			44	
2	Freibach	5	5					8	43
3	Diessbach	3						2	
4	Gepatsch	58	58	285	285	32	51	3	20
5	Durlassboden	18	18	143	140	44	6	17	23
6	Eberlaste (Stillupp)	21	6					16	11
7	Wurten	11	6	32	32			5	
8	Latschau II	102	29	5		16		6	
9	Galgenbichl	37	37	6				5	7
10	Gösskar	64	64	8		6		8	6
11	Oscheniksee	62	62	47	47			4	
12	Hochwurten	31	31	34	34			4	11
13	Gross-See	25	25	22	22			4	
14	Längental	22	22					11	2
15	Finstertal*)	110	110	114	118	12	110	3	13
16	Bolgenach	28	28	20	29	28	10	5	3
17	Bockhartsee*)	23	23	36	104		21	8	2
18	Zirmsee	14	14	46	20			7	1
19	Feistritzbach (Koralpe)	39	39	95	95		62	7	28
20	Rotgüldensee	38	38	81	81	10	24	11	8

Table 8 *from [9]: Main monitoring equipment in Austrain fill dams over 25 m high. *) Plumpline shaft*

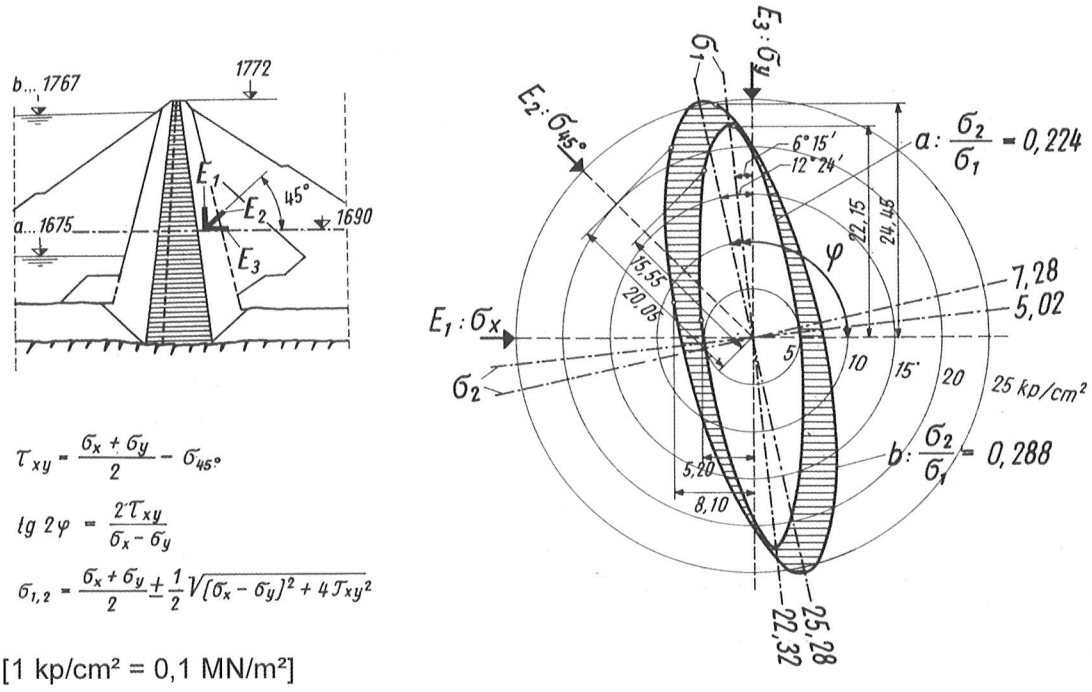

Fig. 82 *from [28]: Dam no. 4*
Soil pressure ellipses in the main dam cross-section for reservoir level at 1675 m (a) and at 1767 m (b). E 1-3: Soil pressure cells.

8.2 Incidents

The term „incidents" is used to describe events requiring immediate corrective measures or major remedial works in excess of routine maintenance, as the following examples show.

During the third filling of Dam no. 13 (Gross-See) in 1981, as reported in [73], an increase in seepage flows was detected at 4 a.m. on 19 July from approx. 15 l/s to 31 l/s and a first-level alarm was given. On 20 July, a second-level alarm was triggered at 47 l/s followed by a third-level alarm at 62 l/s. The seepage flows then increased rapidly and peaked at approx. 145 l/s. That constituted a dangerous situation requiring immediate action.

The cause was found to be erosion damage in the asphaltic concrete surface membrane affecting an area of some 5 m² of the blanket about 3 m under the level reached by the impounded water. To avoid having to interrupt reservoir filling, a temporary repair was performed with underwater concrete applied to the leak by divers, and the asphaltic concrete facing was not renovated until routine annual drawdown. Repairs were also needed elsewhere on the facing. As mentioned above, the cause of the damage is thought to be creeping ice with the ploughshare effect of enclosed stones.

Immediate action was also required in response to slope movements that occurred during the first partial filling of the Gepatsch reservoir. This event is dealt with in detail in section 9.4.

All other measures required for the twenty dams in this report can be considered remedial works that could be performed without any acute risk. That applies in particular to repairs or the replacement of asphaltic concrete surface diaphragms as a result of aging. The relief wells on Dams nos. 5 and 6 had to be replaced and, in the case of Dam no. 6, new ones constructed. Following pronounced settlements at Dam no. 4 (Gepatsch), the crest had to be raised to bring the dam back up to the planned height.

Another remedial measure was post-construction sealing works for the cutoff wall at the contact with the asphaltic concrete core at Dam no. 6. As stated in section 5.1.2, monitoring after five years of reservoir operation showed a gradual increase in seepage from 125 l/s to 175 l/s.

As explained in [38], dye tests were used to locate the main seepage flows. The additional sealing works took the form of a 50 m long and 36 m deep two-line grout curtain placed in front of the cutoff. The grout, a mix of 300 kg cement and 40 kg bentonite with 850 l water, was injected via a sleeve pipe working in three passes. Thanks to these additional sealing works, the dam was restored to its original state. As mentioned above, additional sealing works were also necessary for Dam no. 2.

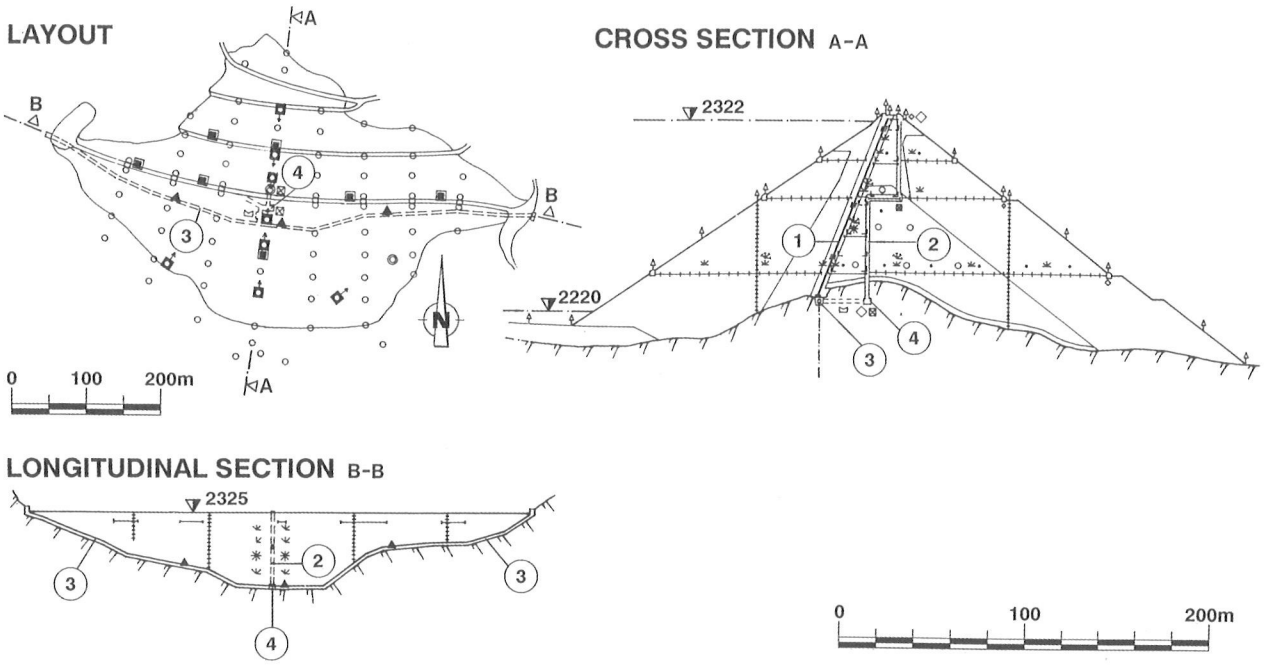

Symbol	Monitoring equipment	Number
	TWO DIMENSIONAL GROUP OF EARTH PRESSURE CELLS	92
	THREE DIMENSIONAL GROUP OF EARTH PRESSURE CELLS	18
	PORE PRESSURE CELLS	12
	RESISTANCE THERMOMETERS	9
	PEAK RECORDING ACCELEROGRAPHS	3
	STRONG MOTION ACCELEROGRAPHS (THREE DIMENSIONAL)	2
	PIEZOMETER IN BOREHOLE	13
	RECORDING OF SEEPAGE WATER LOSSES	3

Symbol	Monitoring equipment	Number
	SURFACE MONUMENTS	110
	HORIZONTAL PLATE GAUGES	8
	VERTICAL PLATE GAUGES	7
	EXTENSOMETERS	13
	GROUPS OF 4 STRAIN METERS	4
	FLUID LEVEL SETTLEMENT DEVICES (PERMANENTLY INSTALLED)	9
	PLUMB-LINES	2
	MEASURING DEVICES FOR DETERMINATION OF CORE-WALL THICKNESS VARIATIONS	3

Fig. 83 *from [9]: Dam no. 15 Monitoring equipment.*

1: Asphaltic concrete core wall.
2: Accessible plumbline shaft.
3: Inspection and grouting gallery.
4: Central measuring chamber.

9. Dam safety

In general it can be said that structural safety has been a main focus of research in the last few decades. Working on the basis of probability theory, researchers have considered load effects and resistances to develop the concept of the probability of failure as a measure of safety. This interesting approach has not yet gained acceptance among the dam engineering community, however, and in the field of geotechnics, too, standardization for embankment safety remains based, with minor modifications, on the proven ultimate load methods.

The most frequent causes of fill dam failure to date have been surface erosion as a result of overtopping or internal erosion caused by seepage. In the first half of the 20th century there were also cases of dam failure due to pore water pressure problems, especially during the construction phase or in connection with seismic activity. Given today's standards of dam safety and our knowledge of potential causes of damage, however, such dam failures can now be largely excluded. For Austria's twenty high embankment dams, it is reasonable to assume that any negative developments would be recognized in good time.

Additional remarks on dam safety concern the following:

9.1 Safety against overtopping

Reliable design is essential for the fill dam spillways needed to discharge the overflow in an extreme flood event. In Austria it is standard practice to base spillway design on a 5000-year flood, and older dams are being upgraded accordingly. Such factors as wave height and wind friction receive detailed treatment in [2]. They are used to calculate the necessary freeboard, which must also be done with due regard for the risk of an additional mass suddenly entering the reservoir in the form of a landslide or avalanche and of a fault in a flood control gate. Appropriate measures must be taken to prevent obstructions forming in spillways.

9.2 Safety against internal erosion

Internal erosion is an extremely complex subject. The hydraulic redistribution of solids is all the more dangerous as the processes often remain undetected for years or even decades. That is the reason for the continuous turbidimetric monitoring of seepage with data transmission for dams nos. 2, 5 and 6, which have a hazard potential with regard to internal erosion. A solid load of 0.5 mg/l, which is often present in the impounded water itself, is considered unproblematical.

The reduction of seepage is seen as the only reliable countermeasure to internal erosion. That goal was achieved in the case of the smaller embankment dams at Gosausee and Feldsee. The extent of the reduction of seepage flows through additional sealing works can also been seen as a measure of safety against internal erosion.

9.3 Calculated safety factors

However high today's standards may be in calculating dam safety factors, it must nevertheless be said that they can only offer approximations of varying degrees of accuracy of complex natural states. This is a general truth; it is not intended to detract in any way from the standards or guidelines issued by the Austrian Reservoir Commission [79], which are mandatory for all embankment dams in Austria. In accordance with those guidelines and international practice, two earthquake load cases must be studied: OBE (Operating Basis Earthquake) and MCE (Maximum Credible Earthquake).

The relevance in the field of all such calculations depends on the quality of the data employed. Obtaining reliable data is often only possible up to a certain limit, which cannot be significantly exceeded no matter how much work is done.

By way of example, Fig. 84 shows the results of the stability analysis for the maximum cross-section of the Gepatsch rockfill dam using the ultimate load method. The analysis takes account of the influences of fluctuations in storage level and a core side pressure. As can be seen from Fig. 5, design changes were made during the construction phase and load transfer occurred. That necessitated revised safety calculations on completion of the construction works using the characteristic material values obtained from on-site quality controls. Fig. 85 shows the result for several potential sliding bodies on the downstream side of the dam based on the measured stresses. It is interesting to see that the results obtained with different calculation methods show relatively little scatter and that the safety factors of all the sliding bodies studied are higher than that of the dam slope fs.

The problem of load transfers in narrow valleys

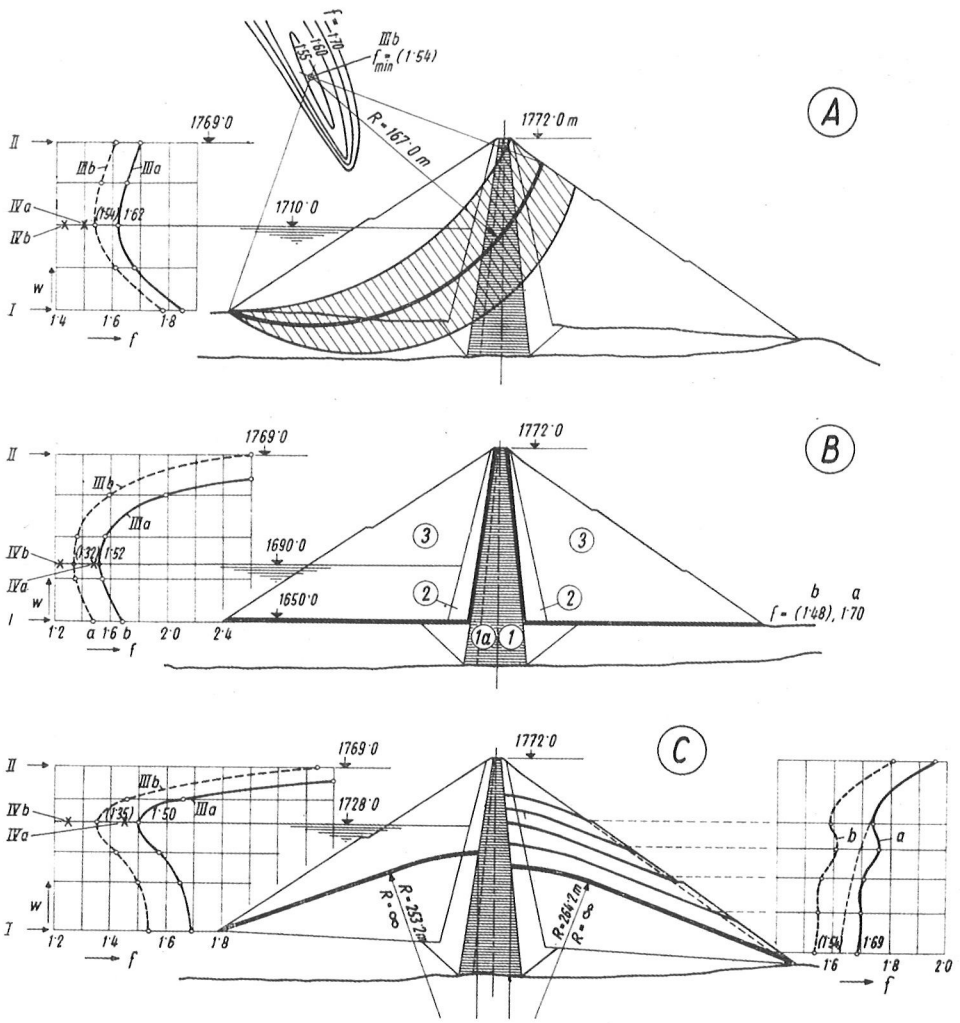

(I) (II) (III) Normal load cases.
(IV) Exceptional load case (earthquake).
(a) Final stage.
(b) Completion stage.
(f) Safety factor.
(w) Water level of reservoir.
(1) (1a) (2) (3) Dam zones.

Fig. 84 *from [27]: Dam no. 4*
Results of stability analyses.
(A) (B) (C) Supposed slide and shearing surfaces.

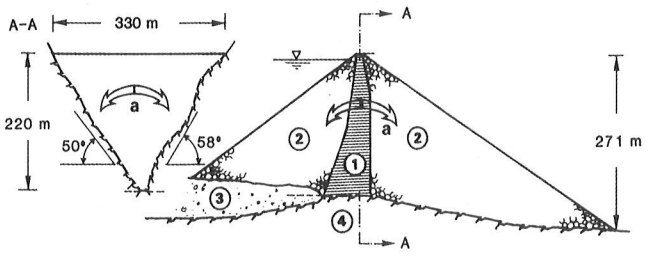

Fig. 86 *from [17]: Dabaklamm research project.*
(1) Earth core.
(2) Shell zones.
(3) Overburden.
(4) Bedrock
(a) Arching effect.

was studied in the framework of the BFG's embankment dam research program with reference to plans to build Dabaklamm Dam. For LC deadweight, the results of the analysis indicated not only load transfers within the cross-section but also transverse to the valley into the flanks of the gorge-shaped valley [13, 16] (see Fig. 86). Fig. 87 shows load transfers within the cross-section, which are caused by the compressible upstream overburden. The analysis indicated a material utilization of 100 % in the stiff earth core, with an arching effect across the crest area between the two shell zones. The transverse load transfers are presented in Fig. 88. The shielding effect reducing the vertical pressures is shown in Fig. 88/b. To mitigate this effect it would be necessary to modify the valley section as shown in Fig. 89.

With regard to the spatial bearing effect of an earth core fill dam, the proposal presented in Fig. 90 was developed for the Dabaklamm project [17], adapting the basic concept of the well known Trial Load

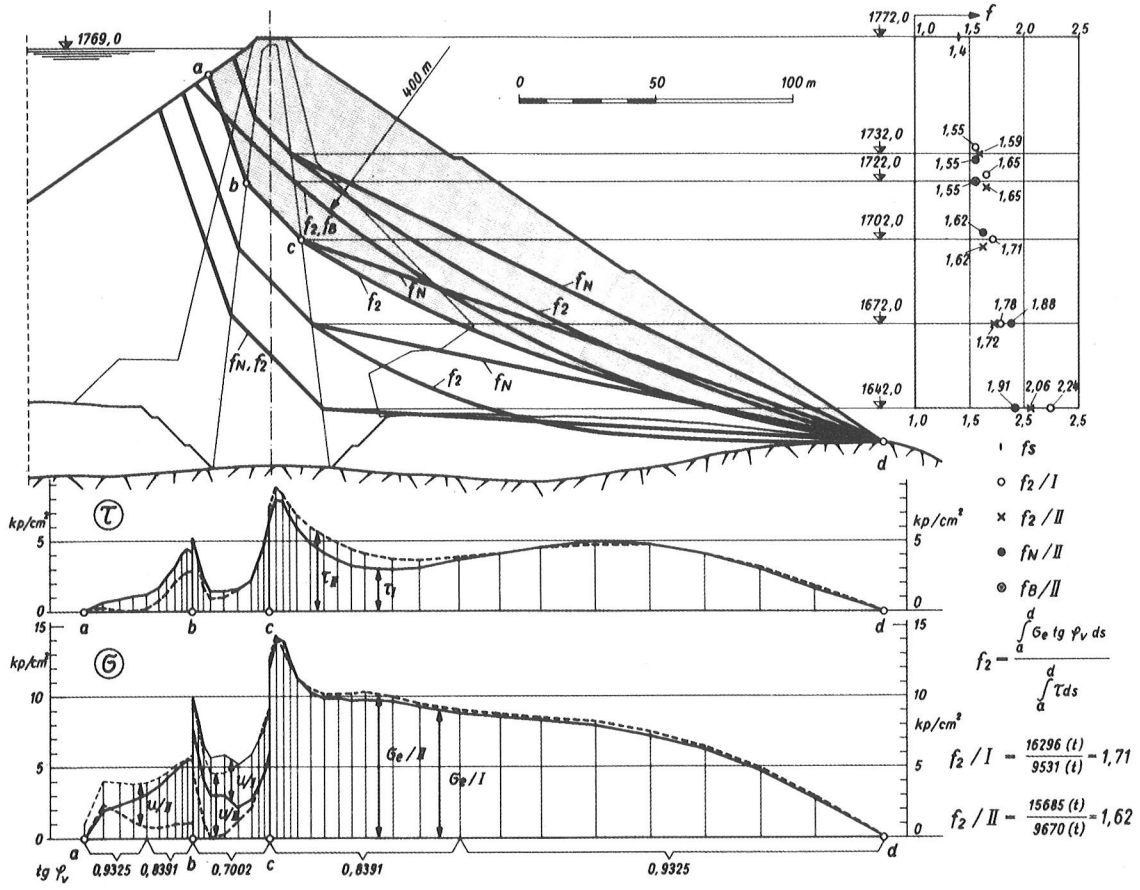

Fig. 85 *from [30]: Dam no. 4*
Safety factor f2 for the downstream side for load case I (f2 /I) and II (f2 /II).

fN/II, fB/II:Safety factors according to Nonveiller and Bishop for load case II.
fs: Safety factor for the dam slope.

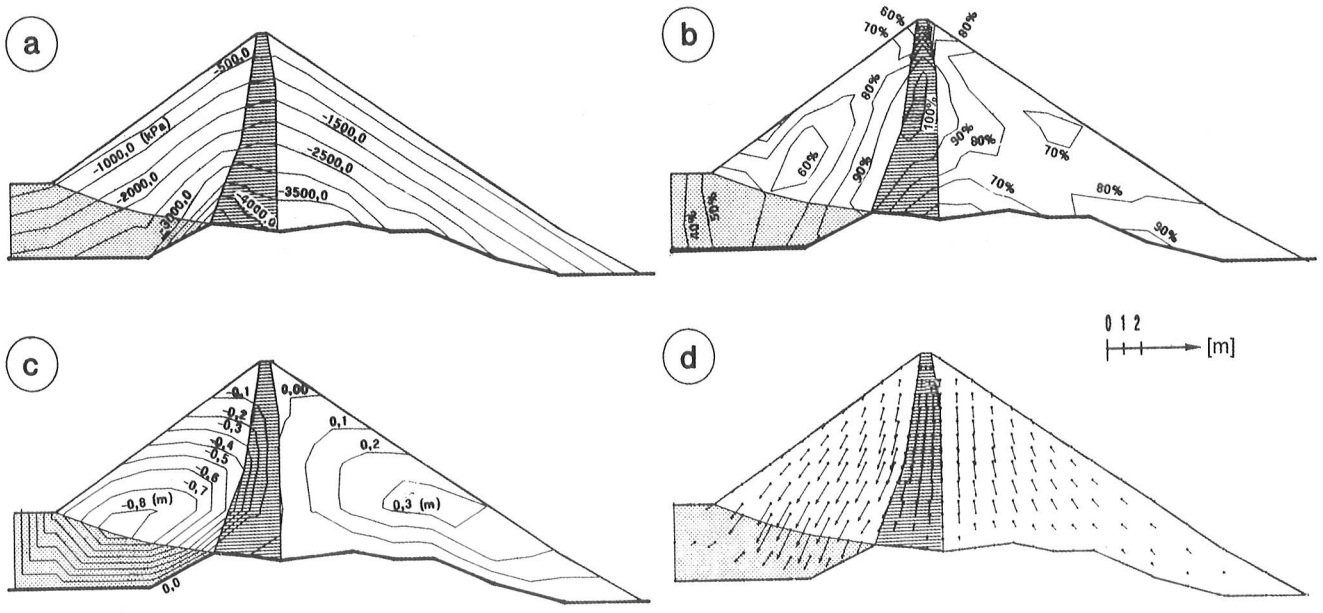

Fig. 87 *from [17]: Dabaklamm project.*
Results of 2-D/FEM Calculations; LC deadweight.

(a) σ_V isolines,
(b) Material utilization factor isolines.
(c) Horizontal displacement isolines.
(d) Vectors of deformation.

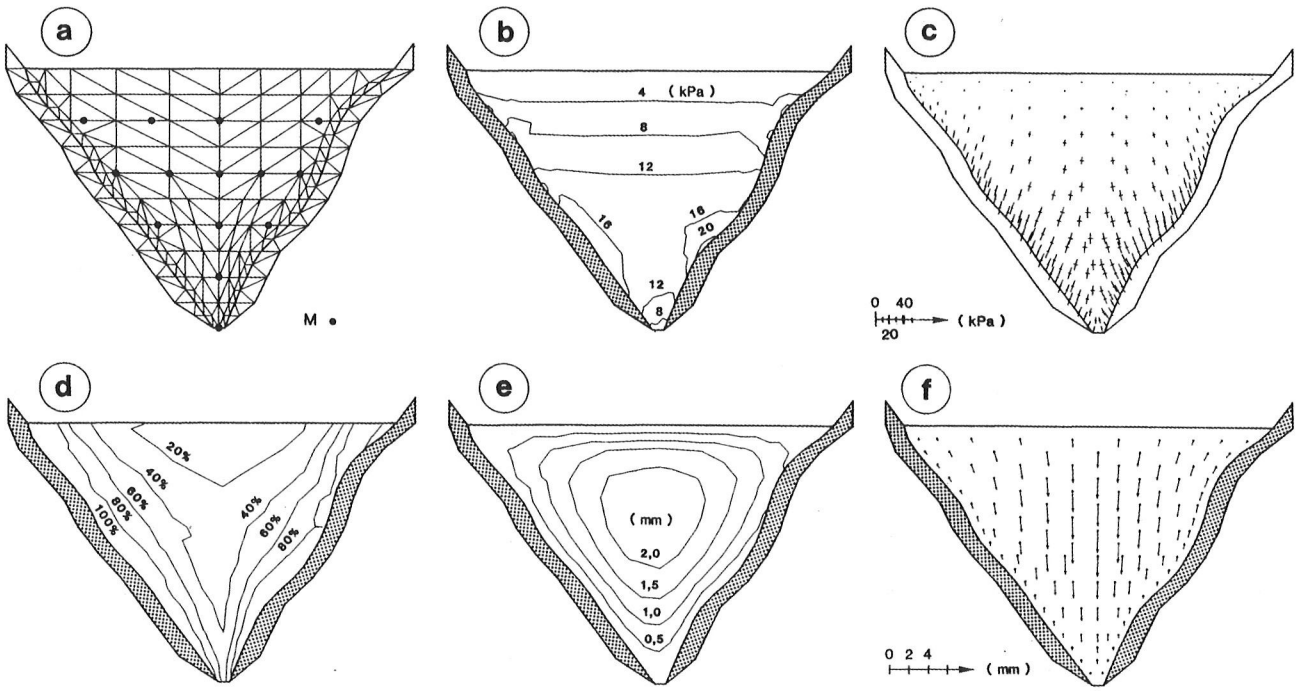

Fig. 88 *from [17]: Dabaklamm project.*
FEM Calculations of the physical model in Fig. 47.
(a) FEM grid; M points of measurement.
(b) σ_V isolines.
(c) Main stress axis.
(d) Isolines of material utilization factors.
(e) Settlement Isolines.
(f) Vectors of deformation.

Method for arch dams to an embankment dam.

As the diagrams show, the load bearing effect in the downstream shell zone in a vertical slice is linked to that of the three horizontal slices S1, 2 and 3. The iterative steps in the process are also shown in Fig. 91. As a first step, a division of headwater pressure was assumed, with p_{W1} representing the horizontal load bearing effects and p_{W2} the vertical load bearing effects. In the FEM analysis, p_{W2} is used to calculate the horizontal displacements

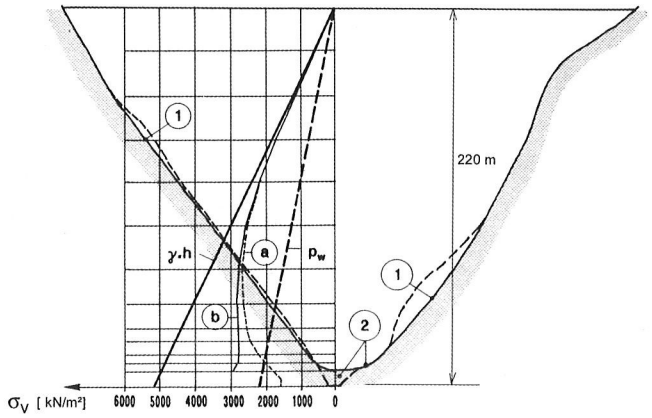

Fig. 89 *from [17]: Dabaklamm project.*
Results of FEM calculations. Vertical stresses in the valley section.
(1) Concave shaping.
(2) Concrete filling and rounded shapes.
(a) σ_V stresses without applying measures.
(b) σ_V stresses with measures 1 and 2.

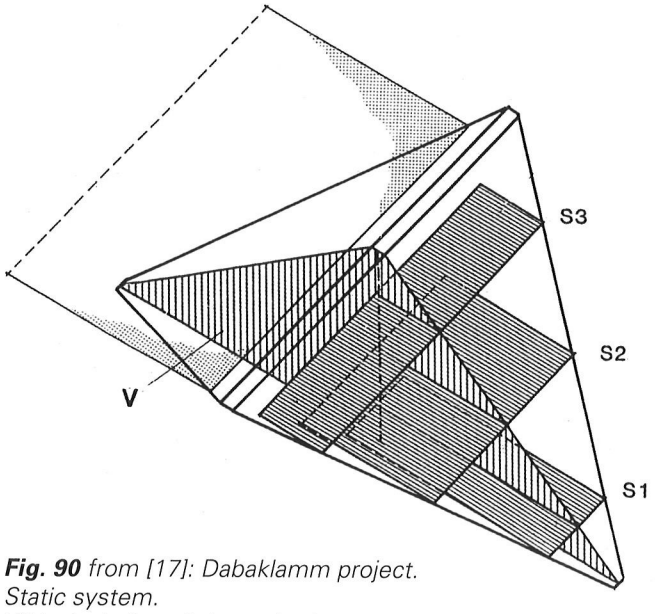

Fig. 90 *from [17]: Dabaklamm project.*
Static system.
V Vertical slice of the main dam section. S1, S2, S3 Horizontal slices.

δ1,2 and 3 at levels S1,2, and 3. The latter are applied to the horizontal slices, and FEM analysis is used to determine the resulting activatable load bearing effect p_{W1}. That in turn produces a new

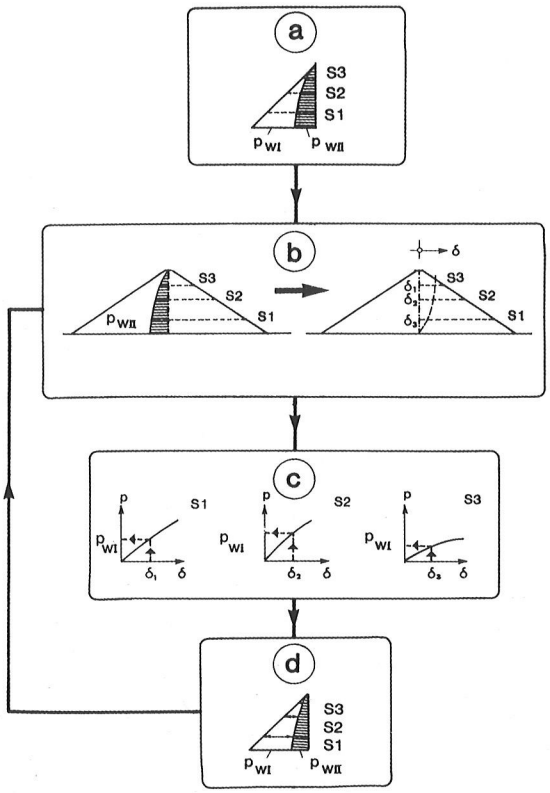

Fig. 91 *from [17]: Dabaklamm project. Iteration sequence.*

(a) Assumption of a load distribution: p_{wI} Proportion of horizontal bearing effect, p_{wII} Proportion of vertical bearing effect

(b) Determination of the horizontal displacements δ1, δ2, δ3 in the vertical slice at p_{wII}.

(c) Determination of p_{wI} using displacements according to (b).

(d) Improved assumption for load distribution.

load distribution, which requires the iteration process to be continued until agreement is reached with the improved assumption. The result for this example is given in Fig. 92. It shows the great influence of the spatial effect, with a reduction in horizontal displacements compared with the 2D case of approx. 60 %. Good agreement was also found with the results of testing with physical models presented in [4] (e in diagram d).

9.4 Stability of the reservoir slopes

The catastrophic damage caused by the major landslide into the Vajont reservoir in the Venetian Alps in October 1963 generated public awareness worldwide for the problem of the stability of reservoir slopes. One year later, in 1964, slides and creep developed in the post-glacial sagging slopes of the Gepatsch reservoir during first partial filling. Before impounding continued, it was therefore necessary, as mentioned above, to perform extensive investigations into predicted slope behavior and its effects on impounding up to top water level. The results of these studies are presented in [31] and [80]. A mathematical model was used (Fig. 93) to determine the sliding movements that continued filling could be expected to produce up to a state of equilibrium. The results obtained were largely confirmed during reservoir filling in 1965 and 1966. The movements that actually occurred are shown in Fig. 94.

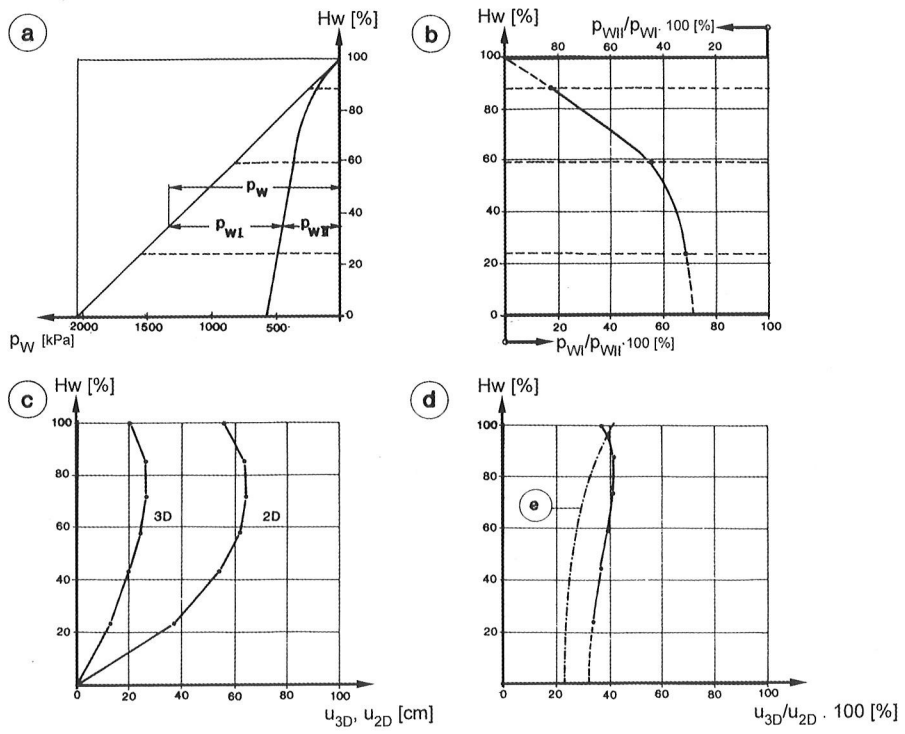

Fig. 92 *from [17]: Dabaklamm project. Results of the 3-D effects. Explanation, see Fig. 91.*

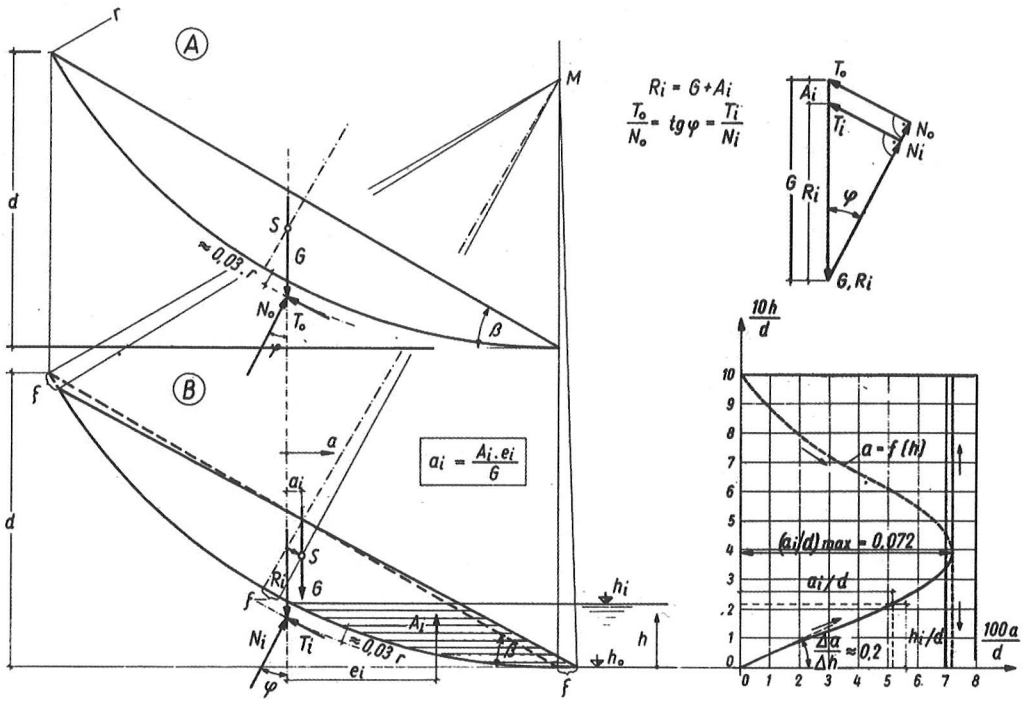

Fig. 93 *from [31]: Dam no. 4*
Necessary displacement of a sliding body of circular segment shape (r/d=2, β= 30°) to compensate uplift.

(A) Equilibrium limit before reservoir filling.
(B) Equilibrium limit at reservoir level hi.
(G Weight of the slope before reservoir filling.
(φ) Friction angle.
(A_i) Uplift at reservoir level hi.
(R_i) Resultant at reservoir level h_i.
(a_i) Horizontal displacement of the center of gravity of the slope required to maintain equilibrium limit at reservoir level h_i.

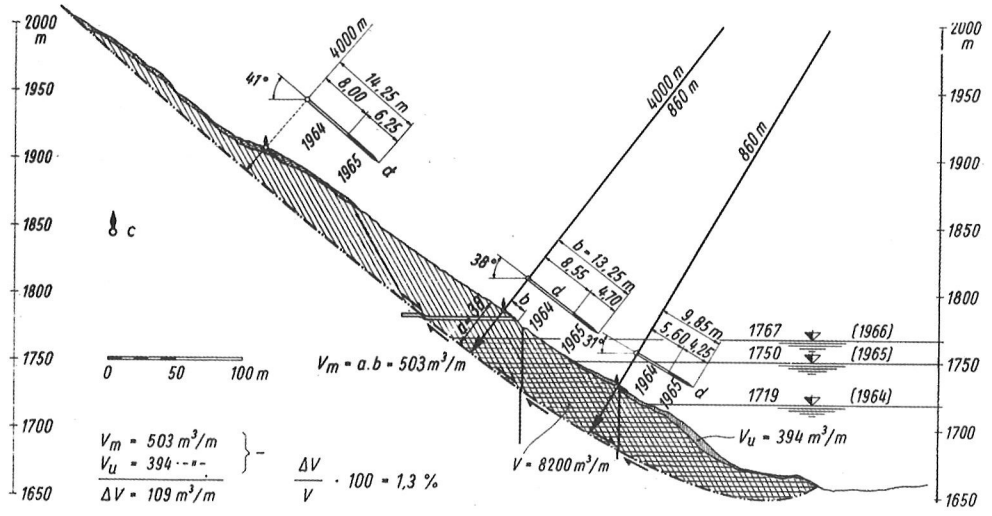

Fig. 94 *from [31]: Dam no. 4*
Profile of the original and deformed slope at Hochmaiss with vectors of movement, radii of curvature of the sliding area and the deformed slope.

(V) Saturated slope zone.
(V_m) Passage of masses per meter at medium slope elevation.
(V_u) Increase in masses at the slope toe.
(c) Observation point.
(d) Vector of movement on enlarged scale.

In contrast to the use of stability analysis for embankment dams, it is not possible to work with absolute safety factors in the case of reservoir slopes. All calculations operate with the limit equilibrium state $\eta = 1$, so that only relative values can be calculated. The assessment must be based primarily on measured movements. It is also necessary to consider whether surge waves formed when the mass of an unstable slope or an avalanche slides into the reservoir could cause overtopping at the crest of the dam. To perform the relevant analysis for the Gepatsch reservoir, hydraulic tests were conducted on the model shown in Fig. 95 [81].

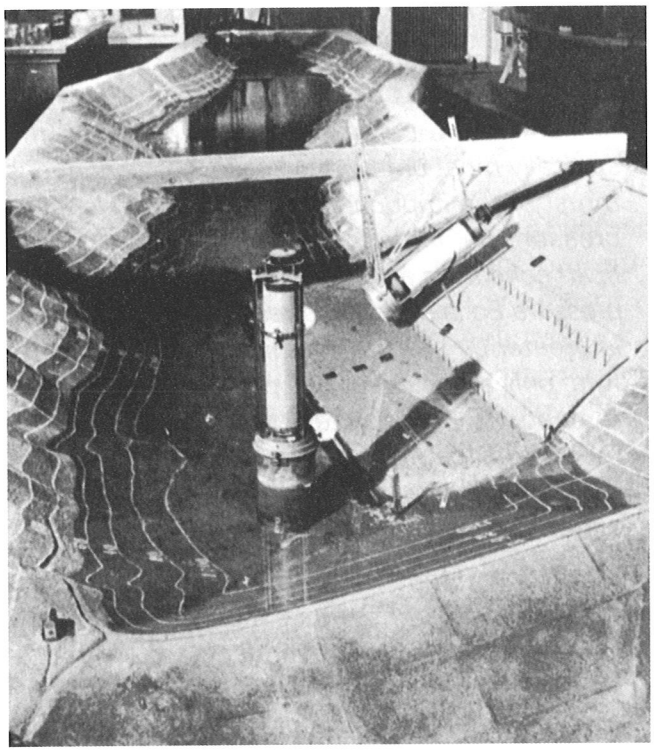

Fig. 95 *from [31]: Dam no. 4*
Reservoir model at scale of 1/500 with dam and deformation sliding slope of Hochmaiss at full elevation 1767 m.

Since 1966 creep has continued in all the submerged sagging slopes at Gepatsch reservoir, with annual increments of between a few mm and a few cm [82]. These movements are comparable with the ongoing settlements in the upstream shell of the dam due to grain redistribution caused by fluctuations in the level of the impounded water. They do not pose a threat to dam stability. As shown in Fig. 96, the sliding slope in Fig. 97 has been made the subject of continuous monitoring with fluid levels and extensometers. A geodetic surveillance system is also in place, with automatic theodolites providing continuous monitoring of the surface monuments installed in the sagging slopes. A

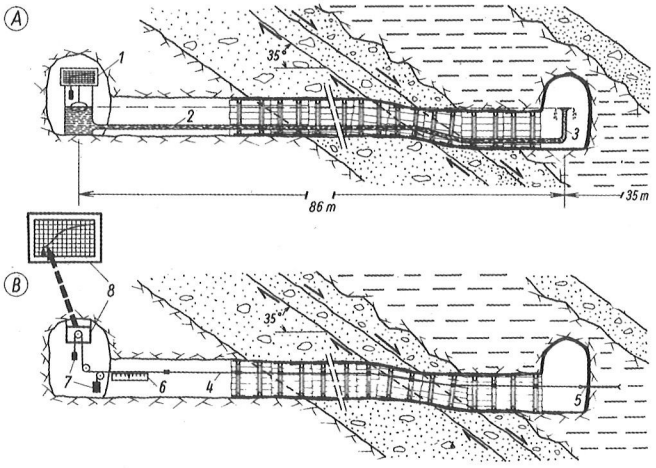

Fig. 96 *from [31]: Dam no. 4*
Equipment for continuous monitoring of movement.
(A) Hose pipe scale with recording device.
(B) Wire deformometer with teletransmission and recording device.
(1) Tank with floating body and recording device.
(2) Hose pipe with protecting tube.
(3) Stand pipe with overflow.
(4) Measuring wire, 1 mm diameter.
(5) Anchorage.
(6) Scale.
(7) Stretching weight.
(8) Measuring value transmitter and receiver with recording device.

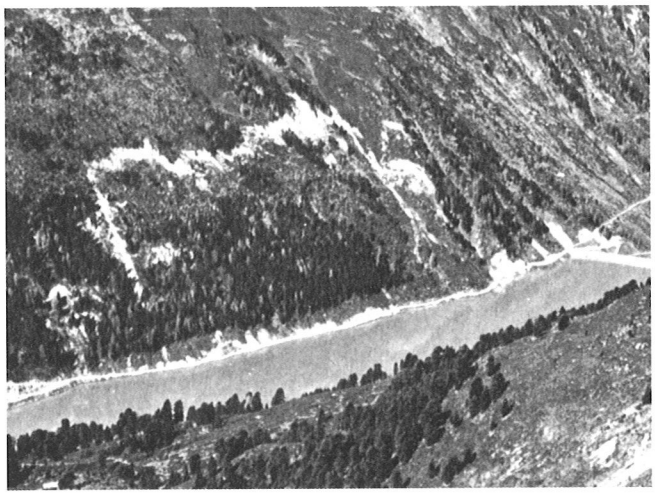

Fig. 97 *from [31]: Dam no. 4*
Sliding slope at Hochmaiss with dam and reservoir at full level 1767 m.

similar system is in operation at Dam no. 5 (Durlassboden), where the reservoir also has post-glacial sagging slopes.

As discussed in [65], extensive investigations were also required for stability analysis of the reservoir slopes at Dam no. 16 (Bolgenach). Slope stability is monitored by measuring the changes in distance across the valley between surface monuments on the two slopes.

10. Spillways and bottom outlets

The reservoirs formed by Austria's high embankment dams are provided with a bottom outlet and a spillway. Bottom outlets must be designed with due regard for the safety of downstream residents, and the stability of the reservoir slopes and the upstream slope of the dam. Only in exceptional cases will it be possible to draw down a reservoir via the outlet works during extremely high inflows. Nor can one rely on the possibility of using turbine water for flood relief purposes. The design of the spillway is thus of crucial importance for the protection of a dam against overtopping.

Frequently the tunnel for the bottom outlet also served to divert the water during the construction period. In the case of dams with surface diaphragms, the bottom outlet may also take the form of a pipe laid in a gallery through the dam body. A bottom outlet normally has a service gate and a safety gate. Both must be capable of operation at maximum discharge.

Austrian fill dams are generally constructed with free overflow spillways, e.g. of the morning glory type. Flood discharge from the spillways is often via shafts and tunnels, although chute discharge is also to be found. Stilling basins are normally built for energy dissipation in the tailwater, although a downstream rocky streambed may also be used.

The mechanical installations for bottom outlets and spillways are subject to annual inspections by the Austrian authorities.

11. Final remarks

11.1 Embankment dam research

Embankment dam construction based on fill placement and compaction can be traced back to the ancients, but it was not until the 20th century that the technologies were developed to ensure a high standard of dam safety.

As far as the central research topic of bearing behavior in fill dams is concerned, the following conclusions can be drawn.

- *As long as surface erosion and internal erosion can be excluded, and the decrease in piezometric level takes place mainly in the impermeable zone, embankment dams have very considerable reserves in terms of bearing capacity. Even in a fill dam with a central core membrane, as the statically most unfavorable case, the continuous thrust of the impounded water and active earth pressure Ea' in the upstream shell zone under uplift conditions are countered by a passive earth pressure Ep in the downstream shell zone, which is greater by several magnitudes. Since, therefore, only a fraction of this passive earth pressure needs to be activated, the horizontal movements required to achieve a state of equilibrium are slight relative to movements of the boundary state.*
- *In addition to the stiffness of the shell materials, the magnitude of horizontal movements deriving from hydrostatic load depends on the shear prestress in these shells caused by LC deadweight. This prestress reduces the displacement effect of the effective acting loads on the dam body. It is a result of the triangular shape of the dam section and is highest in dams with plastic earth cores.*
- *In order to generate an artificial shear prestress, the concept of the prestressed embankment dam was developed. It constitutes a new approach to dam safety as both impermeability testing and bearing behavior monitoring take the form of trial loading with an empty reservoir and thus zero risk. The prestressed dam concept also contributes to a better understanding of the bearing behavior of embankment dams.*

The other research subjects are above all relevant for the planning stage in the construction of an embankment dam. The results take the form of simple design procedures. The research work involved, as in the case of spatial effects, also contri-

butes to a greater awareness of the problems involved.

11.2 Embankment dam construction in Austria

It was not until the second half of the previous century that high embankment dams came to be constructed in Austria. That made it possible to take advantage of international experience in the field. As repeatedly stated in this report, fill dam construction in Austria would not have been possible without the theoretical counseling and practical advice given by the Austrian Professor H. Breth of the Technical University of Darmstadt.

The various embankment dams presented in this report confirm the truth of the general statement made in the preface that dam construction in the individual case is always a unique proposition.

But even if direct comparisons between dams can rarely be drawn with any degree of certainty, a number of conclusions can nevertheless be drawn in retrospect:

- *An embankment dam designed on the basis of the accepted codes and standards has the stability needed to safely transfer all loads imposed into the foundations. It constitutes an extremely adaptable composite system comprising the impervious element, the dam body and the foundations.*
- *The main problem is sealing the dam and its foundations. The sealing works must meet two requirements: the ability to withstand deformations without cracking and the ability to handle seepage without erosion damage. All the other dam and foundation zones must also be erosion-resistant.*
- *The use of FEM to determine 2D and 3D bearing behavior permits more reliable predictions on dam performance to be made and also offers a better understanding of the influence of various effects.*
- *Continuous monitoring is essential for any embankment dam. The Austrian standard of monitoring, with continuous surveillance and alarm systems, guarantees dam safety.*
- *It is safe to say that, following the phase of plastic deformations, elastic movements between high and low water levels are generally minor.*
- *The stability assessment of sagging slopes in reservoir basins must focus on deformation behavior. Creep movements that can be seen from the topography of the terrain to have developed over the centuries without triggering spontaneous mass movements could be considered a safety criterion.*

Given the unimaginable potential for destruction in the case of a dam failure, effective co-operation between the supervisory authority and the operator is essential. Austrian law does full justice to this requirement. Today's high standard is an excellent point of departure for future embankment dam construction projects

Dam construction and operation is doubtless one of the fields of building and civil engineering that imposes the highest degree of responsibility on the engineer. The author was involved with all twenty dams covered by this report, either as an engineer, consultant, expert or agent of the supervisory authority. In addition to long years of membership in the Austrian Reservoir Commission, that explains the decision - taken with a feeling of gratitude - to write this report.

12 Bibliography

1 Schober, W.
Staudammforschung - ein Schwerpunkt am Institut für Bodenmechanik, Felsmechanik und Grundbau der Universität Innsbruck
Heft 5/6 der Österreichischen Wasserwirtschaft, Jg. 31, 1979

2 Kjaernsli, B., Valstad T. and K. Höeg, K.
Rockfill Dams - Design and Construction
Norwegian Institute of Technology, Division of Hydraulic Engineering, Publication 10,1992

3 Symposium on Rockfill Dams
Transactions of the American Society of Civil Engineers, Volume 125, Part II 1960
New York, published by the Society 1961

4 Schober, W.
A study on the behaviour of embankment dams with diaphragms
Q. 61, R 53, XVI ICOLD, San Francisco 1988

5 Schober, W.
Besonderheiten beim Entwurf, bei der Ausführung und im Verhalten Österreichischer Staudämme
Österr. Wasserwirtschaft, Heft 9/10, 1977

6 Tschernutter, P.
Experience gained with asphaltic concrete facings on high-level embankment dams of the Fragant group of power schemes
Q61, R59, XVI ICOLD, San Francisco 1988

7 Sherard, Woodward, Cizienski, Clevenger
Earth and Earth-Rock Dams
John Wiley & Sons, 1967

8 Pinto, N.L. and al.
Design and perfomance of Foz do Areia Concrete membrans as related to Basalt Properties
Q55, R51, XIV ICOLD, Rio de Janeiro 1982

9 Schober, W., Schwab, H.
Dams in Austria - Chapter G:
Embankment Dams,
Austrian National Committee on Large Dams
XVII ICOLD Vienna 1991

10 Schober, W., Lackinger, B.
Model studies of the bearing behaviour of dams with an interior membrane seal
Colloquium on Physical-Geomechanical Models, ISMES Bergamo 1978

10a List, F., Sadgorski, W.
Stress and strain measurements in Mauthaus Dam
Q 52, R 15, XIV ICOLD Rio de Janeiro 1982

10b Lackinger, B.
Das Tragverhalten von Staudämmen mit membranartigen Dichtungen
Mitteilung 4 des Instituts BFG 1980

11 Schober, W., Rostek, R.
The shear resistance in the interface of the fill material or the rock overburden and the bedrock
Q48, R56, XIII ICOLD New Dehli 1979

12 Schober, W., Teindl, H.
Filter criteria for geotextiles
VII. ECSMFE Brighton 1979

13 Schober, W., Rammer L.
High embankment dams in ravine like valleys
XI. ICSMFE, San Francisco, 9/B/5, 1985

14 Schober, W.
Concrete core diaphragm walls for high embankment dams
Q.55, R.12, XVI. ICOLD Rio de Janeiro 1982

15 Schober, W., Lercher, H.
The concrete core diaphragm wall of the embankment dam Bockhartsee
Monitoring and interpretation
Q.56, R.66, XV. ICOLD Lausanne 1985

16 Schober, W., Hammer, H., Hupfauf, B.
Load transfer in embankment dams - Model testing
XII. ICSMFE Rio de Janeiro, 11/24, 1989

17 Schober, W., Hupfauf, B.
The bearing behaviour of embankment dams in narrow vallys
Q.67, R.5, XVII. ICOLD Vienna 1991

18 Schober, W.
Considerations and investigations for the design of a rockfill dam with 92 m high bituminous mix core
Q.42, R.34, XI. ICOLD Madrid 1973

19 Schober, W., Hupfauf, B, Hechenblaickner, K.
The prestressed Dam - A new approach to safety in embankment dams
Q.71, C17, XVIII. ICOLD Durban 1994

20 Schober, W., Atzl, G.
Special tests with well-graded core material: Stress and strain behaviour and internal erosion
Q.73, R.1, XIX. ICOLD Florence 1997

21 Schober, W., Henzinger J.
Membranartige Betonkerndichtungen für hohe Staudämme
Henzinger, J.: Staudämme mit membranarti-

gen Betonkerndichtungen
Tragverhalten, Anwendungskriterien, Bemessungsrichtlinien
Mitteilung 6 des Instituts BFG, 1985

22 Rammer, L.:
Wirklichkeitsnahe Ermittlung der Spannungs- und Verformungszustände von Staudämmen mit membranartigen Dichtungen unter Berücksichtigung der räumlichen Tragwirkungen
Mitteilung 8 des Instituts BFG, 1987

23 Schober, W., Lercher, H., Rammer, L., Hupfauf, B.:
Der Staudamm Bockartsee - Bauerfahrungen und Auswertung der Kontrollmessungen
Mitteilung 9 des Instituts BFG, 1987

24 Hammer, H.
Spannungsumlagerungen in Erdkörpern unter besonderer Berücksichtigung des Dammbaus
Hupfauf, B.:
Das Tragverhalten von Staudämmen in Abhängigkeit von der Dichtungsart
Mitteilung 10 des Instituts BFG, 1992

25 Atzl, G.
Belastungsermittlung von eingeschütteten starren Bauwerken
Mitteilung 11 des Instituts BFG, 1992

26 Lauffer, H., Schober, W.
Investigations for the earth core of the Gepatsch rockfill dam with a height of 150 m
Q.27, R.92, VII. ICOLD Rome 1961

27 Lauffer, H., Schober, W.
The Gepatsch rockfill dam in the Kauner valley
Q. 31, R.4, VIII. ICOLD Edinburgh 1964

28 Schober, W.
Behaviour of the Gepatsch rockfill dam
Q.34, R. 39, IX. ICOLD Istamboul 1967

29 Neuhauser E., Wessiak, W.
Placing the shell zones of the Gepatsch rockfill dam in winter
Q.35, R.30, IX. ICOLD Istamboul 1967

30 Schober, W.
The interior stress distribution of the Gepatsch rockfill dam
Q.36, R.10, X. ICOLD Montreal 1970

31 Lauffer, H., Neuhauser, E., Schober, W.
Uplift responsible for slope movements during the filling of the Gepatsch reservoir
Q.32, R.41, IX. ICOLD Istamboul 1967

32 Schober, W.
Damm auf 310 m Höhe geschüttet
VDI Nachrichten Nr. 19, 1974

33 Breth, H., Günther, K.
Die Anwendung von Entspannungsbrunnen zur Verhütung von Erosionsschäden beim Erddamm Eberlaste
Der Bauingenieur Jg. 42, Heft 8, 1967

33a Verbund Austrian Hydro Power AHP
Jahresbericht - Staudamm Eberlaste, 1997/98

33b Vorarlberger Illwerke AG
Stauanlagen - Meflbericht Bielerdamm 1997

34 Breth, H., Günther, K.
Betrachtungen über die Bemessung von Staudämmen auf heterogenem Untergrund
Mitteilungen des Instituts für Verkehrswesen, Grundbau u. Bodenmechanik der TH Aachen Heft 51, 1970

35a Melbinger, R., Niel, A.
Surveillance and emergency measures for dams in Austria
G.P.6, XIV ICOLD - Rio de Janeiro 1982

35b Heigerth, G., Melbinger, R., Obernhuber, P., Tschernutter, P.
Assessing and improving the safety of existing dams in Austria
Q.68, R58, XVIII ICOLD Durban 1994

35c Melbinger, R.
The Austrian approach to dam safety: a symbiosis of rules and engineering judgement
Proc. International Symposium on Dam Safety, Balkena Rotterdam 1998

35d Melbinger, R.
Die Überwachung der Talsperren Österreichs - 12 Thesen suchen Zustimmung.
Österr. Wasser- u. Abfallwirtschaft, 54. Jg., Heft 11/12, 2002

36 Breth, H., Günther, K.
Die Dichtungselemente des Erddammes Eberlaste
Strabag - Veröffentlichungen, 8. Folge, Heft 2, 1964 - 1967

37 Kieflling, H. Rienössl, R., Schober, W.
Embankment dams in Austria
General Paper (G.P.4) XII. ICOLD Mexico 1967

38 Widmann, R.
Die Sanierung einer Leckstelle in der Dichtwand des Erddammes Eberlaste
Mitteilung 5 des Instituts BFG 1984

39 Pircher, W., Schwab, H.
Design, construction and behaviour of the Asphaltic concrete core wall of the Finstertal dam

Q. 61, R. 49 XVI ICOLD San Francisco 1988

40 Schwab, H.
Verformungsmechanismen von Aspahltbeton-Kerndichtungen in Staudämmen
Mitteilung 5 des Instistuts BFG 1984

41 Schwab, H., Pircher, W.
Structural behaviour of a high rockfill dam, comprehensive interpretation of measurements, and conclusions on stress-strain relationships
Q. 56, R. 67 XV ICOLD Lausanne, 1985

42 Breth, H.
Messungen an einem Damm mit Asphaltbeton-Kerndichtung
Strabag - Schriftenreihe, 7. Folge Heft 1, 1964

43 Schober, W.
Comments on Q. 55 - R. 12
Q55, Volume V, XIV ICOLD Rio de Janeiro 1982

44 Schwab, H., Pircher, W.
Monitoring and alarm equipment at the Finstertal and Gepatsch rockfill dams
Q 52, R. 64 XIV ICOLD Rio de Janeiro 1982

45 Kjaernsli, B., Kvale, G., Luside, J., Baade-Mathiesen, I.
Design, construction control and performance of the Svartevann earth-rockfill dam
Q.55, R.19 XIV ICOLD Rio de Janeiro 1982

46 Tschernutter, P. Nackler, K.
Construction of Feistritzbach dam with central aspahltic concrete membrane and the influence of poor quality rock on fill behaviour
Q.67, R. 27 XVII ICOLD Vienna 1991

46a Tschernutter, P.
Influence of soft rockfill material on a central bituminous concrete membrane
USCOLD Lectures Series, San Diego 1997

47 Neuschitzer, F.
Sperre Feistritzbach - Entwurf und Ausführung des Dammbaues und der Asphaltbetoninnendichtung
Österr. Zeitschrift f. Elektrizitätswirtschaft, 46. Jg., Heft 12, 1993

48 Kelag TK - Talsperrenüberwachung
KW Koralpe - Sperre Feistritzbach, Jahresbericht 1992

49 Posch, E., Wintersteiger, A.
Die Steindamm-Talsperre am Rotgüldensee
Österr. Ingenieur-Zeitschrift, Heft 2, 1959

50 Schober, W.
Discussion to Q 61
Minutes of Sessions, Volume V, XVI ICOLD San Francisco 1988

51 Salzburg AG - Talsperrenüberwachung
Damm Rotgüldensee Meflbericht 1998

52 Leonhardt, G.
Die Belastung starrer Rohrleitungen unter Dämmen
Mitteilung des Instituts f. Grundbau und Bodenmechanik, TU Hannover, Heft 4, 1973

53 Orel, A.
Gesteuerte Dichtungsarbeiten beim Erddamm des Freibachkraftwerkes - Kärnten
ATCOLD-Schriftenreihe - „Die Talsperren Österreichs", Heft 13, 1964

54 KELAG TK - Talsperrenüberwachung
Sperre Freibach - Jahresbericht 2002

55 KELAG - Kraftwerk Freibach
ÖZE Österr. Zeitschrift f. Elektrizitätswirtschaft, 12. Jg., Heft 4, 1959

56 Strabag Bau -AG
Asphalt - Wasserbau
Strabag-Schriftenreihe, 3. Folge, Heft 2, 1957

57 Strabag Bau-AG
Asphalt-Wasserbau. Neue Entwicklungen und Ausführungen
Strabag-Schriftenreihe 7. Folge Heft 1, 1964

58 Schwab, H.
Staudamm Gepatsch, Analyse zum langjährigen Verhalten (1962 - 1978)
Österr. Wasserwirtschaft, Jg. 31, Heft 5/6 1979

59 Schober, W.
Large scale application of Gloetzl Type hydraulic stress cells at the
Gepatsch rockfill dam, Austria
Baumefltechnik, Report 1, Special information from F. Gloetzl, 1965

60 Trollope, D.M.
The systematic arching theory applied to the stability analysis of embankments
IV. ICSMFE 25, 1957

61 Kropatschek, H., Breth, H., Rienössl, K., Widmann, R.
Durlaflboden
ÖZE: Österr. Zeitschrift für Elektrizitätswirtschaft, Heft 8, Aug. 1968

61a Verbund Austrian Hydro Power AHP
Staudamm und Speicher Durlaflboden Jahresbericht, 1998/99

62 Schober, W.
Über das Tragverhalten von Staudämmen
Wasserwirtschaft Jg. 71, Heft 4, 1981

63 Innerhofer, G.
Der 100 m hohe Kiesdamm Bolgenach mit Moränenkern
Wasserwirtschaft 70, Heft 3, 1980

64 Innerhofer, G., Loacker, H.
The connection of the core of the Bolgenach dam to weathered marl
Q53, R15, XIV ICOLD - Rio de Janeiro 1982

65 Innerhofer, G., Loacker, H.
The stability of the rock rim of the Bolgenach reservoir
Q54, R6, XIV ICOLD - Rio de Janeiro 1982

66 Vorarlberger Kraftwerke AG
Staudamm Bolgenach - Bauwerksbeobachtung 1980 bis 2001

67 Schwab, H.,Pircher, W.
Roughening of smooth and steeply sloping rock surfaces in the foundation of Finsterstal rockfill dam
Q 48, R 22, XIII. ICOLD - New Dehli 1979

68 Rostek, R.
Der Scherwiderstand von Lockergestein auf Felsuntergrund
Mitteilung 1 des Instituts BFG, 1977

69 Teindl, H.
Filterkriterien von Geotextilien
Mitteilung 3 des Instituts BFG 1980 und Heft .153 der Straflenforschung im Bundesministerium, 1980

70 Busch, K.F. Luckner, L.
Geohydraulik
F. Enke, Stuttgart 1974

71 Lorenz, W., List, F.
Trench diaphragms as sealing elements in earth dams
Q.55, R 13, XIV ICOLD Rio de Janeiro 1982

72 Lorenz, W.
The sealing element of the dam of Mauthaus drinking water reservoir
Q.42, R.6, XI ICOLD Madrid 1973

73 Wellacher, H. Tschernutter, P.
Repair of a high-altitude Rockfill Dam with an upstream asphalt concrete membrane
Q59, R 40, XV. ICOLD - Lausanne 1985

74 List, F.
Die Staudämme der bayerischen Trinkwassertalsperren Mauthaus und Frauenau
Heft 5 der Mitteilung des Instituts f. BFG 1984

75 Hechenblaikner, K.
Der vorgespannte Damm
Dissertation an der Technischen Fakultät der Univ. Innsbruck 1995

76 Lauffer, H.
Discussion to Q. 27Vol.V, VII-ICOLD Rome 1961

77 Nackler, K., Neuschitzer, F.
Talsperrenüberwachung mit Hilfe digitaler dezentraler Datenerfassung und Informationsbereitstellung
Österr. Wasser- u. Abfallwirtschaft, H.11 - 12, 2002

78 Rostek, R.
Eine Methode zur Bestimmung der Einbaudichte von grobkörnigen Schüttmaterialien.
Bauingenieur Jg.55, 1980

79 Richtlinien zur Ermittlung der Standsicherheit von Staudämmen
Staubeckenkommission im österr. Bundesministerium f. Land- u. Forstwirtschaft 1996

80 Breth, H.
The dynamics of a landslide produced by filling a reservoir
Q.32, R.3, IX ICOLD - Istamboul 1967

81 Neuhauser, E.
Modellversuche über die Wirkung von Schwallwellen am Staudamm Gepatsch
Österr. Wasserwirtschaft, 31. Jg., Heft 5/6, 1979

82 Neuhauser, E., Schober, W.
Das Kriechen der Talhänge und elastische Hebungen beim Speicher Gepatsch
2. Kongreß der int. Gesellschaft f. Felsmechanik - Belgrad 1970

Published in series

„Die Talsperren Österreichs" (Large Dams in Austria)

Volume 1: Prof. Dr. A.W. REITZ: Beobachtungseinrichtungen an den Talsperren Salza, Hierzmann, Ranna und Wiederschwing (1954)

Volume 2: Dipl. Ing. Dr. techn. Helmut FLÖGL: Der Einfluß des Kriechens und der Elastizitätsänderung des Betons auf den Spannungszustand von Gewölbesperren (1954)

Volume 3: Prof.Dr.A.W. REITZ, R. KREMSER und E. PROKOP: Beobachtungen an der Ranna-Talsperre 1950 bis 1952 mit besonderer Berücksichtigung der betrieblichen Erfordernisse (1954)

Volume 4: Prof.Dr. Karl STUNDL: Hydrochemische Untersuchungen an Stauseen (1955)

Volume 5: Prof.Dr. Josef STINI: Die baugeologischen Verhältnisse der österreichischen Talsperren (1955)

Volume 6: Dipl.Ing.Dr. Hans PETZNY: Meßeinrichtungen und Messungen an der Gewölbesperre Dobra (1957)

Volume 7: Dozent Dipl.Ing.Dr.techn. Erwin TREMMEL: Limbergsperre, statische Auswertung der Pendelmessungen (1958)

Volume 8: Dr.techn. Dipl.Ing. Roland KETTNER: Zur Formgebung und Berechnung der Bogenlamellen von Gewölbemauern (1959)

Volume 9: Dipl.Ing. Hugo TSCHADA: Sohlwasserdruckmessungen an der Silvrettasperre (1959)

Volume 10: Dipl.Ing. Wilhelm STEINBÖCK: Die Staumauern am Großen Mühldorfersee (1959)

Volume 11: Dipl.Ing.Dr.techn. Ernst FISCHER: Beobachtungen an der Hierzmannsperre (1960)

Volume 12: Prof.Dr. Hermann GRENGG: Statistik 1961 (1962) Ausgabe in englischer Sprache (1962)

Volume 13: Dipl.Ing. Alfred OREL: Gesteuerte Dichtungsarbeiten beim Erddamm des Freibachkraftwerkes, Kärnten 1964

Volume 15: Sammel-Ergebnisse des 8. Talsperren-Kongresses in Edingburgh 1964 (1966)

Volume 16: Dipl.Ing. Otto GANSER: Die Meßeinrichtungen der Staumauer Kops 1968

Volume 17: 9. Talsperren-Kongress in Istanbul 1967 (1969)

Volume 18: Österreichische Beiträge zum Talsperrenkongress Montreal (1970)

Volume 19: Prof.Dr. Hermann GRENGG: Statistik 1971 der Talsperren, Kunstspeicher und Flußstauwerke (1971)

Volume 20: Dipl.Ing.Dr.tech. Joser KORBER: Die Entlastungsanlagen der österreichischen Talsperren (1973)

Volume 21: Österreichische Beiträge zum Talsperrenkongreß in Madrid 1973 (1974)

Volume 22: Österreichische Beiträge zum 12. Talsperrenkongreß in Mexico 1976 (1975)

Volume 23: Dipl.Ing.Dr.techn. Hans PETZNY, Prof.Dipl.Ing.Dr.tech. Walter SCHOBER, Dipl.Ing.Dr.techn. Richard WIEDMANN: Messungen an österreichischen Talsperren (1977)

Volume 24: Dipl.Ing. Rudolf PARTL: Statistik 1977 (Ausgabe auch in Englisch)

Volume 25: Österreichische Beiträge zum 13. Talsperrenkongreß 1979 in New Delhi

Volume 26: Österreichische Beiträge zum 14. Talsperrenkongreß 1982 in Rio de Janeiro

Volume 27: Fernüberwachung österreichischer Talsperren

Volume 28: Langzeitverhalten österreichischer Talsperren und Flußstauwerke

Volume 29: Hydro power schemes and large dams in Austria

Volume 30: Österreichische Beiträge zum 15. Talsperren-Kongreß 1985 in Lausanne

Volume 31: Österreichische Beiträge zum 16. Talsperren-Kongreß 1988 in San Francisco

Volume 32: Dams in Austria (1991)

Volume 33: R. WIDMANN, Die Talsperren Österreichs, Gewölbemauern (Erfahrungen - Probleme - Entwicklungen) (1999)

Kufferath

Austrian National Committee on Large Dams
Elisabethstrasse 59/4, A-8010 Graz, Phone ++43/316/354708, Fax ++43/316/354706, secretary@atcold.at, www.atcold.at